**Applied Battery Research for Transportation
(B&R No. VT-1102000)**

**Progress Report
for
Second Quarter FY 2012**

**Contributions from
Argonne National Laboratory
Army Research Laboratory
Brookhaven National Laboratory
Idaho National Laboratory
Jet Propulsion Laboratory
Lawrence Berkeley National Laboratory
National Renewable Energy Laboratory
NAVSEA Carderock
Oak Ridge National Laboratory
Sandia National Laboratories**

May 2012

Applied Battery Research for Transportation Program
Second Quarter Progress Report for FY 2012

This quarterly progress report describes the activities to be conducted in support of DOE's Applied Battery Research for Transportation (ABR) Program. This program focuses on helping the industrial developers to overcome barriers for Li-Ion batteries for use in plug-in hybrid electric vehicles (PHEVs). In its goal of developing low-emission high fuel economy light-duty HEVs and PHEVs, the FreedomCAR and Fuels Partnership established requirements for energy storage devices in these applications. The Vehicle Technologies Program at DOE has focused the efforts of this applied battery R&D program on the PHEV application.

Through the U.S. DRIVE Partnership, DOE is currently supporting the development of advanced Li-Ion batteries with industry for HEV, PHEV, and EV applications. The industrial developers have made significant progress in developing such batteries for HEV applications and there are new challenges associated with developing viable battery technologies for the PHEV application, especially when targeting the 40-mile all electric range. In addition to the calendar life, abuse tolerance, and cost challenges that exist for Li-Ion batteries in the HEV application, now the issue of providing sufficient energy within the weight and volume requirements becomes a huge challenge, as does cycle life. Also, the abuse tolerance and cost challenges become even greater. The Applied Battery Research for Transportation program is directed at assisting the industrial developers to identify the major factors responsible for the technical barriers and to find viable cost-effective solutions to them. The goal is to facilitate the development of low-cost cell chemistries that can simultaneously meet the life, performance, abuse tolerance, and cost goals that have been established by the U.S. DRIVE Partnership.

The ABR Program is organized into three main technical tasks to address these issues for PHEVs:

(1) Battery Cell Materials Development—focuses on research, development, and engineering of advanced materials and cell chemistries that simultaneously address the life, performance, abuse tolerance, and cost issues.
(2) Calendar & Cycle Life Studies—deals with understanding the factors that limit life in different Li-Ion cell chemistries, which are used as feedback to Task 1. This task also deals with the establishment and operation of in-program cell fabrication capabilities for use in these life studies.
(3) Abuse Tolerance Studies—deals with understanding the factors that limit the inherent thermal and overcharge abuse tolerance of different Li-ion cell materials and chemistries, as well as developing approaches for enhancing their abuse tolerance.

A list of the projects is given in the table, with the individual reports compiled in the Appendix.

Organization	AMR Project ID	AOP Project ID	Title	PI/Contact Point	Page Number
			Task 1: Battery Cell Materials Development		
ANL	ARRA VT076		Materials Scale-Up Facility	Gregory Krumdick	6
ANL	ES167	IV. E.1.1	Process Development and Scale up of Advanced Cathode Materials	Gregory Krumdick	10
ANL	ES168	IV. E.1.2	Process Development and Scale up of Advanced Electrolyte Materials	Gregory Krumdick	14
ANL	ES015	1.1A	Engineering the High Energy Cathode Material	Khalil Amine	17
ANL	ES016	1.1B	New High Energy Gradient Concentration Cathode Material	Khalil Amine	23
ANL	ES019	1.1G	Development of High-Capacity Cathode Materials with Integrated Structures	Michael Thackeray	27
ANL	ES020	1.1C	Developing High Capacity, Long Life anodes	Ali Abouimrane	31
ARL	ES024		High Voltage Electrolytes for Li-ion Batteries	Richard Jow	34
ANL	ES025	1.1D	Development of Advanced Electrolyte Additives	Zhengcheng Zhang	42
JPL	ES026		Electrolytes for Use in High Energy Li-Ion Batteries with Wide Operating Temperature Range	Marshall Smart	46
INL	ES027		Novel Phosphazene Compounds for Enhancing Electrolyte Stability and Safety of Lithium-ion Cells	Kevin Gering	52
ANL	ES028	1.1E	Streamlining the Optimization of Lithium-Ion Battery Electrodes	Wenquan Lu	59
ANL	ES028	1.3	Screen Electrode Materials, Electrolytes, and Additives	Wenquan Lu	62
LBNL	ES029	1.2.2	Scale-up and Testing of Advanced Materials from the BATT Program	Vincent Battaglia	65

Organization	AMR Project ID	AOP Project ID	Title	PI/Contact Point	Page Number
			Battery Chemistries		
			Task 2: Calendar & Cycle Life Studies		
BNL	ES034	2.4 and 3.3	Life and Abuse Tolerance Diagnostic Studies for High Energy Density PHEV Batteries	Xiao-Qing Yang	121
ORNL	ES039		Online and Offline Diagnostics for Electrodes for Advanced Lithium Secondary Batteries	David Wood	124
ANL	ES111	2.2A	Battery Design Modeling	Kevin Gallagher	136
			Task 3: Abuse Tolerance Studies		
ANL	ES035	3.1	Develop & Evaluate Materials & Additives that Enhance Thermal and Overcharge Abuse	Zonghai Chen	141
SNL	ES036	3.2	Abuse Tolerance Improvements	Chris Orendorff	145
LBNL	ES037	1.2.1	Overcharge Protection for PHEV Batteries	Guoying Chen	151

APPENDIX

Individual Project Progress Reports

TASK 1
Battery Cell Materials Development

Project Number: ARRAVT076   **2012 Q2 update**

Project Title: Materials Scale-Up Facility

Project PI, Institution: Gregory Krumdick, Argonne National Laboratory

Collaborators (include industry):
Barton Malow, Design Build Subcontractor

Project Start/End Dates: start: 4/1/2010; end: 3/31/2012

Objectives: The objective of this project is to design and build a pilot-scale battery-materials production facility (Materials Engineering Facility) to scale up bench-scale battery chemistries and produce bulk quantities of new materials for evaluation in prototype cells to enable quick turnaround validation of new materials chemistries. Such a facility is a key missing link between the bench-scale development of battery technology and high-volume manufacturing of large-format advanced batteries for transportation applications. One of the primary contributing factors to the lack of a significant domestic Li-ion battery manufacturing capability is the lack of adequate facilities to enable the research community to produce quantities of materials for prototype cells to enable quick-turnaround validation screening of new materials chemistries throughout the R&D process.

Approach: To enable the process development and scale-up of new battery materials, the facility is planned to have:
- Suitable space – The Materials Engineering Facility will contain high hazard Group H-Occupancy labs to accommodate the larger volumes of hazardous materials used as processes are scaled up.
- Modular process equipment – The facility and equipment design will incorporate modular equipment to enable quick change out of unit operations, as required for a range of materials process R&D.
- Analytical lab for materials analysis – A dedicated analytical lab to characterized materials during scale up allows for rapid process optimization and can also provide materials quality assurance analysis.
- Staff experienced in process scale-up R&D – Scientists and engineers trained and experienced in process development and scale up are a critical component to the program.

The approach to achieve the facility plan is to:
- Establish conceptual design of facility (CDR), Establish Design Build contract for facility.
    - Following the principals of the DOE Project Management Process.
- Establish interim scale-up labs during the design and construction of the facility.

- o To allow for the scale up of battery materials to begin now.
- Prepare the environmental and safety plans and NEPA for the facility construction and interim labs.
- Begin work in interim labs to demonstrate that scaling is possible.

Milestones:

Materials Engineering Facility Construction

Milestone / Deliverable	Description	Date	Status
Milestone 1	Complete full facility design (CDR)	10/1/2010	COMPLETED 8/19/2010
Milestone 2	Award full facility construction contract	2/1/2011	COMPLETED 11/22/2010
Deliverable 1	Open interim facility (3 facilities) 2 opened 9/17/10, 1 opened 6/13/11	9/30/2010	COMPLETED 9/17/2010
Deliverable 2	Complete full facility construction	2/1/2012	COMPLETED 1/31/2012
Deliverable 3	Open full facility	3/31/2012	COMPLETED 3/30/2012

Interim Facilities and Equipment

Milestone / Deliverable	Description	Date	Status
Milestone 1	Interim facility equipment purchased & installed (3 facilities)	12/31/2010	COMPLETED 9/17/2010
Milestone 2	Production scale-up facility equipment purchased & accepted	12/31/2011	No Funding Allocated
Deliverable 1	Interim facility open (3 facilities) 2 opened 9/17/10, 1 opened 6/13/11	9/30/2010	COMPLETED 9/17/2010
Deliverable 2	Full facility open	3/31/2012	COMPLETED 3/30/2012

Financial data:
Total project duration: 24 mo.
Construction funds for facility: $3.3M
Capital equipment for process and analytical equipment: $2.5M

Progress towards construction milestones:
- The environmental and safety plans and NEPA for the facility construction and interim labs have been approved.
- First Construction milestone completed – 8/19/2010
    - Jacobs Engineering drafted the Conceptual Design Report and Fire Protection Assessment
- Second Construction milestone completed – 11/22/2010
    - Design Build contract was awarded to Barton Malow
- Construction deliverable #1 completed – 9/17/2010
- Construction deliverable #2 completed – 2/1/2012
    - **Beneficial occupancy was issued on 1/31/2012**
- Construction deliverable #3 completed – 3/31/2012
    - **Final occupancy was issued on 3/30/2012**

Figure 1. Materials Engineering Research Facility Construction Site – March 28, 2012

Progress towards interim facilities and equipment milestones:

- All interim labs are fully operational
- Electrolyte materials scale up lab – fully operational
    - Equipment has been delivered and installed
- Battery materials analytical lab – fully operational
    - Equipment has been delivered and installed
- Cathode materials scale up – fully operational
    - 4L reactor system is fully functional
    - 20L reactor system is fully functional
    - Powders hood has been delivered and installed

Capital equipment delivery status – **ALL EQUIPMENT DELIVERED AND INSTALLED**

Item	Status
Cilas Particle size analyzer	Delivered
Netzsch TGA-DSC-MS	Delivered
Agilent GC-MS	Delivered
Agilent ICP-MS	Delivered
Bruker FTIR	Delivered
Bruker XRD	Delivered
Powrex Vertical mixer	Delivered
NGK Batch furnace	Delivered
Nissin Particle classifier	Delivered
GL Filtration washer dryer 1	Delivered
GL Filtration washer dryer 2	Delivered
Physical Electronics XPS	Delivered
Maccor cycler	Delivered

TASK 1
Battery Cell Materials Development

Project Number: IV.E.1.1 (ES167)　　　　　　**2012 Q2 update**

Project Title: Process Development and Scale up of Advanced Cathode Materials

Project PI, Institution: Gregory Krumdick, Argonne National Laboratory

Collaborators (include industry):
Young-Ho Shin, Argonne National Laboratory
Kaname Takeya, Argonne National Laboratory

Project Start/End Dates: start: 10/1/2011; end: 9/30/2013

Objectives: Next generation cathode materials have been developed at the bench scale by a number of researchers focusing on developing advanced lithium ion battery materials. Process engineers will work with these researchers to gain an understanding of the materials and bench-scale processes used to make these materials and then scale–up and optimize the processes.

The objective of this task is to conduct process engineering research for scale-up of Argonne's next generation high energy cathode materials. These materials will be based on NMC chemistries and may include lithium rich technology, layered–layered and possibly layered–spinel classes of cathode materials. The current multistep batch processes, capable of producing approximately 2 kg of material per week using a 4L reactor will be optimized and scaled up. Scaling up the process involves modification of the bench-scale process chemistry to allow for the semi–continuous production of material, development of a process engineering flow diagram, design of a mini-scale system layout, construction of the experimental system and experimental validation of the optimized process. The design basis for scale-up will be based on a 20L reactor capable of producing a 10 kg batch of cathode materials per week.

Last quarter, it was reported that process optimization of $Li_{1.14}Mn_{0.57}Ni_{0.29}O_2$ on the 4L system was completed and work had begun on scaling the process to the 20L system. A primary issue identified on the 4L system was the fact that prior to reaching steady state, particles continued to grow past the optimal size forming a mixture of sized particles both larger and smaller than optimal. A technique was identified and tested to overcome this issue to allow for continuous processing.

Approach: A particle growth control technology was installed on the 20L system and tested on the synthesis of $Li_{1.14}Mn_{0.57}Ni_{0.29}O_2$. Further system optimization and coin cell testing continues next quarter.

Schedule and Deliverables: Deliverables will include scaled materials for independent testing, publications and a topical report.

Financial data:
Total project duration: 12 mo.
Staff and M&S: $500K with an additional $500K to be allocated in Q2.

Progress towards deliverables: A particle growth control technology was installed on the 20L system and the particle size and distribution of precursor growth was further tested. Initial results are promising, indicating the ability to reduce particle growth and narrow and control the particle size distribution, see figure 1. A new method for the prevention of plugging was installed and tested, results were very promising. We are unable to provide details about this addition at this time due to possible new IP. An invention disclosure has been filed on this new particle growth technology and has been expanded to include plugging prevention.
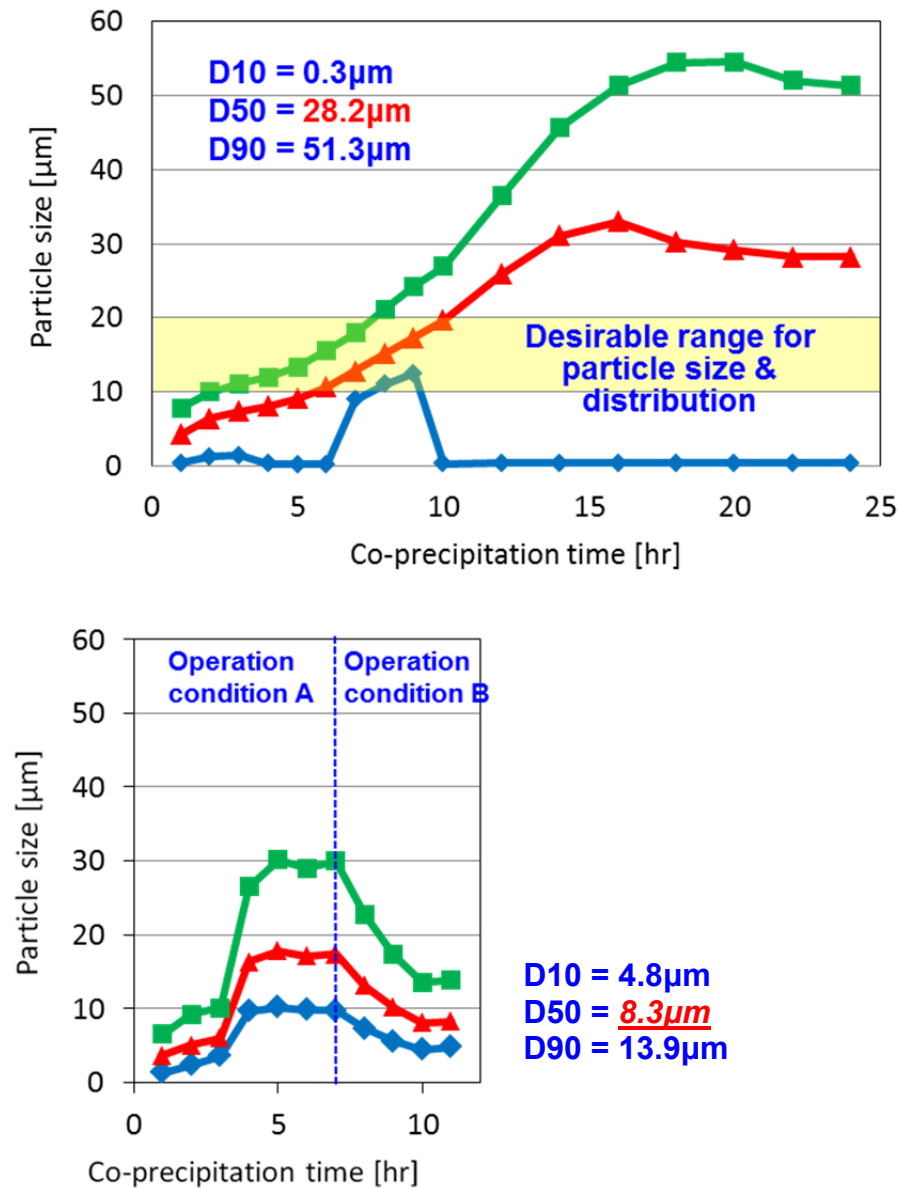

Figure 1. Particle size distribution without and with growth control technology.

7.157 kg of cathode materials was produced from the 1st 20L run; coin cells were generated and tested. Results are below in figure 2. A 2nd 20L run was conducted which produced 10.128 kg of cathode materials, 1 kg was delivered to the Materials Screening group to be made into pouch cells for validation testing (figures 3&4).
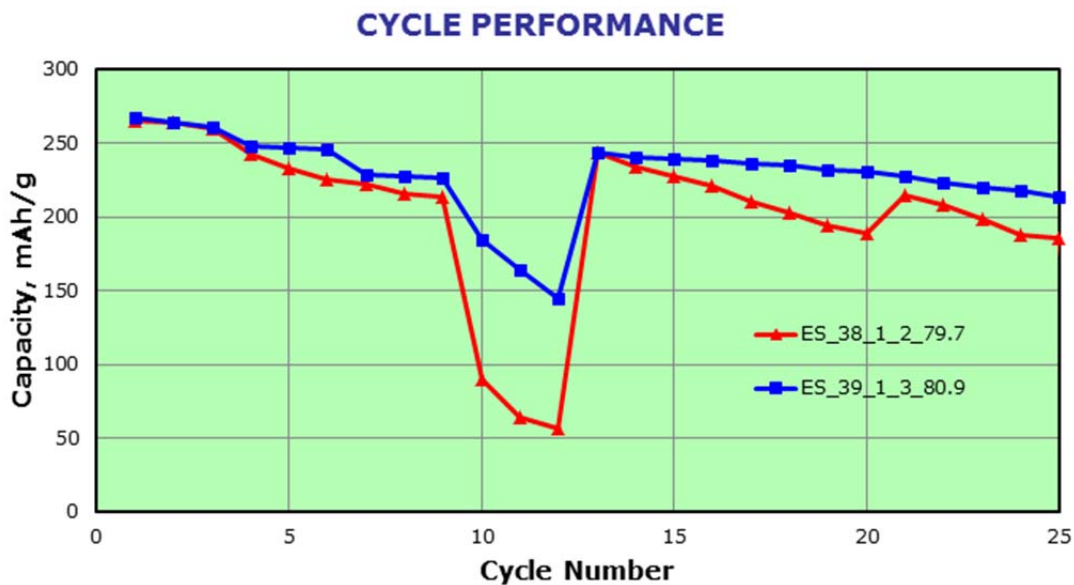

Figure 2. Coin cell results from 1st 20L run.

Figure 3. Precursor generated from 2nd 20L run.

Figure 4. 10 kg of cathode material generated from 2nd 20L run.

TASK 1
Battery Cell Materials Development

Project Number: IV.E.1.2 (ES168)   **2012 Q2 update**

Project Title: Process Development and Scale up of Advanced Electrolyte Materials

Project PI, Institution: Gregory Krumdick, Argonne National Laboratory

Collaborators (include industry):
Krzytof Pupek, Argonne National Laboratory
Trevor Dzwiniel, Argonne National Laboratory

Project Start/End Dates: start: 10/1/2011; end: 9/30/2013

Objectives: The objective of this task is to conduct process engineering research for scale-up of Argonne's new electrolyte and additive materials. Advanced electrolytes and additives are being developed to stabilize the interface of lithium ion batteries by forming a very stable passivation film at the carbon anode. Stabilizing the interface has proven to be key in significantly improving the cycle and calendar lift of lithium ion batteries for HEV and PHEV applications. Up to this point, these advanced electrolytes and additives has only been synthesized in small batches. Scaling up the process involves modification of the bench-scale process chemistry to allow for the semi–continuous production of materials, development of a process engineering flow diagram, design of a mini-scale system layout, construction of the experimental system and experimental validation of the optimized process. The mini system will be assembled utilizing an existing synthesis reactor system. Electrolyte materials produced will be analyzed to confirm material properties and for quality assurance. The electrochemical properties of the material will be validated to confirm a performance match to the original materials.

Approach: A formal approach for the scale-up of electrolyte materials has been defined. This approach starts with the initial discovery of a new electrolyte material and an initial electrochemical evaluation. This determines if the material is to be added to the inventory spreadsheet, ranked and prioritized. At this point, the scale-up process begins with the initial feasibility study, proof of concept testing, 1st stage scale-up and 2nd scale scale-up. Go/No go decisions are located after feasibility determination and electrochemical validation testing. See Figure 1 for more details.

Schedule and Deliverables: The schedule of electrolyte materials to scale will be determined once the scale-up spreadsheet has been ranked and prioritized. This will reflected in the project milestones. Deliverables will include scaled materials for independent testing and a technology transfer package of information on each material scaled.

Financial data:
Total project duration: 12 mo.
Staff and M&S: $500K with an additional $500K to be allocated in Q2.

Progress towards deliverables:
Work on the passivation additive LiDFOB has ended. Work on the solvent 1S1M3 has been completed. Work on the passivation additive HFiPP for the Army Research Lab has been completed.
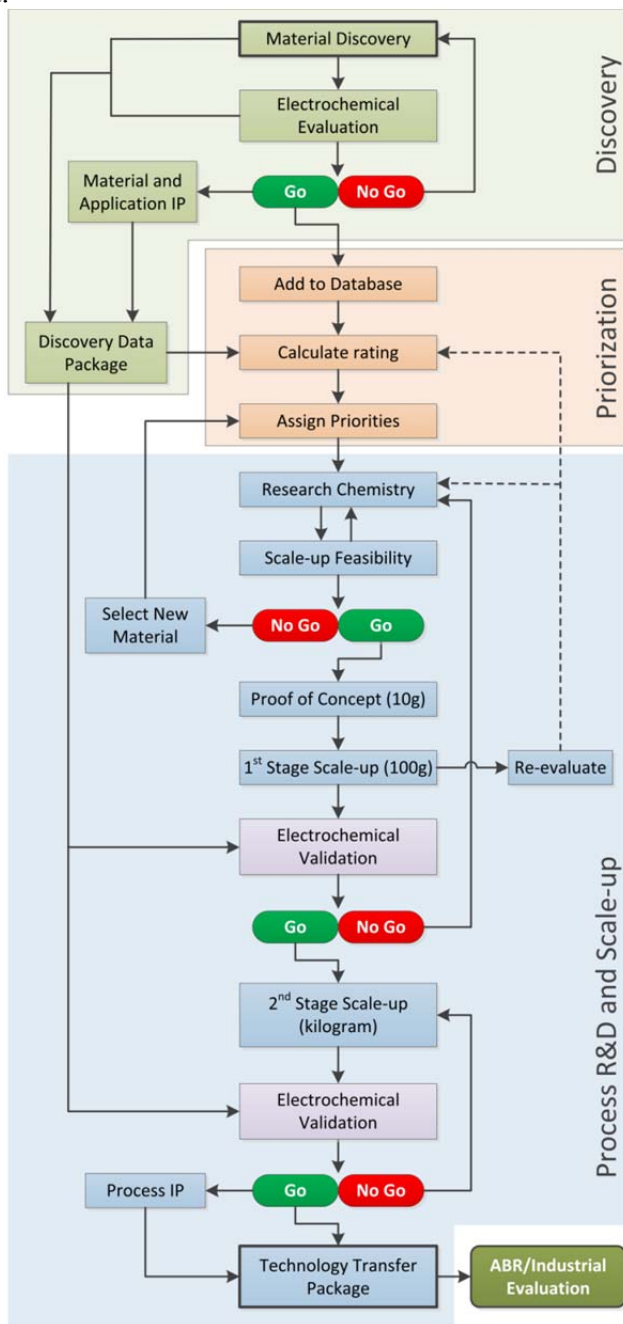

Figure 1. Electrolyte Materials Process R&D Flowchart

Milestones: Note: additional electrolyte materials will be added for FY12 upon prioritization of the current materials to scale spreadsheet.

MILESTONE	DATE	STATUS	COMMENTS
LiDFOB (Continued from FY11)			
Select CSE material to scale	01/07/2011	Completed	
Assess scalability of CSE process	08/12/2011	Completed	
WP&C documentation approved	06/22/2011	Completed	
Develop and validate scalable process chemistry (10g scale)	08/26/2011	Completed	
First process scale-up (100g bench scale)	11/07/2011	Completed	The material (~150 g) was synthetized, purified and analyzed.
Second process scale-up (1000g pilot scale)	March 2012	Ended	The usefulness and need of this material were re-evaluated and determined to be insufficient to justify further work. MERF is willing to prepare larger batches of this material on request.
1S1M3 (Continued from FY11)			
Select CSE material to scale	01/04/2011	Completed	
Assess scalability of CSE process	08/03/2011	Completed	
WP&C documentation approved	02/22/2011	Completed	
Develop and validate scalable process chemistry (10g scale)	09/02/2011	Completed	The reaction was successfully run in several 2 g-scale batches
First process scale-up (100g bench scale)	11/04/2011	Completed	The material was synthesized, purified and analyzed (80 g, >99%)
Second process scale-up (1000g pilot scale)	02/28/12	Completed	The material was synthesized, purified and analyzed (1327 g, 99.63%)
HFiPP, tris(1,1,1,3,3,3-hexafluoro-2-propyl) phosphate			
Assess scalability of disclosed process	10/07/2011	Completed	
WP&C documentation approved	10/21/2011	Completed	
Develop and validate scalable process chemistry (10g scale)	11/30/2011	Completed	
First process scale-up (100g bench scale)	12/22/2011	Completed	
Second process scale-up (1000g pilot scale)	01/27/2012	Completed	1230g produced in a single batch, purity >99.5%.

MILESTONE	DATE	STATUS	COMMENTS
Relocation to Materials Engineering Research Facility			
Decommission Interim Lab	04/06/2012	Completed	
Transfer Equipment	April 2012	Scheduled	Dependent on MERF completion.
Set up Equipment in MERF	May 2012	Scheduled	Dependent on MERF completion.
Electrolyte Lab Operational	May 2012	Scheduled	Dependent on MERF completion.

TASK 1
Battery Cell Materials Development

Project Number: 1.1A (ES015)

Project Title: Engineering of high energy cathode material

Project PI, Institution: Khalil Amine (Argonne National Laboratory)

Collaborators (include industry):
Huiming Wu (ANL); Ilias Belharouak (ANL); Ali Abouimrane (ANL);Y.K. Sun (Hangyang University); Army Research Lab; Toda Corporation, USA & Japan; BASF, USA & Germany

Project Start/End Dates:
October 1, 2008 /September 30, 2014

Objectives:
Develop high-energy composite layered cathode of $xLi_2MnO_3 \cdot (1-x)LiNiO_2$ for use in 40-mile plug-in hybrid vehicle, having following characteristics:

- Capacity of over 250 mAh/g
- High packing density (2.2~2.4 g/cc)
- Good rate capability
- Excellent cycle and calendar life
- Excellent abuse tolerance

Approach:
Argonne's high-energy composite layered cathode $xLi_2MnO_3 \cdot (1-x)LiNiO_2$ (M=Ni, Co, Mn) delivers a high capacity of ~250 mAh/g. However, charging the material to a high voltage (4.6 V) is a huge challenge for commercial electrolyte. high-voltage electrolyte additives where then used to stabilize the performance of the electrode since this material shows different charge and discharge behavior from the conventional cathode. It is believed that the high energy composite releases a gas during the first charge which may affect the integrity of the electrode. Therefore, a new binder with high binding strength is neededto hold the electrode together. The packing density of the high-energy composite layered cathode must also be improved, which was described in a previous report. Overall, there are three major tasks:

- Investigate High high-voltage electrolyte additive to improve the performance of the high-energy composite material.
- Investigate carboxy-methyl cellulose **(**CMC) binder to improve the performance of the high-energy composite material.
- Modify the precursor fabrication process to improve the strength of the powder and tap density. In the past, the precursor was prepared by the carbonate process using

the co-precipitation method. Currently, we use the hydroxide process to prepare spherical metal hydroxide precursor.

Milestones:
Kilogram levels of Co-free high-energy cathode material ($Li_{1.2}Ni_{0.3}Mn_{0.6}O_{2.1}$) were prepared at Argonne, and cathodes of this material were used in pouch cells to complete the following milestones:

a) Determine the electrochemical performance of a $Li_{1.2}Ni_{0.3}Mn_{0.6}O_{2.1}$/graphite full cell with Hfip high-voltage electrolyte additive cycled at room temperature and high temperature. Hfip additive could improve the performance at high temperature (ongoing).

b) Determine the stability of the high-energy electrode using CMC and conventional polyvinylidene fluoride (PVDF) binders (ongoing).

c) Use hydroxide process for preparing the metal hydroxide precursor (ongoing).

Financial data:
Total project funding
– DOE share: $300K

PROGRESS TOWARD MILESTONES

Summary of work in the past quarter related to milestone (c).
One of the main reason behind moving to the hydroxide process in the making of the high energy material is the cracking of the particle that are made by the carbonate process, especially during the calendaring of the electrodes as shows in Fig. 1. This cracking of the particle is caused by the large porosity inside particle when the carbonate process is used (Fig.2). The material shows high surface area of 5.5 m^2/g and a porosity of 16.5% (see table 1)
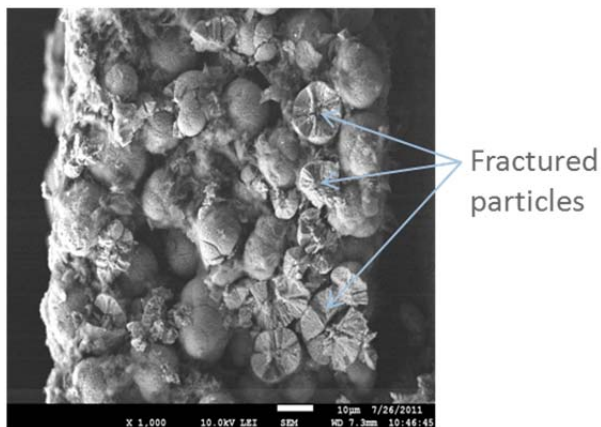

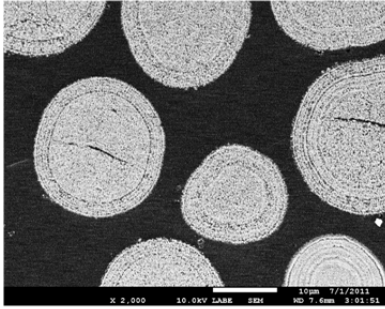Figure 1. SEM images of high energy electrode made by the carbonate process.

Figure 2 Cross section of high energy cathode particles made by the carbonate process.

BET	$Li_{1.14}Ni_{0.29}Mn_{0.57}O_2$ Carbonate process
Surface area	5.5 m^2/g
Average pore size	14 nm
Pore volume	3.766e-02 cc/g
Porosity (particle level, calculated)	16.5%

Table 1 physical characteristics of high energy material prepared by carbonate process

Fig.3 shows the SEM image of a high energy electrode made from the hydroxide process. The active particle in the electrode remains intact after repeated calendaring of the electrode. This positive result is caused by the fact that the porosity of the particles is 6.6% which is far much less than that of particles made by the carbonate process. As a result, the surface area of the material made by hydroxide process is smaller (3.8m^2/g)
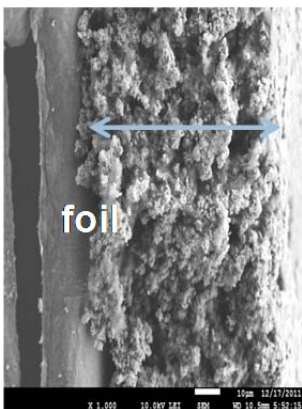

Figure 3. SEM images of high energy electrode made by hydroxide process.

BET	$Li_{1.14}Ni_{0.29}Mn_{0.57}O_2$ From hydroxide precursor
Surface area	3.862 m²/g
Average pore size	8 nm
Pore volume	1.582e-02 cc/g
Porosity (particle level, calculated)	6.6%

Table 2 physical characteristics of high energy material prepared by the hydroxide process

Fig 4 shows the initial charge and discharge as well as cycling performance of cells made from high energy cathode made by the carbonate and hydroxide process. Both materials show high capacity of 250~260mAh/g during the initial cycling. The cell based on material made by the hydroxide process shows higher first cycle efficiency. At C/3 cycling, both material shows over 200mAh/g with good cycle life.

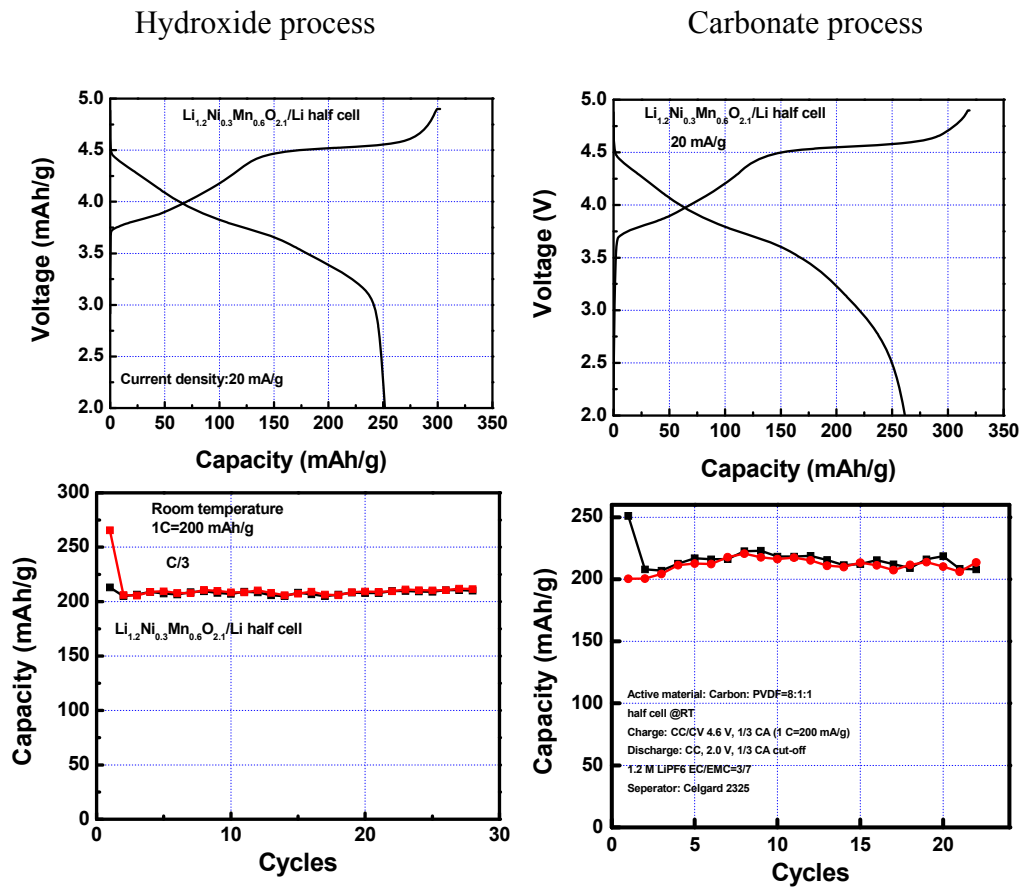Hydroxide process   Carbonate process

Figure 4 first charge and discharge cycle and capacity vs cycling tie of cells based on cathodes made by the hydroxide and the carbonate process.

Fig. 5 compares the rate performance of cells made by cathodes from hydroxide and carbonate processes. At high rate (1C and 2C rate), the cell based on cathode made by the hydroxide process shows higher capacity than that of cells made by the carbonate process.
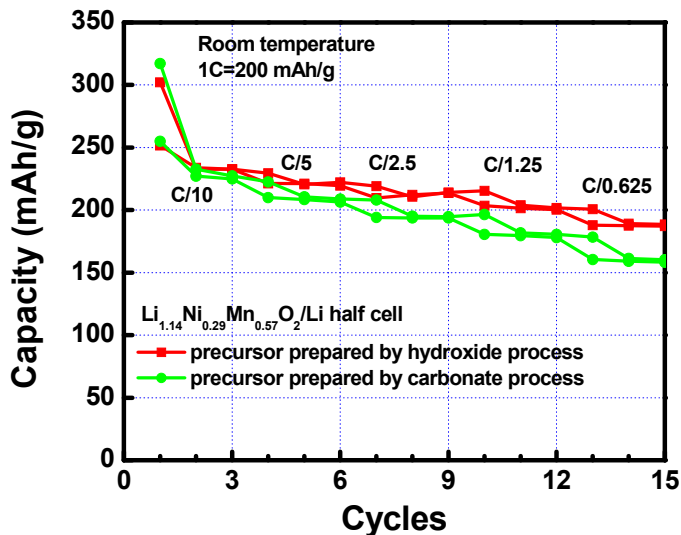

Figure 5 Rate performance of cells based on cathodes made by hydroxide and carbonate process

Fig.6 compares the DSC of charged high energy cathode made by hydroxide and carbonate process. Both electrodes show very high onset temperature of over 250°C. However, a close look at the onset temperature shows that the charged cathode made from hydroxide process has slightly higher onset temperature (265°C) than that made from carbonate process (250°C). In addition the overall heat from the cathode made by the hydroxide process was lower. This is because the hydroxide process yielded lower surface area than the carbonate process which means that less active material is reacting with the electrolyte.
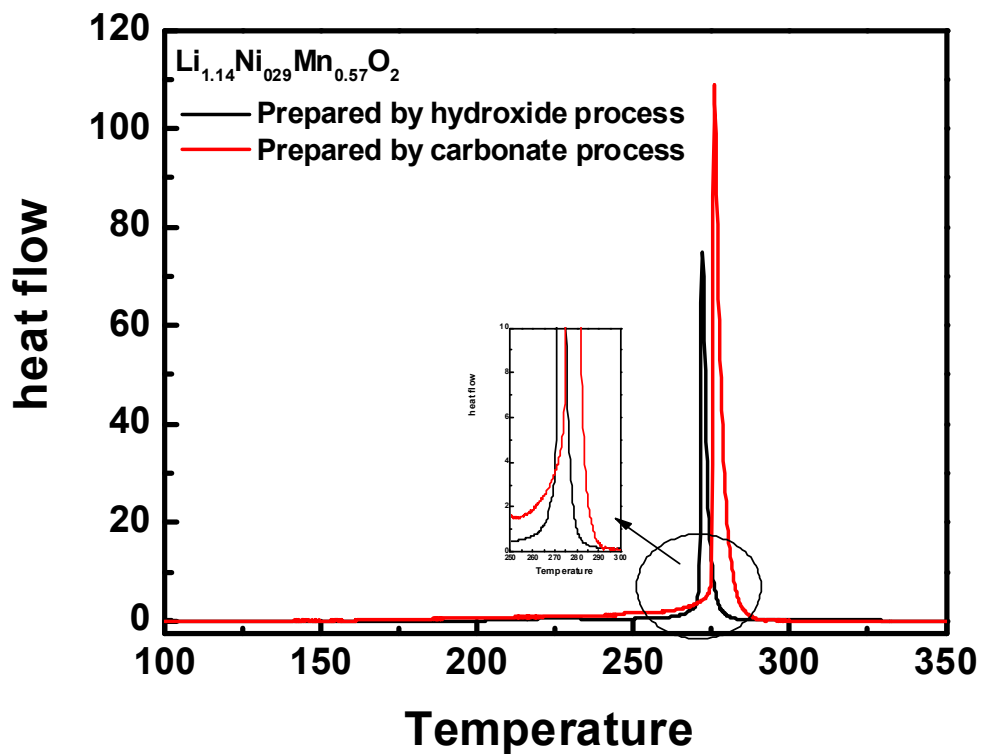
Figure 6. DSC of charged cathodes made by the hydroxide and the carbonate process

Publications, Reports, Intellectual property or patent application filed this quarter. (Please be rigorous, include internal reports--invention records, etc.)
No publications, reports, or patents were submitted this quarter.

TASK 1
Battery Cell Materials Development

Project Number: 1.1B (ES016)

Project Title: New High Energy Gradient Concentration Cathode Material

Project PI, Institution: Khalil Amine, Argonne National Laboratory

Collaborators (include industry): Gary Koenig and Ilias Belharouak, Argonne National Laboratory; Prof. Yang-Kook Sun, Hanyang University; ECPRO; TODA

Project Start/End Dates: October 1, 2008-September 30, 2014

Objectives: Develop a high energy cathode material for PHEV applications that provides over 200 mAh/g reversibly capacity, good rate capability, excellent cycle and calendar life, and good abuse tolerance. The cathode material capacities being investigated have capacities exceeding 200 mAh/g, which exceeds that of the NMC baseline.

Approach: Our approach is to develop a general synthetic method to tailor the internal composition gradient in cathode particles. This will be achieved by depositing a gradual composition gradient throughout particles to suppress stress during lithium intercalation and diffusion. We also aim to further enrich materials in Mn at the surface to enhance safety.

Milestones:

a) Develop a model to predetermine the concentration gradient in particles produced via co-precipitation. This is necessary to have reproducibility of synthesized cathode materials. Complete.

b) Develop a process for precursors with a gradient in transition metal composition that was enriched in manganese. Manganese enriched materials have shown excellent safety and cycle life. Complete.

c) Demonstrate in a proof-of-principle experiment that precursors could be synthesized with predetermined compositional profiles. Complete.

d) Demonstrate high capacity (>200 mAh/g) in final materials produced using the gradient precursors. On schedule

e) Demonstrate that a tailored relative transition metal composition at the surfaces of gradient particles influences safety and cycle life. Complete.

f) Develop hydroxide co-precipitation process at Argonne and implement gradient concentration materials in hydroxide process to achieve higher tap density particles and larger relative core nickel concentrations for increased rate capability and high level of Mn concentration at the outer layer. On schedule.

Financial data: $300K/year

PROGRESS TOWARD MILESTONES (f)

To demonstrate the need of maximizing the concentration of Mn at the outer layer of the particle of the gradient material, we carried out several experiments where we made a) one material with thicker shell 2.3 m) having lower Mn concentration at the outer layer of particle (CSCG B) , and b) an other material with thinner shell (2.1   m) having higher Mn concentration at the outer layer of the particle (CSCGA). Both materials were made using hydroxide process described in the past report.

Fig. 1 represents the EPA result of a cross section of CSCGA and CSCGB particles showing the atomic ratio of Ni, Mn, and Co from the bulk to the surface of the particle. The CSCG-B shows lower Mn (20%) concentration at the surface of particle when compared the CSCG-A material which shows higher level of Mn (37%).
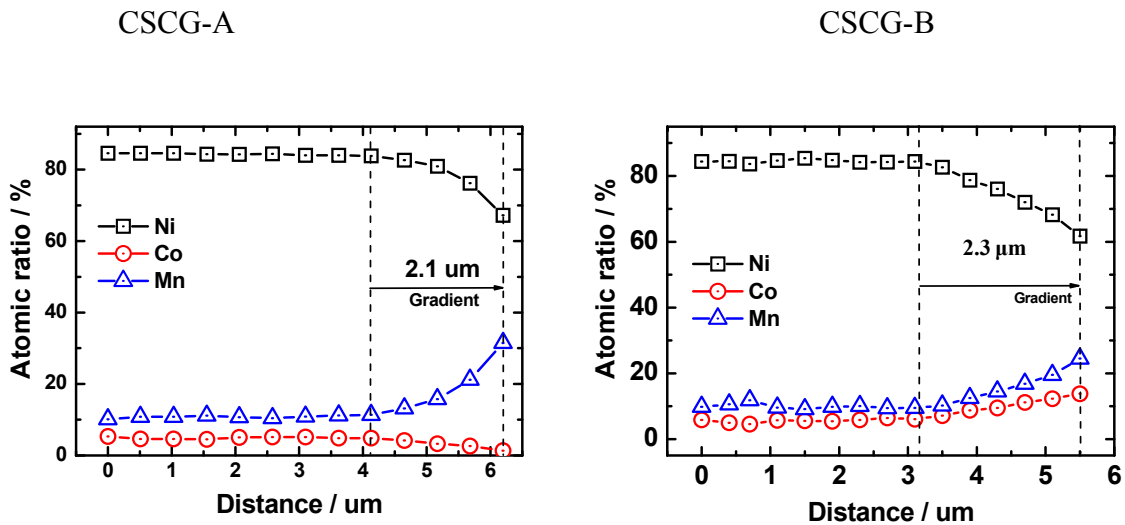
CSCG-A   CSCG-B

Fig.1 EPMA of a cross section of CSCG-A and CSCG-B gradient materials.

Fig.2 shows the cycling performance of the composition of the core ($LiNi_{0.85}Co_{0.05}Mn_{0.1}O_2$), and the gradient materials CSCG-A and CSCG-B. The anode used in this case is lithium metal. All cells were cycled up to 4.4V and 55°C to accelerate any possible degradation at the surface of the particle during cycling. All cells show capacity as high as 220mAh/g but different trend in the degradation process was observed. The core composition shows rapid degradation of the capacity with cycling with 40% capacity fade after only 50 cycles. The cells based CSCG-A shows far much better capacity retention because of the existence of high level of Mn at the outer layer

of the gradient material. In this case, the cell lost only 6% capacity after 100 cycle at 55°C. The gradient material with less Mn concentration at the outer layer of the particle (CSCG-B) shows little more degradation upon cycling when compared to CSCG-A. In this case, the cell lost 16% capacity after 100 cycles.
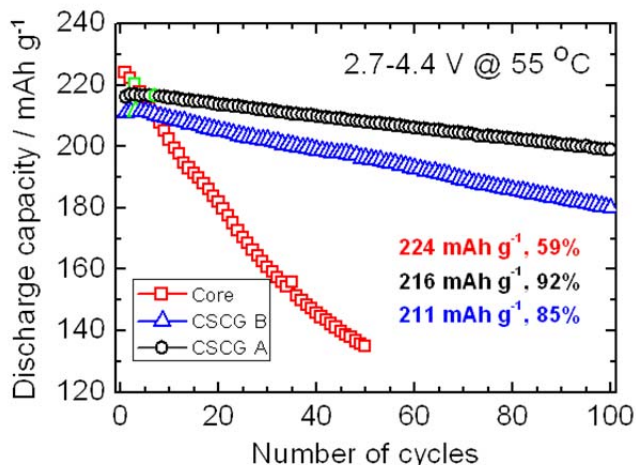

Fig.2 Cycling performance of cells based on core composition, CSCG-A and CSCG-B gradient materials at 55°C.

Fig. 3 shows the AC impedance during cycling of cells based on the core composition, the CSCG-A and CSCG B. While the core shows significant growth of the interfacial impedance during cycling, both gradient materials show far much less increase in the interfacial impedance of their corresponding cells. The cell based on CSCG-A shows the least increase in the interfacial impedance when compared to the cell based on CSCG-B. This is because the CSCG-A has higher concentration of Mn at the outer layer of the particle, which stabilizes the surface of the material and reduces any surface reactions with the electrolyte.
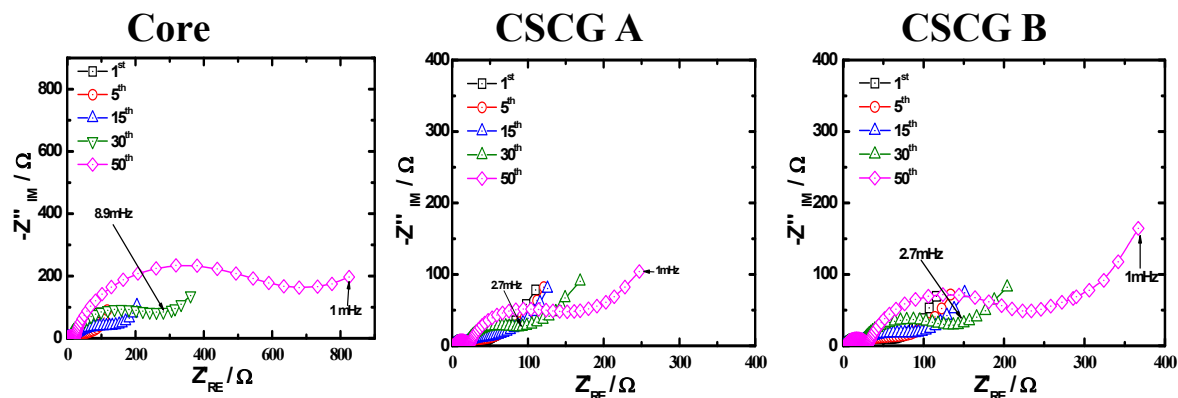

Fig.3 AC impedance of cells based on core composition, CSCG-A and CSCG-B gradient materials.

Fig.4 shows the DSC of the charged core, CSCG-A and CSCG-B in the presence of 1.2MLiPF$_6$/EC:EMC. The Charged core shows an onset temperature of reaction of 200°C with large heat generation caused by the instability of Ni^{4+} that reducesto Ni^{2+}, leading to oxygen release which oxidizes the electrolyte. The charged CSCG-A and CSCG-B shows higher onset temperature of 240°C and lower heat generation due the stable Mn4+ at the surface of the particles. The CSCG-A shows lower heat generation than CSCG-B, because of the high degree of Mn at the surface of this material. From all these studies, it is clear that high Mn level at the surface of the gradient particle will lead to better cycling and improved safety. Our next step is to maximize the ratio of Mn in the full gradient to at least 50%. This will result in operating reversible at 4.5 V which can lead to capacities as high as 240mAh/g
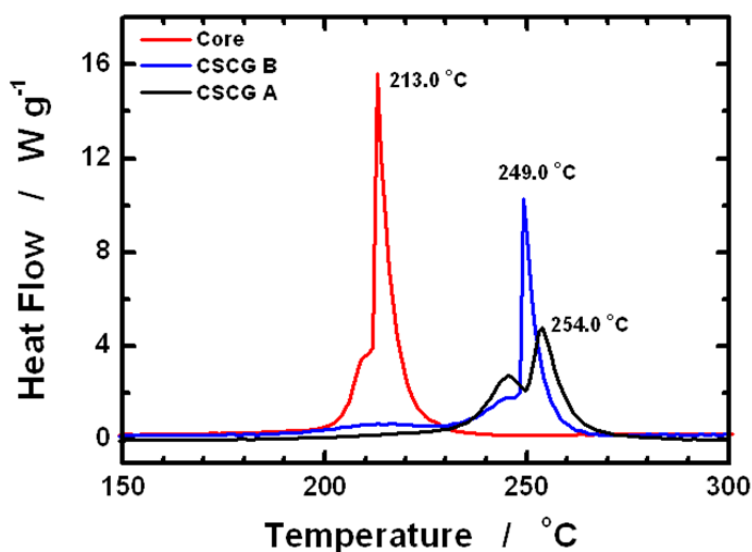

Fig.4 DSC of charged Core, CSCG-A and CSCG-B gradient materials in the presence of 1.2MLiPF6/EC:EMC (30:70)electrolyte.

Publications, Reports, Intellectual property or patent application filed this quarter.
Publication in preparation
High energy cathode material for lithium battery.
Nature Material, 2012, (under revision)

TASK 1
Battery Cell Materials Development

Project Number: 1.1G (ES019)

Project Title: Development of High-Capacity Cathode Materials with Integrated Structures

Project PI, Institution: Michael Thackeray, Argonne National Laboratory

Collaborators (include industry):
Donghan Kim, Giselle Sandí, Argonne National Laboratory
Peter Chupas, Karena Chapman, Matthew Suchomel, APS, Argonne National Laboratory
Yang Shao-Horn, Chris Carlton, Massachusetts Institute of Technology

Project Start/End Dates: October 2009/September 2014

Objective: The objective of this work is to develop low cost Li- and Mn-rich cathode materials with integrated structures that offer good thermal stability, high capacity (~240 mAh/g), good rate capability (≥200 mAh/g at C/1 rate) and high first-cycle efficiency. The targeted performance values are 240 mAh/g of reversible capacity and a first-cycle efficiency of at least 85%. If successfully developed, the energy density of a cell coupled with graphite would be ~460 Wh/kg (assuming 300 mAh/g graphite, 3.7 V nominal).

Approach: 'Layered-layered' composite cathode materials, $xLi_2MnO_3 \bullet (1-x)LiMO_2$ (M=Ni,Co,Mn) can deliver a high capacity of 240-260 mAh/g. However, these materials have drawbacks such as low first-cycle efficiency, voltage fade on cycling, transition metal dissolution and poor power performance. The concept of embedding a spinel component into 'layered-layered' structures is being exploited to improve their electrochemical properties and cycling stability. Studies of blending $xLi_2MnO_3 \bullet (1-x)LiMO_2$ with high-power cathode materials, such as $LiFePO_4$, are being continued to improve impedance at low states of charge.

Milestones:
(a) Optimize the chemical composition of 'layered-layered-spinel' electrodes, including coatings such as AlF_3;
(b) Characterize 'layered-layered-' and 'layered-layered-spinel' electrodes to determine, in particular, the causes for the voltage fade phenomenon;
(c) Identify performance degradation mechanisms, particularly voltage fade phenomena in structurally-integrated 'layered-layered-spinel' electrodes;

Financial data: $400K

PROGRESS TOWARD MILESTONES

Summary of work related to milestone (a)

The concept of embedding a spinel component into composite $xLi_2MnO_3\bullet(1-x)LiMO_2$ (M=Mn, Ni) 'layered-layered' structures to improve their electrochemical properties and cycling stability is being exploited. In this project, efforts are focused predominantly on the preparation and electrochemical characterization of three-component 'layered-layered-spinel' electrodes, synthesized, for example, by lowering the lithium content of a parent 'layered-layered' $0.3Li_2MnO_3\bullet0.7LiNi_{0.5}Mn_{0.5}O_2$ material (and Mg-substituted derivatives) while maintaining a Mn:Ni ratio of 0.65:0.35; such compounds can be designated generically by the system, $Li_xNi_{0.35}Mn_{0.65}O_y$, for which the end members are $0.3Li_2MnO_3\bullet0.7LiNi_{0.5}Mn_{0.5}O_2$ (x=1.3; y=2.3), in which the average manganese and nickel oxidation states are 4+ and 2+, respectively, and $LiMn_{1.3}Ni_{0.7}O_4$ (x=0.5; y=2) in which the corresponding average oxidation states are expected to lie between 4+ and 3.77+ for Mn, and 2.57+ and 3+ for Ni, respectively. In particular, Mg-substituted cathode materials with composition $Li_{1.25}Mn_{0.65}Ni_{0.33}Mg_{0.02}O_y$ were synthesized and targeted to contain

Figure 1: Effect of coating time on spinel content for $Li_{1.25}Mn_{0.65}Ni_{0.33}Mg_{0.02}O_y$ samples coated with AlF_3 at pH=4

6% spinel. In order to stabilize the surface and to suppress Mn dissolution, samples were coated with AlF_3 at different stirring times. After acidic treatment (pH=4), however, the content of spinel increased to 27%, corresponding to '$Li_{1.15}Ni_{0.33}Mg_{0.02}Mn_{0.65}O_y$'. Thus, coating under acidic conditions increased the spinel content and decreased the capacity relative to uncoated 'layered-layered-spinel' samples. Figure 1 shows the effect of coating time on the spinel content; calculations were based on electrochemical, elemental analysis, and spectroscopic data. Further studies will be focused on optimizing the spinel content by controlling the surface characteristics of these composite cathodes. Electrochemical evaluations of the electrode materials in full cells and DSC experiments at various states of charge are currently being undertaken.
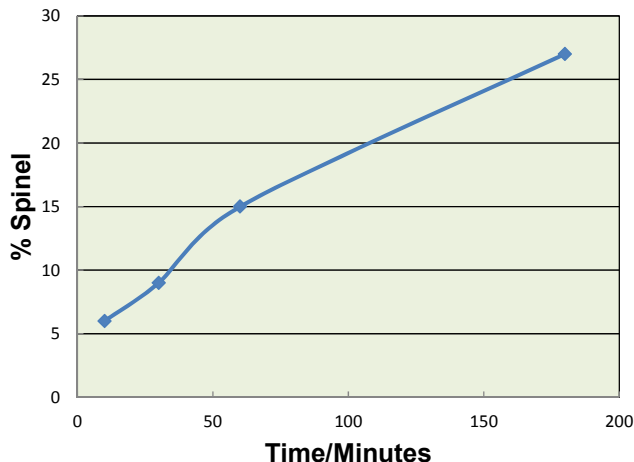
Summary of work related to milestone (b)

Electrodes with the composition $Li_{1.44}Ni_{0.219}Co_{0.125}Mn_{0.656}O_{2.44}$ (alternatively, in composite notation, $0.44Li_2MnO_3\bullet0.56LiNi_{0.39}Co_{0.22}Mn_{0.39}O_2$) were synthesized and electrochemically monitored to evaluate the voltage fade phenomenon when cells were cycled over different voltage windows. During the activation cycle (Fig. 2), half cells were charged to 4.6 V and discharged to 2.0 V at a 15 mA/g rate, yielding a 84% first-cycle efficiency. Extended cycling was performed under the same conditions. From the 3rd to 20th cycle, the capacity decreased from 275 mAh/g to 250 mAh/g and voltage

decay was evident (Fig. 3). Electrochemical testing was also performed with a reduced voltage window, from 4.4 to 2.0 V (Fig. 4); although the cathode capacity was lowered to 215 mAh/g, it was compensated by enhanced cycling stability but not by any significant suppression of the voltage fade for this Mn-rich composition.
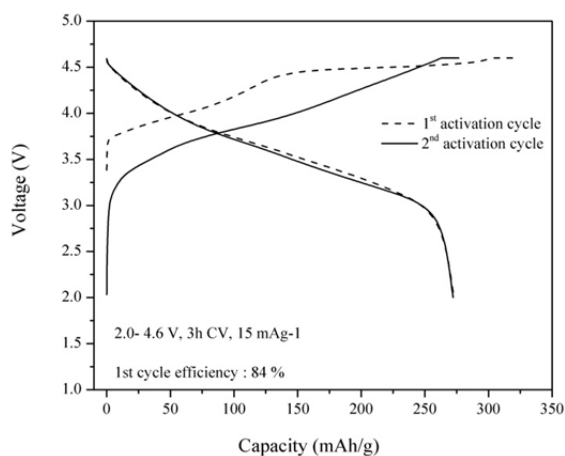

Figure 3: Activation of a $Li_{1.44}Ni_{0.219}Co_{0.125}Mn_{0.656}O_{2.44}$ cathode when charged and discharged between 4.6 and 2.0 V at 15mA/g.
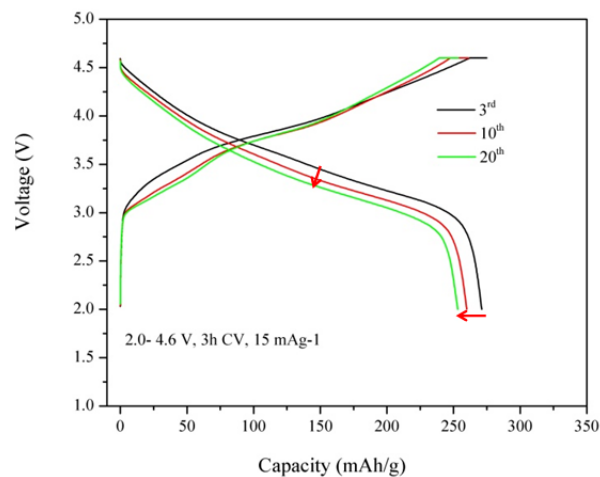

Figure 2: Cycling of the same cathode as in Figure 2 under the same electrochemical conditions. (Cycles 3, 10 and 20 shown)
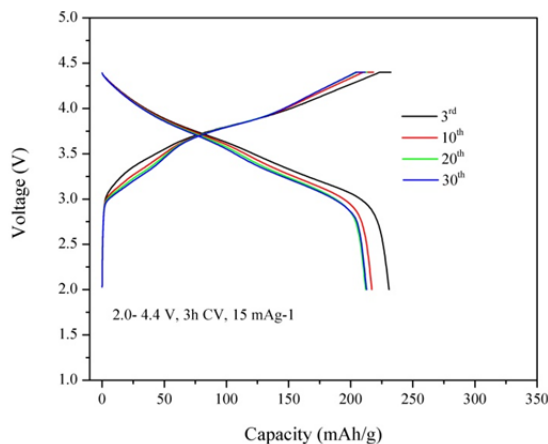

Figure 4: Cycling of the same cathode as in Figure 2 between 4.4 and 2.0 V at 15 mA/g. (Cycles 3, 10, 20 and 30 shown)

Summary of work in the past quarter related to milestone (c)
Studies of the voltage decay phenomenon exhibited by 'layered-layered' lithium-metal-oxide cathode materials, using high-resolution X-ray diffraction (HRXRD) and pair-distribution function (PDF) analytical techniques were continued at the Advanced Photon Source using the composition, $0.5Li_2MnO_3 \cdot 0.5LiCoO_2$, annealed at temperatures ranging from 450 to 950 °C. Preliminary HRXRD and PDF data suggest the formation of a "layered-layered" composite structure at 750 °C from a 'layered-spinel' precursor, which is synthesized at lower temperature. Structural refinements before and after cycling and correlations to electrochemical performance are expected to provide

valuable insights into the formation and electrochemical behavior of these highly complex electrode materials. This project is a work-in-progress.
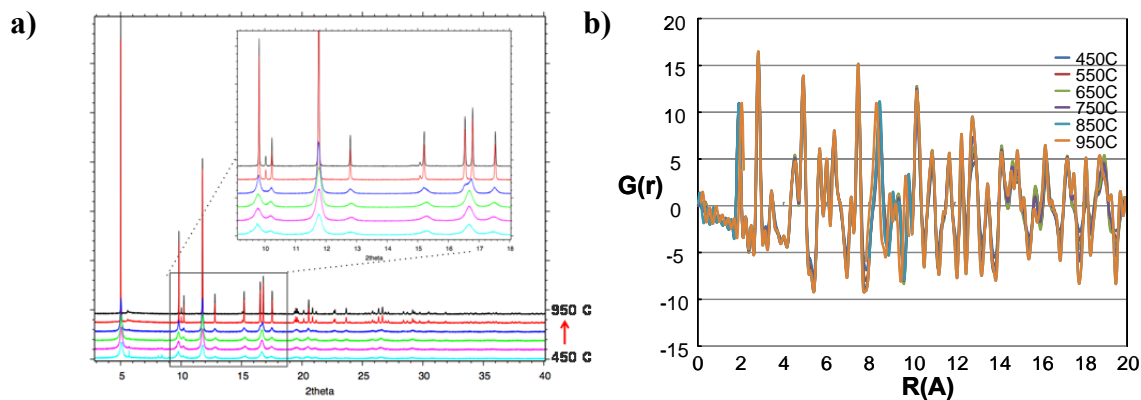

Figure 5: a) X-ray powder diffraction patterns and b) PDF spectra of 0.5Li₂MnO₃•0.5LiCoO₂, annealed at 450, 550, 650, 750, 850, and 950 °C.

TASK 1
Battery Cell Materials Development

Project Number: 1.1C (ES020)

Project Title: Developing High Capacity, Long Life anodes

Project PI, Institution: A. Abouimrane and K. Amine Argonne National Laboratory

Collaborators (include industry):
- B. Liu, D. Dambournet (CSE/ANL).
- P. Chupas, K. Chapman, Y. Ren Advanced Photon Source, (APS/ANL).
- Z. Fang (University of Utah).
- FMC, Northwestern University,

- **Project Start/End Dates:** October [1st], 2009/September 2014

Objectives:
- ❑ Develop new advanced high energy anode materials with long life and improved Safety for PHEV and EV applications
- ❑ Develop a low cost synthesis methods to prepare high energy anodes
- ❑ Full structural and electrochemical characterizations of the prepared anode materials.
- ❑ Demonstrate the applicability of these anodes in half and full cells systems.

.

Approach:
- ❑ MO-$Sn_xCo_yC_z$ (MO=SiO, SiO_2, SnO_2, MoO_2, GeO_2) anode materials were selected for investigation as high energy anode based on the following criteria:
  - SnxCoyCz alloys are known to provide a capacity of 400-500mAh/g for hundreds of cycles.
  - MO anodes are known to provide more than 1000 mAh/g with poor cyleability.
  - The formation of $Sn_xCo_yC_z$ and MO composite could lead to the increase in the capacity, reduce the amount of cobalt in the material and improve the cyleablity as SnxCoyCz play the role of buffers against the volume expansion of MO.
  - This anode system is more safer than the graphite and possess low potentials in the range of 0.3-0.75V (expect high voltage cells when combined with high cathodes)

Milestones:

1- Prepare materials with at least 800 mAh/g capacity with cycleability more than hundred cycles (2011-2012);
2- Identify the best material in term of cost, voltage output, cycling performance, and deliverable capacity (2011-2012);
3- Prepare a scalable amount of anode material (~ 200 grams) with 800 mAh/gas capacity for 100 cycles (2012);
4- Deliver a full cell battery (coin cell configuration) with a least 420 Wh/kg energy density (when combined with NMC) (2013-2014);

Financial data: Project budget/year, amount subcontracted if appropriate
300K/year

PROGRESS TOWARD MILESTONES

(a) Summary of work in the past quarter related to milestone (1)

We used ultra-high energy ball milling (UHEM) and SPEX milling methods to prepare $SiO-Sn_{30}Co_{30}C_{40}$ anode materials. UHEM, as compared with SPEX milling, showed remarkably more-reversible specific capacity, excellent cycling performance, and good rate capability. The UHEM sample powder had a particle size distribution whose main peak was located at ~2 μm, and the 50% cumulative particle size was less than 2.5 μm. The SPEX sample had 50% particles smaller than ~13 μm, which was much larger than that of the UHEM sample. This millstone is achieved now at 100%.

(b) Summary of work in the past quarter related to milestone (2)

We have successfully prepared three anodes materials based $M_aO_b-Sn_xCo_yC_z$ (where MO: SiO, MoO_3, GeO_2). Based on the price and the voltage profile and for industrial application our work will focus on the cheapest $SiO- Sn_xCo_yC_z$ system. Furthermore, good electrochemical performance was also obtained at high temperature performance. This millstone is achieved now at 100%.

(c) Summary of work in the past quarter related to milestone (3)

250 grams of the material was prepared by ultra-high energy ball milling (UHEM). The material shows ~ 900 $mAhg^{-1}$ under 100 mA/g. The high temperature did not affect the electrochemical performance of the material .As a result, after 100 cycles, the capacity retention was 97.3% for the anode cycled under conditions of 1C at 25ºC, but 91.6% and 90% for the anodes cycled under conditions of 1C at 55ºC and C/3 at 25ºC, respectively. (En schedule) "The progress to this milestone is achieved at 90%".

(d) Summary of work in the past quarter related to milestone (4)

Before evaluating our anode system in full cell, we lithiated our anode and it was cycled with 5V spinel $LiNi_{0.5}Mn_{0.5}O_4$ material. 4.3V battery was delivered with ~115 $mAh.g^{-1}$ based on the cathode weight. Promising cycleability was obtained as no capacity fade was noticed for more than 30 cycles. (En schedule) "The progress to this milestone is achieved at 10%".

FY 2011 Publications/Presentations

1. 2011 DOE Annual Peer Review Meeting Presentation, May 9th-13th 2011, Washington DC.

2. Provisional patent application A. Abouimrane & K. Amine "Anode materials for lithium batteries: ANL-IN-10-013"

3. "A new anode material based on SiO-$Sn_{30}Co_{30}C_{40}$ for lithium batteries" B. Liu, A. Abouimrane, D. Wang, Y. Ren, Z. Fang and K. Amine (submitted paper).

4. New anode materials based on MO-$Sn_{30}Co_{30}C_{40}$ (MO=SiO, SiO_2, SnO_2, MoO_3, GeO_2) for lithium batteries Materials Challenges in Alternative & Renewable Energy, Clearwater FL, Feb. 28th 2012.

5. New anode materials based on MO-$Sn_{30}Co_{30}C_{40}$ (MO=SiO, SiO_2, SnO_2, MoO_3, GeO_2) for lithium batteries. IBA meeting, Waikoloa Village, HW, Jan. 10th 2012.
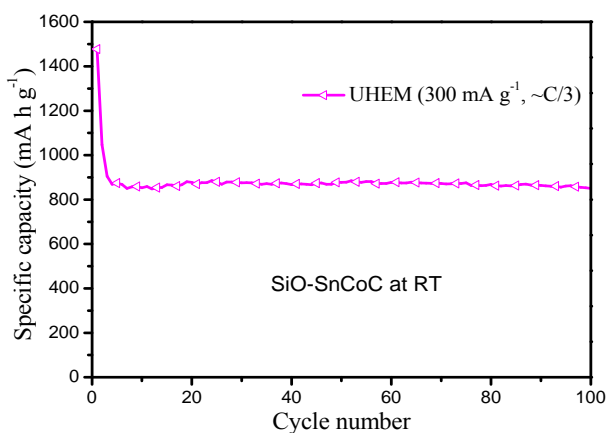
Fig.1 Room temperature cycling performance of SiO-SnCoC/Li half-cell under C/3 current rate.
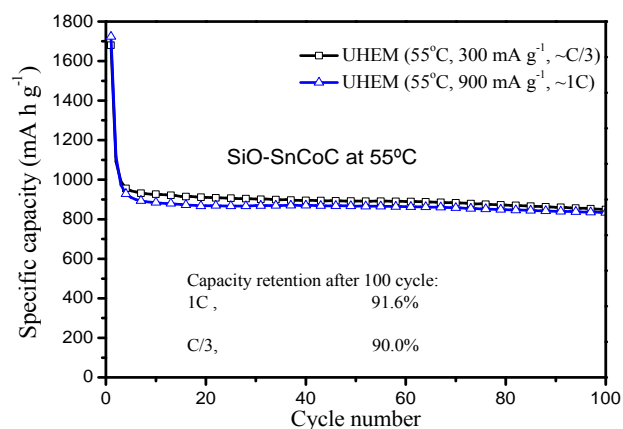

Fig.2 High temperature cycling performance of SiO-SnCoC/Li half-cell under C/3 and 1C current rate.
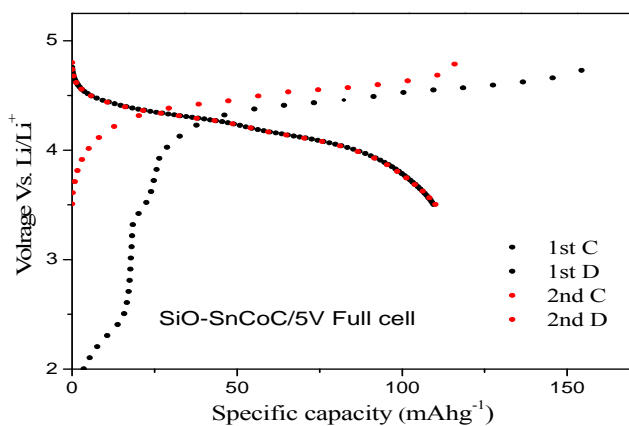

Fig.3 Voltage profile of SiO-SnCoC/ $LiNi_{0.5}Mn_{0.5}O_4$ full cell under 45 mA/g current rate.

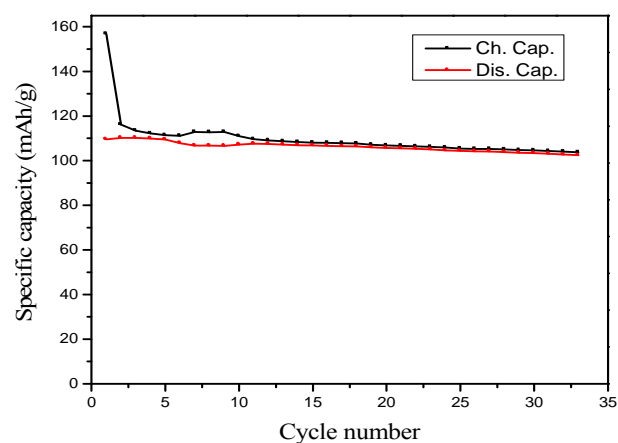**Fig.4** Cycling performance of SiO-SnCoC/ $LiNi_{0.5}Mn_{0.5}O_4$ full cell under 45 mA/g current rate.

TASK 1
Battery Cell Materials Development

Project Number: ES024

Project Title: High Voltage Electrolytes for Li-ion Batteries

Project PI, Institution: T. Richard Jow/Kang Xu, U.S. Army Research Laboratory

Collaborators (include industry): Dr. Jan L. Allen, Dr. Oleg Borodin, Dr. Arthur von Cresce, Army Research Laboratory; Y. F. Lam, U. of Maryland; Lidan Xing, U. of Utah; K. Amine, D. Abraham, D. Dees, ANL

Project Start/End Dates: June 2011 / May 2014

Objectives: Develop high voltage electrolytes that enable the operation of 5 V Li Ion Chemistry. With a 5-V high voltage electrode materials and a capacity similar to that of the state-of-the-art cathode, the energy density will be increased more than 25% than that of the-state-of-the-art Li-ion batteries for HEV/PHEV. Our other objective is to understand the surface chemistry at the high voltage cathode and electrolyte interface through surface characterization and computational effort. With better understanding, better electrolyte components and cathode materials can be developed.

Approach: Three approaches were taken.
1. **Develop additives for carbonate based solvents for high voltage cathodes**
    a. Search additives that would decompose and form protective interface on cathode
    b. Formulate electrolytes using fluorinated phosphate ester as additives for the state-of-the-art electrolytes
2. **Characterize interfacial chemistry at the cathode/electrolyte interface**
    a. Use high resolution XPS
    b. Use mass spectroscopy method, NMR, AFM, etc
3. **Computational effort**
    a. Understand oxidative stability of solvents/electrolytes
    b. Understand reactive pathways of additives and electrolytes
    c. Develop ability to predict and design electrolyte components

Milestones:
 (a) Explored new additives for high voltage cathodes (June 2012)
 (b) Evaluate electrolytes with additives in both half cells and full cells (Dec 2012)
 (c) Diagnostic studies: surface characterization and SEI chemistry (Dec 2012)
 (d) Understand reactive pathways of electrolyte components through computational effort (June 2012)
 (e) Develop stable high voltage cathodes and understand their electronic structures (Dec 2012)

Financial data: $250,000/year

PROGRESS TOWARD MILESTONES

(a) Perfluorinated new additives for the interphase on cathode/electrolyte
Two new additives directions were considered. One is perfluorination and the other is phosphazene. As shown in Fig. 1, higher degree of fluorinatedphosphates help the capacity retention. The structure of HFiP, phosphazene and perfluorinated HiFP, PFBP, are are shown in Structures S1-S3, respectively. In collaboration with Drs. X.Q. Yang and H.S. Lee of BNL, perfluorinated additive PFBP with structure S3 was synthesized.
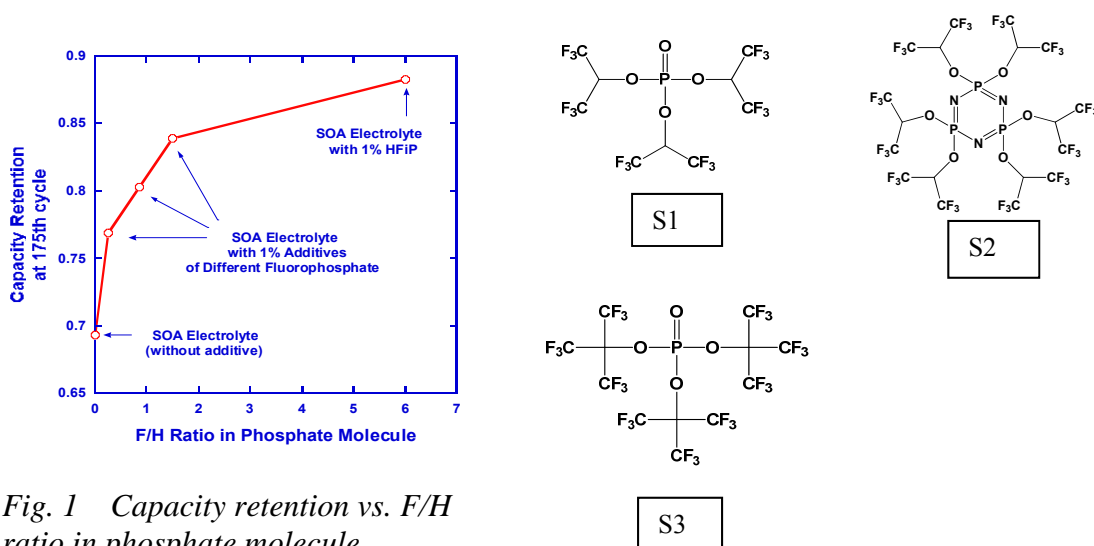

Fig. 1   Capacity retention vs. F/H ratio in phosphate molecule.

The baseline electrolyte made of 1.2 m $LiPF_6$ in EC:EMC (3:7 wt. ratio) with the additive PFBP was tested in full cells made of $LiNi_{0.5}Mn_{1.5}O_4$ cathode and graphite anode (A12), both received from Argonne National Laboratory. The capacity retention as a fundtion of cycle life is plotted as shown in Fig. 2. The same plot for the baseline electrolyte was included for comparisons. In the baseline electrolyte, the cell capacity lost more than 50% of the capacity in 200 cycles. In the electrolyte with the PFBP, the cell capacity lost only 10% in 200 cycles. The coulombic efficiency as shown in the insert of Fig. 2 reached 99.8% in 200 cycles from 99% in initial cycles.

(b) Double intercalation in graphite electrodes
The concept of double intercalation, in which Li cation is intercalated into graphite anode and anion is intercalated into graphite cathode at the same time, was introduced in 1990s by Jeff Dahn but was not realized due to the lack of electrolyte allowing the anion intercalation that occurs at voltages close to 5 V. The electrolyte with the PFBP additive, which enables the stable operation to 5 V, makes the double intercalation into graphite possible as shown in Fig. 3.
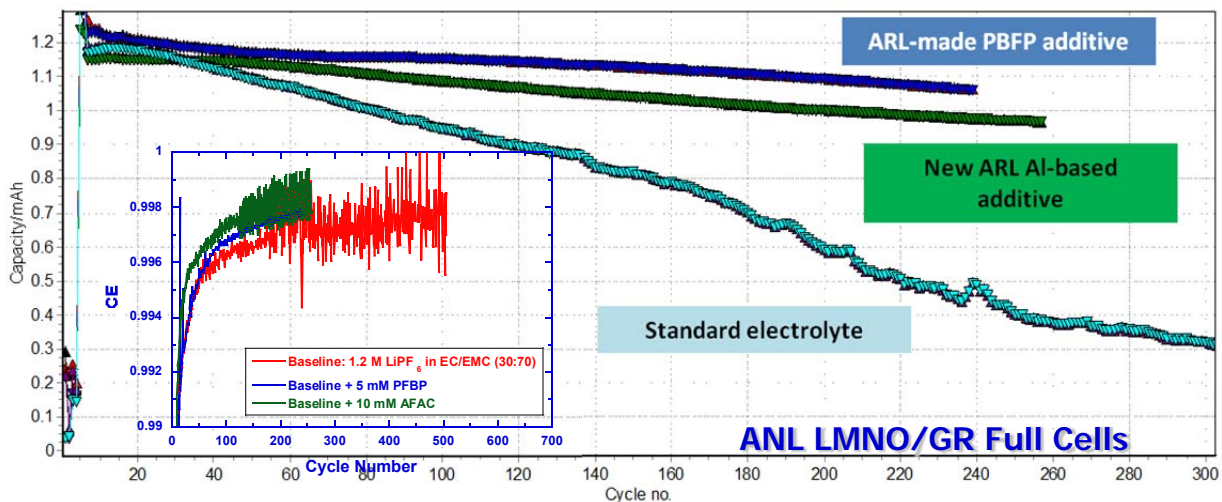
Fig. 2   Discharge capacity of LiNi$_{0.5}$Mn$_{1.5}$O$_4$/Graphite full cell (electrodes provided by ANL) versus cycle number in electrolytes including standard baseline electrolyte, baseline electrolyte with new ARL Al-based additive and baseline electrolyte with PBFP additive.
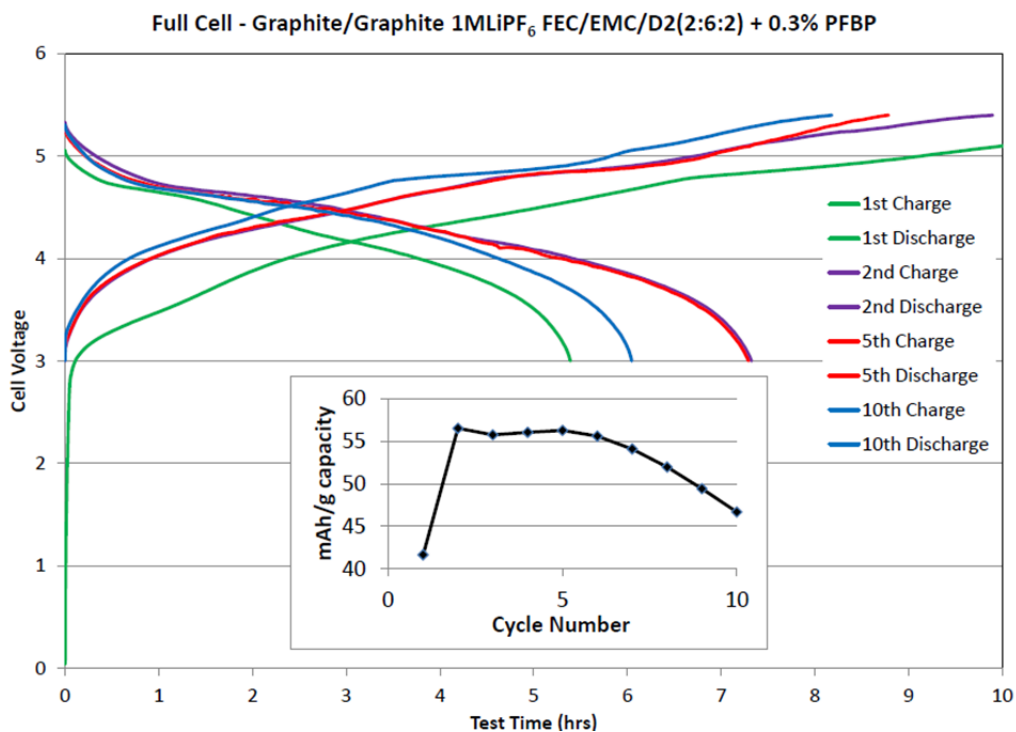
Fig. 3   Cell charge and discharge voltage profiles versus cycle number for a cell made of Graphite/Graphite in 1M LiPF$_6$ in FEC/EMC/D2 (2:6:2) with 0.3% PFBP. The cell capacity as a function of cycle number is shown in the insert.

(c) Modeling of dilithium ethylene dicarbonate, Li$_2$EDC, a SEI component

In order to address the origins of interfacial impedance on the negative electrode MD simulations were performed on the Li$_2$EDC (Li(O$_2$COCH$_2$))$_2$ melt that commonly found in the anode SEI. Initial simulations of the Li$_2$EDC | EC:DMC(3:7)/LiPF$_6$ interface were performed. The revised force field for Li$_2$EDC and Li$_2$DBC (Li(O$_2$COCH$_2$CH$_2$))$_2$ was developed in a manner consistent with APPLE&P force field for EC:DMC/LiPF$_6$ electrolytes.[1-2] MD simulations were conducted on Li$_2$EDC in the crystal-like phase and amorphous (disordered) phase as shown in Figure 4. The crystal was orthorhombic in agreement with experimental data. The disorderered (amorphous) phase is expected to form during fast deposition of Li$_2$EDC from electrolyte on the electrode or due presence of impurities. MD simulations indicated that the average conductivity of the molten (amorphous) and crystalline phases are similar. The conductivity from MD simulations extrapolated to room temperature was found around 10^{-9} S/cm, which is in excellent agreement with the Li$_2$EDC conductivity of ~10^{-9} S/cm estimated by Phil Ross group as reported in the BATT program 2006 report. We conclude that the revised force field predicted Li$_2$EDC conductivity in better agreement with experimental data than the previous FF06 force field (shown in pink in Figure 4) and the revised force field should be used for future studies of SEI compounds.
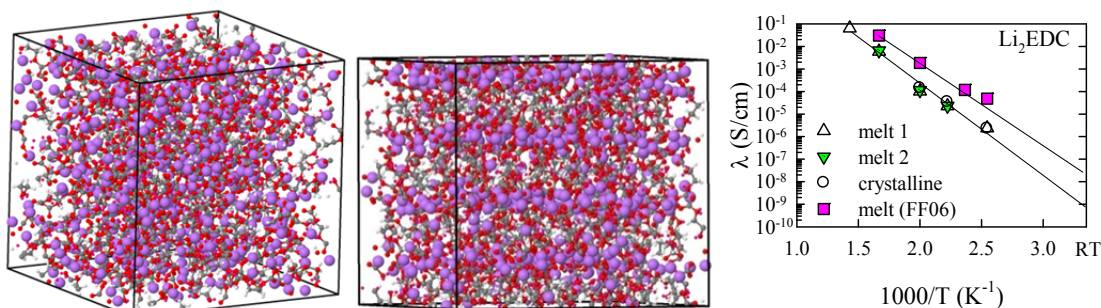

Fig. 4   Snapshot from MD simulations of Li$_2$EDC of the amorphous (molten phase) and crystalline phases (lithium are highlighted as pink balls). Conductivity of Li$_2$EDC melts 1 and 2 from two independent simulations and crystalline Li$_2$EDC from MD simulations is shown on the right. Results from MD simulations using previous force field FF06 are also shown for comparison (pink squares).

Fits to the temperature dependent conductivity of Li$_2$EDC yielded activation energy of ~70-80 kJ/mol. Similar activation energy of 68 kJ/mol was found experimentally for the interfacial impedance at the negative graphite electrode in the recent ARL experimental study.[3] Simulations of Li$_2$DBC melts are conducted in collaboration with U. of Utah and BATT program. The activation energy of Li$_2$DBC conductivity was found to be lower that activation energy of Li$_2$EDC conductivity. Simulations of Li$_2$DBC are conducted in collaboration with U. of Utah and BATT program. The Li$_2$EDC | EC:DMC(3:7)/LiPF$_6$ interface simulations are currently performed and are expected to provide information on the desolvation energies.

(d) Modeling of oxidation induced reactions of electrolyte on non-reactive electrodes

Density functional calculations were utilized to provide understanding of the oxidation induced reactions of the EC:EMC/LiPF$_6$ electrolyte components on non-active electrodes and at Li$_x$CoPO$_4$ surfaces. Oxidation potential of the electrolyte components was calculated as a function of the solvent dielectric constant and is shown in Table 1. We have found that oxidation of EC$_2$ results in a spontaneous transfer of a proton from one EC to another as shown in Figure 5. The proton transfer reduces EC oxidation stability compared to the intrinsic oxidative stability of an isolated EC. Similar results were observed for the EC/anion complexes. Predicted oxidation stabilities were found in good agreement with measured values of glassy carbon electrodes.[4-5] The oxidation of EC$_2$ and EC/anion shows different trends as a function of dielectric constant as shown in Table 1 At high dielectric constant solvents, initial oxidation of EC$_2$ is energetically more favorable than oxidation of EC/PF$_6$ and EC/BF$_4$ provided EC$_2$ dimers form at the interface. However, formation of such dimers is relatively improbable at the interfacial layer.

In collaboration with Lidan Xing (U. of Utah) oxidation induced reactions of EC$_2$ were investigates using B3LYP/6-31++G(d) level of theory as shown in Figure 6. The polarized continuum model (PCM) was used to implicitly include the rest of the surrounding solvent. The most exothermic path with the smallest barrier for EC$_2$ oxidation yielded CO$_2$ and ethanol radical cation. The reaction paths with the higher barrier yielded oligo(ethylene carbonate) suggesting a pathway for the experimentally observed poly(ethylene carbonate) formation of EC-based electrolytes at cathodes surfaces and possible pathway for ethylene dicarbonate formation at the anode.[6]. Similar DFT studies of the oxidation reaction were initiated for a number of electrolyte additives.

Table 1　Oxidation potential, V, of electrolyte components corresponding to Fig. 5

	ε=1	ε=4.2	ε=20.5	ε=78.4
(EC)$_2$		6.2	5.9	5.9
EC/BF$_4^-$	4.6	6.0	6.3	6.3
EC/LiBF$_4$	8.7		6.6	
EC/PF$_6^-$	4.9	6.3	6.6	6.6
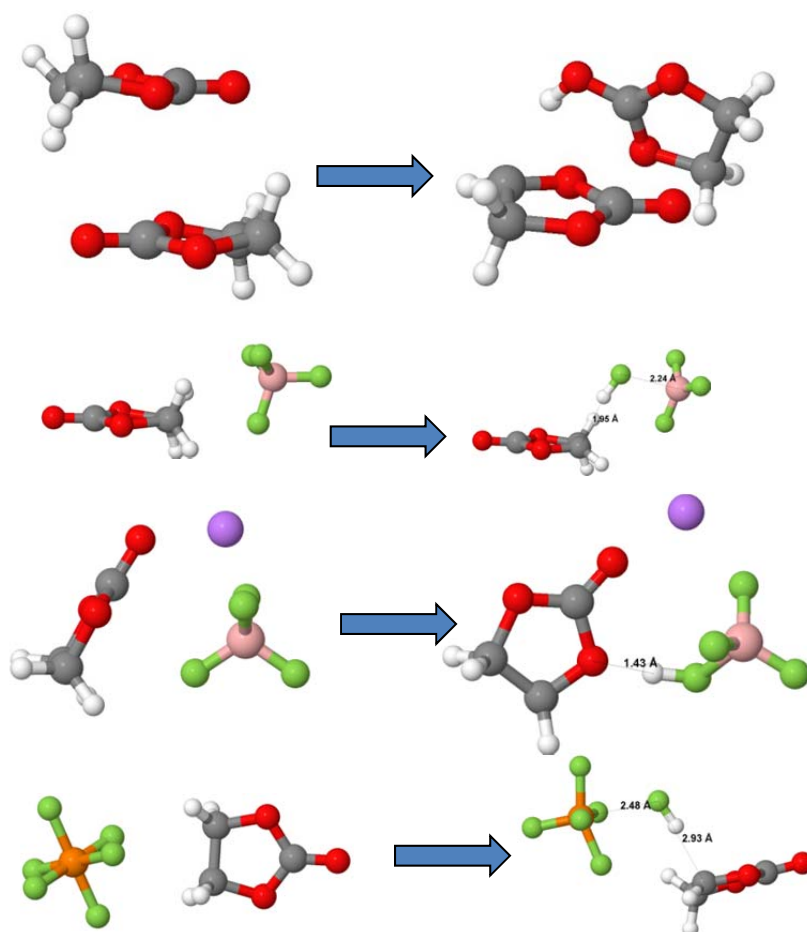
Fig. 5　Initial and oxidized structures from M05-2X/cc-pvTz DFT calculations.
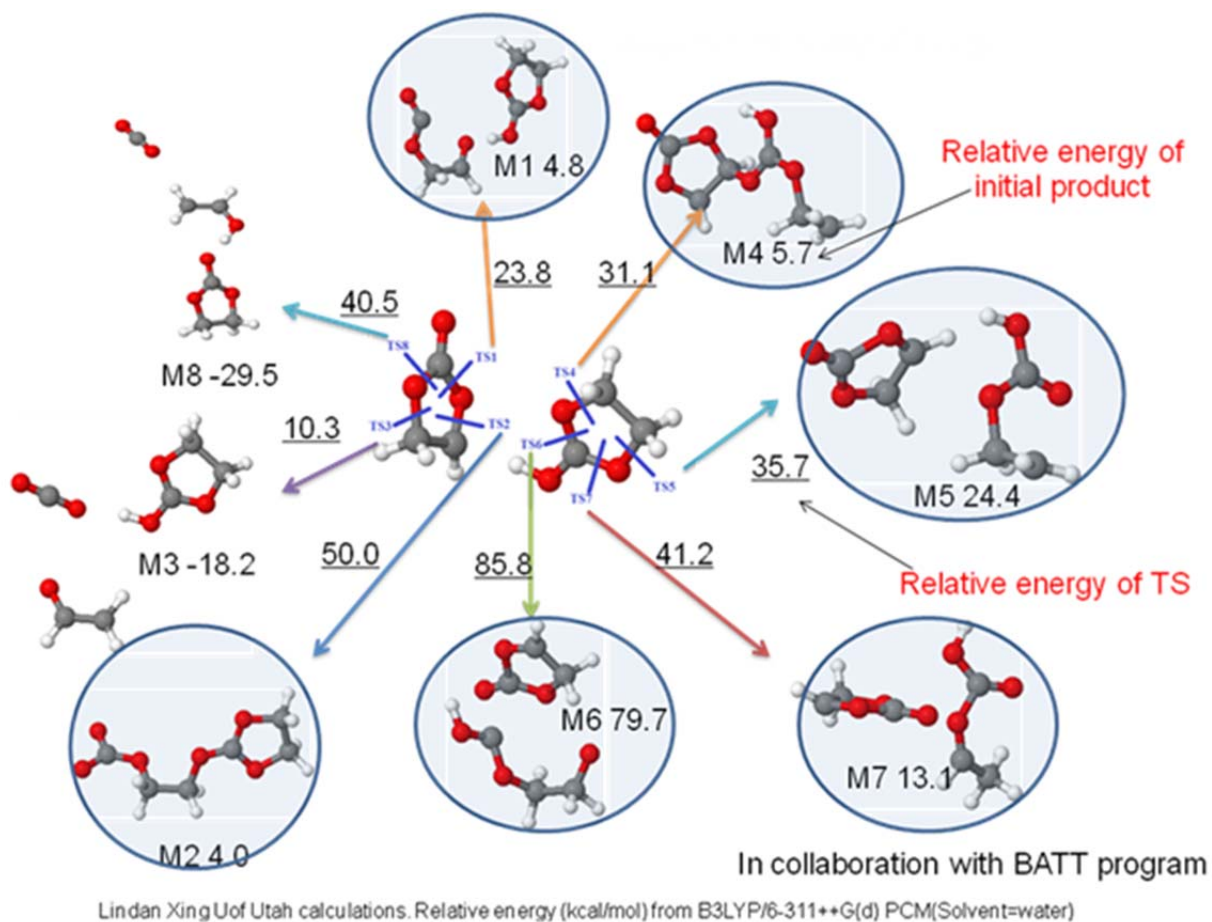
Fig. 6 *The energies (kmol/mol) of transition states and products in EC$_2$-e decomposition paths.*

(e) Modeling of oxidation induced reactions of electrolyte on non-reactive electrodes

We initiated DFT study of the EC$_2$ interactions with CoPO$_4$ high voltage cathode interface using GGA+U periodic DFT calculations. These calculations indicated that carbonyl oxygen from EC reacts with the Co located on the surface supposedly initiating an oxidation cascade of electrolyte decomposition as shown in Figure 7.

Fig. 7   Initial and optimized structure of CoPO4/(EC)$_2$ from GGA+U calculations.

References
1. Borodin, O., Polarizable Force Field Development and Molecular Dynamics Simulations of Ionic Liquids. *J. Phys. Chem. B* **2009**, 113, 11463-11478.
2. Borodin, O.; Smith, G. D., Quantum Chemistry and Molecular Dynamics Simulation Study of Dimethyl Carbonate: Ethylene Carbonate Electrolytes Doped with LiPF$_6$. *J. Phys. Chem. B* **2009**, 113, 1763-1776.
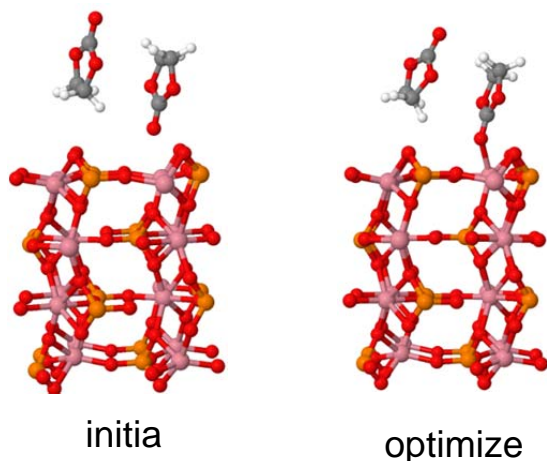3. Jow, T. R.; Marx, M. B.; Allen, J. L., Distinguishing Li$^+$ Charge Transfer Kinetics at NCA/Electrolyte and Graphite/Electrolyte Interfaces, and NCA/Electrolyte and LFP/Electrolyte Interfaces in Li-Ion Cells. *J. Electrochem. Soc*. **2012**, 159, A604-A612.
4. Xu, K.; Ding, S. P.; Jow, T. R., Toward reliable values of electrochemical stability limits for electrolytes. *J. Electrochem. Soc.* 1999, 146, 4172-4178.
5. Ue, M.; Takeda, M.; Takehara, M.; Mori, S., Electrochemical properties of quaternary ammonium salts for electrochemical capacitors. *J. Electrochem. Soc.* 1997, 144, 2684-2688.
6. Xing, L.; Borodin, O. "Oxidation Induced Decomposition of Ethylene Carbonate from DFT Calculations – Importance of Explicitly Treating Surrounding Solvent" *Phys. Chem. Chem. Phys.* (submitted)

TASK 1
Battery Cell Materials Development

Project Number: 1.1D (ES025)

Project Title: Development of Advanced Electrolyte Additives

Project PI, Institution: Zhengcheng (John) Zhang, Argonne National Laboratory

Collaborators (include industry): Khalil Amine, Lu Zhang, Wei Weng, and Peng Du
Project Start/End Dates: 10/01/2008~09/30/2014

Objectives: The objective of this work is to develop new electrolyte additives that could bring additional features to the state-of-the-art lithium-ion battery electrolyte to meet the requirements of PHEV and EV applications.

Approach: The approach for development novel electrolyte additives consists of three phases. The first phase is to screen and evaluate novel electrolyte and additive candidates using DFT theory and relative sample test procedures. Certain criteria are needed to make the screening list. In the second phase, thorough evaluation and mechanism analysis will be conducted to the promising candidates to gain the insights of their superior performance. In the third phase, based on the knowledge earned, new design of promising electrolytes additives should be proposed and organic synthesis will be involved to make these compounds. Evaluations will certainly give feedback to our designs thus leading to modifications and even more new designs.

Milestones
(a) Generate screening list based on the semiempirical rules and establish valid and quick screening procedures, Mar. 2011 (Complete).
(b) Run the screening procedures to find promising additives that could bring superior features to lithium-ion cell system, Sep. 2012 (On schedule).
(c) Evaluate and analyze the interesting additives to further understand the possible mechanism and give feedbacks to screening list, Sep. 2012, (On schedule).

Financial data: $300K/FY2011

PROGRESS TOWARD MILESTONES

(a) Summary of work in the past quarter related to milestone (a).

One empirical rule of degree of unsaturation of chemical structures was established, and new compounds continue to be added to the screening list. New candidates with multiple double bonds have been included due to their high reactivity in polymerization process. The screening process consists of formation, impedance measurements, and fast cycling performance test at elevated temperature. New heterocyclic compounds as shown in Fig.1 has been selected for electrolyte additive study.
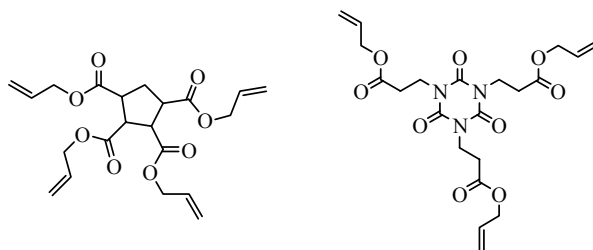
Fig.1. Chemical structures of multiple double-bond containing candidates

(b) Summary of work in the past quarter related to milestone (b)

Additive OHD was screened and exhibited promising capacity retention improvement (Fig.2 9(b)). Fig.2 (a) is the differential capacity profiles of the MCMB/NMC cells with none and 1w% additive OHD. EC decomposition peaks was significantly depressed at 2.8 V and a new peak at around 2.2 V showed up, indicating OHD was effectively involved in the SEI formation process. With 0.2 w% of OHD additive, the cell showed dramatic improvements in capacity retention. In this case, the impedance of the cell with OHD additive (Fig. 3) remains almost same to that with no additive. This result is very encouraging since the SEI formed during the polymerization of OHD is thin but yet very effective.
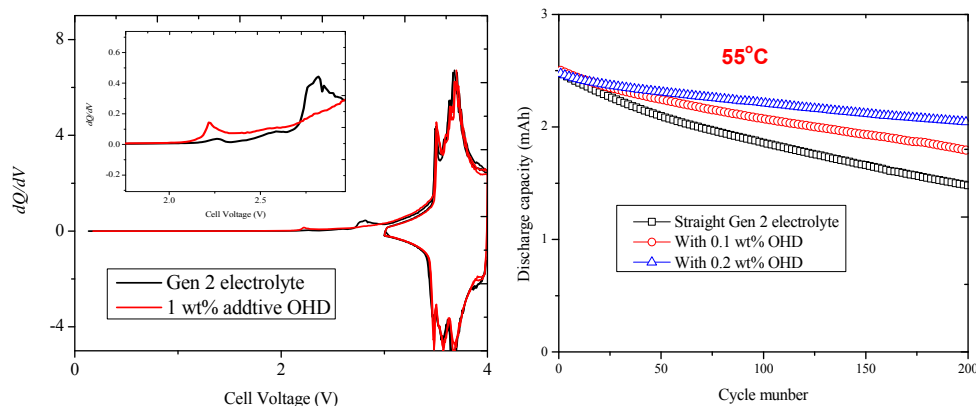

Fig. 2. (a) Differential capacity profiles of MCMB/NCM cells, electrolyte: 1.2M LiPF$_6$ EC/EMC 3/7+1% additive; (b) Capacity retention of MCMB/NCM cells cycled between 2.7 and 4.2V at 55 ◦C in electrolyte of 1.2M LiPF$_6$ EC/EMC 3/7 with no and various amount of additive OHD.
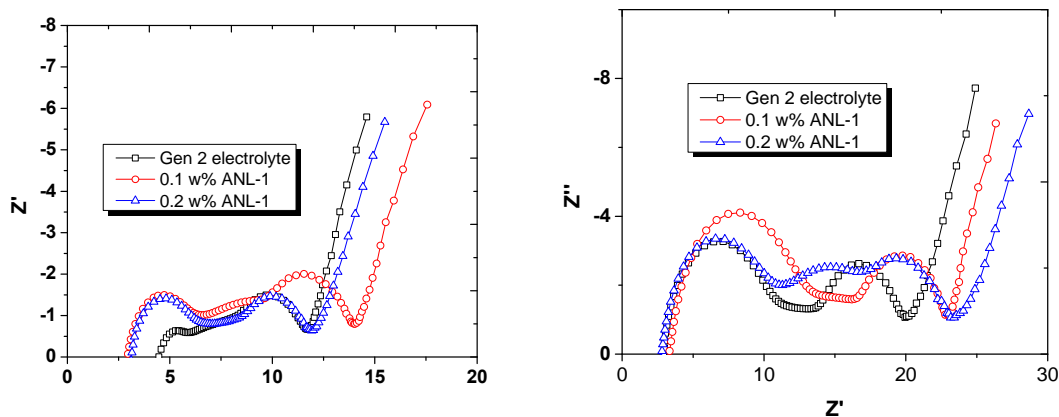
Fig. 3. AC impedance profiles of the MCMB/NMC cells before cycling (left) and after cycling (right) with and without OHD additive.

(c) Summary of work in the past quarter related to milestone (c)

Efforts to look into OHD and its performance were conducted extensively, including FTIR, SEM and XPS. Unlike the maleic anhydride derivatives, OHD additive shows no significant increase in the initial interfacial impedance of the cell. FTIR indicated that at 0.2 wt.% of OHD, the carbonyl group was much reduced and some subtle peaks around 1154 cm^{-1} can be found, indicating possible C=C double bond existed (Fig.4).
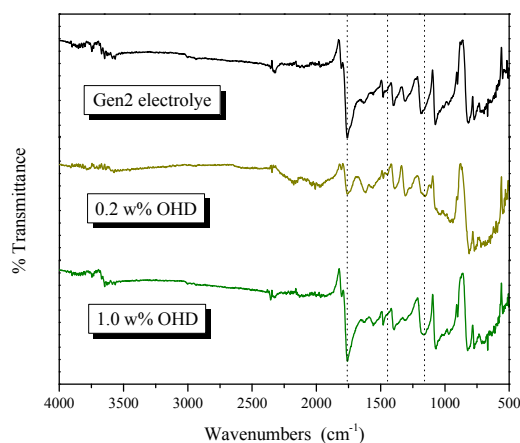
Fig. 4. FTIR spectra of MCMB electrodes harvested from the MCMB/NCM cells containing various amount of OHD after formation.

X-ray Photoelectron Spectroscopy (XPS) is very useful to identify elemental information on the surface and thus help characterizing and understanding the surface chemistry. As shown in Fig. 5, O, F, Li, and C have been studied using XPS on the surface of MCMB electrodes, obtained from the cells containing various amount of OHD after formation. Major difference can be observed from the spectra with none or 1.0wt% OHD additives. In C 1s spectra, five peaks were identified to simulate the raw spectra in the sample containing no OHD additive, however, when OHD was added, only four peaks were obtained. The missing peak is assigned to the Li-C bond,

indicating that addition of OHD might help the delithiation process. For instance, in O 1s XPS spectra, OHD sample did show less O species, indicating the dominated SEI species come from OHD.
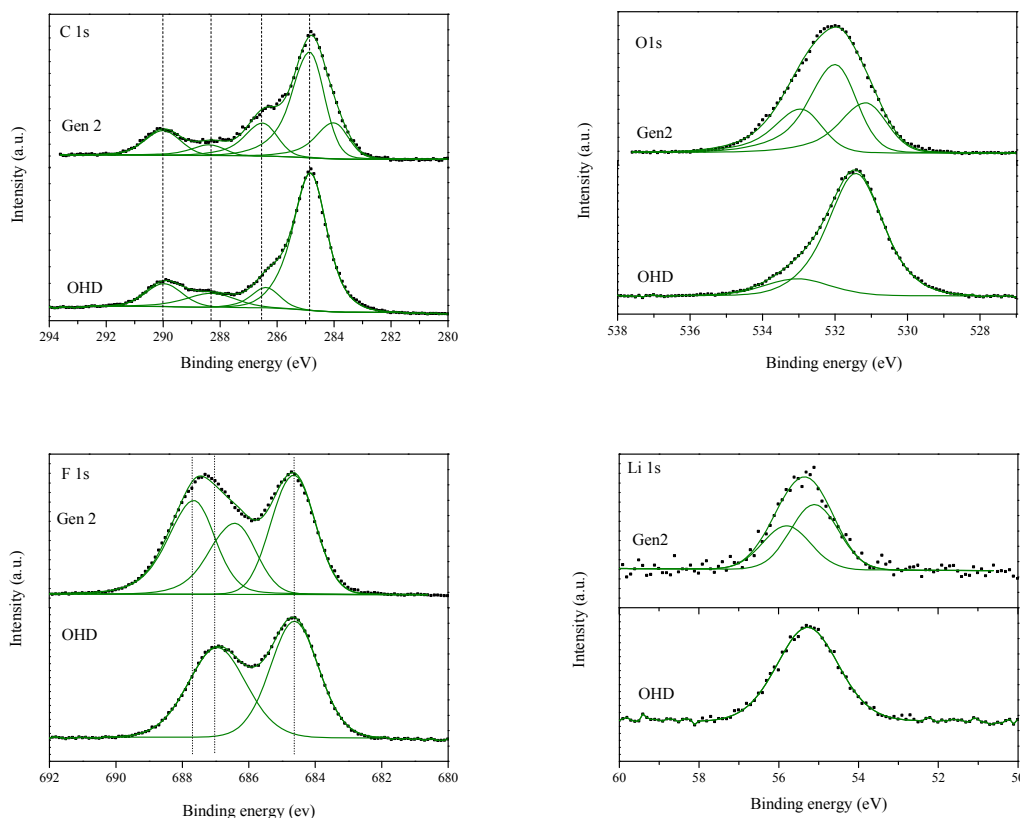
Fig. 5. XPS spectra of C1s, O 1s, F 1s, and Li 1s core peaks of the MCMB electrodes from MCMB/NCM coin cells containing different amounts of OHD in electrolyte of 1.2M LiPF$_6$ with ethylene carbonate/diethyl carbonate (3:7 weight ratio) after 2 cycle C/10 formation process.

Publications, Reports, Intellectual property or patent application filed this quarter. (Please be rigorous, include internal reports--invention records, etc.)

Electrolyte for electrochemical cells. US patent application ANL-IN-12-022.

Functional Electrolyte with Overcharge Protection. US patent application ANL-IN-12-023.

Advanced Electrolyte and Electrolyte Additive for lithium ion batteries, invited talk on 4th International Conference on Advanced Lithium Batteries for Automotive Application (ABAA-4), Sep. 20-23, 2011, Beijing, China.

Advanced Battery Materials for EV Applications, invited talk on EV Battery Tech: 5th Global Cost Reduction Initiative, Feb. 28-29, 2012 London, United Kingdom

TASK 1
Battery Cell Materials Development

Project Number: ES026

Project Title: Electrolytes for Use in High Energy Li-Ion Batteries with Wide Operating Temperature Range

Project PI, Institution: Marshall Smart, Jet Propulsion Laboratory, California Institute of Technology

Collaborators (include industry): (1) University of Rhode Island (Prof. Brett Lucht) (Analysis of harvested electrodes, on-going collaborator), (2) Argonne Nat. Lab (Khalil Amine) (Source of electrodes, on-going collaborator), (3) LBNL (John Kerr, Li Yang) (Evaluation of novel salts), (4) Loker Hydrocarbon Institute, USC (Prof. Surya Prakash) (Fluorinated Solvents and novel salts), (5) A123 Systems, Inc. (Electrolyte development, on-going collaborator), (6) Quallion, LCC. (Electrolyte development, on-going collaborator), (7) Yardney Technical Products (Electrolyte development, on-going collaborator), (8) Saft America, Inc. (Collaborator, industrial partner under NASA program), (9) NREL (Smith/Pesaran)(Supporting NREL in model development by supplying data), (10) Sandia National Laboratory (Safety testing of low flammability electrolyte and supplier of electrode materials), and (11) Hunter College (Prof. Greenbaum) (Ex-situ NMR measurements).

Project Start/End Dates: Start Date: Oct 1, 2009, Projected End Date: September 30, 2014

Objectives:

· Develop a number of advanced Li-ion battery electrolytes with improved performance over a wide range of temperatures (-30 to +60°C) and demonstrate long-life characteristics (5,000 cycles over 10-yr life span).

· Improve the high voltage stability of these candidate electrolyte systems to enable operation up to 5V with high specific energy cathode materials.

· Define the performance limitations at low and high temperature extremes, as well as, identify life limiting processes.

· Demonstrate the performance of advanced electrolytes in large capacity prototype cells.

Approach: The development of electrolytes that enable operation over a wide temperature range, while still providing the desired life characteristics and resilience to high temperature (and voltage) remains a technical challenge. To meet the proposed objectives, the electrolyte development will include the following general approaches: (1) optimization of carbonate solvent blends, (2) use of low viscosity, low melting ester-based co-solvents, (3) use of fluorinated esters and fluorinated carbonates as co-solvents, (4) use of novel "SEI promoting"

and thermal stabilizing additives, (5) use of alternate lithium based salts (with USC and LBNL). Many of these approaches will be used in conjunction in multi-component electrolyte formulations (i.e., such as the use of low viscosity solvents and novel additives and salts), which will be targeted at improved operating temperature ranges while still providing good life characteristics.

The candidate electrolytes are characterized using a number of approaches, including performing ionic conductivity and cyclic voltammetry measurements, and evaluating the performance characteristics in experimental $\sim$ 200-400 mAh three-electrode cells. In addition to evaluating candidate electrolytes in spirally-wound experimental cells, studies will be performed in coin cells, most notably in conjunction with high voltage cathode materials. Cells will be fabricated using a number of electrode couples: (a) MCMB/LiNi$_{0.8}$Co$_{0.2}$O$_2$, (b) graphite/LiNi$_{0.8}$Co$_{0.15}$Al$_{0.05}$O$_2$, (c) graphite/LiNi$_{1/3}$Co$_{1/3}$Mn$_{1/3}$O$_2$, (d) Li$_4$Ti$_5$O$_{12}$ (LTO)/LiNi$_{0.5}$Mn$_{1.5}$O$_2$ (LMNO), and (e) graphite/LiNiCoMnO$_2$. Other chemistries can be evaluated depending upon availability from collaborators. In addition to performing charge/discharge characterization over a wide range of temperatures and rates on these cells, a number of electrochemical characterization techniques will be employed, including: (1) Electrochemical Impedance Spectroscopy (EIS), (2) DC linear (micro) polarization, and (3) Tafel polarization measurements. The electrochemical evaluation in proven three-electrode test cells enables electrochemical characterization of each electrode (and interface) individually and the identification of performance limiting mechanisms for each electrode and for the cell. Electrodes are easily harvested from these test cells and samples will be delivered to collaborators (i.e., URI and Hunter College).

Performance testing of prototype cells containing candidate advanced electrolytes will be performed and evaluated under a number of conditions, i.e., assessment of wide operating temperature capability and life characteristics. JPL has on-going collaborations with several battery vendors and also has the capabilities to perform extensive testing. Typical prototype cell designs that will be considered include (i) Yardney 7 Ah prismatic cells, (ii) Quallion prismatic cells (0.250Ah size and 12 Ah size), and (iii) A123 2.2 Ah cylindrical cells. Cells will be procured and/or obtained through on-going collaborations

Milestones:

Month/Year	Milestone
Sept. 2012	Milestone A: Prepare and characterize experimental laboratory cells containing Gen-3 electrolytes, designed to operate over a wide temperature range in high voltage systems (i.e., Li(NiMnCo)O$_2$ and LiNi$_{0.5}$Mn$_{1.5}$O$_2$), and identify performance limiting characteristics (Sep. 12)
Sept. 2012	Milestone B: Demonstrate improved performance of second generation electrolytes over a wide temperature range (-30° to +60°C) compared with baseline electrolytes, in experimental and prototype cells (Sep. 12).

Financial data:

Total project funding:
  – 875K total (~ 175K/year)
  – Contractor share = 0K

 Funding received:
  FY'10 = 175K (Start Date = Oct 1, 2009)
  FY'11 = 175K
  FY'12 = 170K

Accomplishments and Progress toward Milestones:

In the recent quarter, we continued to characterize a number of 12 Ah cells (MCMB Carbon/LiNiCoAlO$_2$) obtained from our collaborator, Quallion, LCC, that contain electrolytes previously identified to have excellent wide operating temperature range. These cells contain methyl propionate-based electrolytes that have previously been demonstrated to provide wide operating temperature range capability in smaller experimental and prototype cells. In particular,
1.20M LiPF$_6$ in EC+EMC+MP (20:20:60 vol %) and 1.20M LiPF$_6$ in EC+EMC+MP (20:20:60 vol %) + 4% FEC were shown to excellent low temperature performance, with mono-fluoroethylene carbonate (FEC) being introduced with the expectation of improved life characteristics and high temperature resilience.   Current efforts are focused upon performing partial depth of discharge cycle life testing, with periodic full capacity and impedance characterization, with an emphasis upon determining the extent to which the low temperature capability is maintained throughout life.

We are also investigating a number of electrolytes that are permutations of this approach and consist of methyl propionate with varying amounts of mono-fluoroethylene carbonate (4, 10, and 20%).   In one case, we have entirely replaced the cyclic carbonate ethylene carbonate with FEC.   These electrolytes have been investigated in experimental three-electrode cells, and are also being evaluated in hermetically sealed prototype 0.25Ah MCMB/LiNiCoAlO$_2$ cells (manufactured by Quallion, LCC). Cells possessing 1.20M LiPF$_6$ in EC+EMC+MP (20:20:60 vol %) + 0.10M LiBOB were also fabricated, since the use of LiBOB as an additive has been previously identified to result in improved low temperature performance and improved cathode kinetics. These electrolytes were envisioned to have improved high temperature resilience compared to the baseline MP-containing electrolyte.   A number of performance tests are currently being implemented on these cells, including discharge rate characterization as a function of temperature, charge rate characterization, and cycle life performance under various conditions (including cycling at high temperatures).   As illustrated in Fig. 1A, good discharge rate capacity has been observed at low temperature with the cells, with all formulations displaying enhanced performance at -50°C compared with the baseline using a C rate discharge, with the permutation possessing LiBOB delivering the highest capacity.
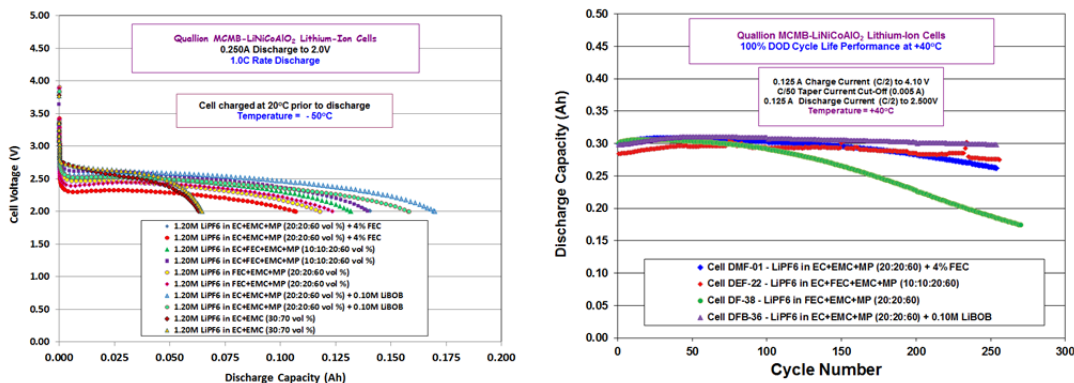
Figure 1: Discharge performance of 0.25Ah MCMB-LiNiCoAlO$_2$ cells (Quallion, LCC) containing various electrolytes -50°C using a C-rate discharge (Figure 1A) and 100% DOD cycling life performance at 40°C, using C/2 rates over a voltage range of 2.50V to 4.10V (Figure 1B).

When these cells were subjected to full depth of discharge cycling at high temperature (i.e., 40°C), the cells that delivered the best performance contain the methyl propionate-based electrolyte with the LiBOB additive. Based on previous results in experimental cells, it is speculated that the decomposition of LiBOB results in a desirable cathode electrolyte interface (CEI), preventing excessive electrolyte oxidation at high temperatures. The presence of FEC also appears to have a beneficial effect upon the cycle life at high temperature when used in moderate amounts. However, when FEC is used in place of EC as the only cyclic carbonate poorer performance is observed. Work is on-going the fully characterize the discharge performance and cycle life performance of these cells over a wide temperature range.

Recent effort has been focused upon investigating wide operating temperature range electrolytes with high voltage systems, including LiNi$_{1/3}$Co$_{1/3}$Mn$_{1/3}$O$_2$ and the excess lithium layered-layered composite Li(NiCoMn)O$_2$ (NMC) (from two sources). In an extension of work performed in coin cells, we have recently investigated a number of methyl butyrate-based electrolytes (with various additives, including vinylene carbonate, lithium oxalate, FEC and LiBOB) in larger three-electrode cells consisting of Conoco graphite anodes and NMC cathodes supplied by Argonne National Labs. Being equipped with lithium reference electrodes enabled us to study the lithium kinetics of the respective electrodes by electrochemical techniques. In particular, both anodes and cathodes were subjected to a number of electrochemical measurements, including Electrochemical Impedance Spectroscopy (EIS), Tafel polarization, and linear micro-polarization measurements. Upon performing Tafel polarization measurements on each electrode (which possess relatively heavy loadings), it was observed that the NMC-based cathode displayed poor lithium kinetics (limiting electrode) compared to the anode, as shown in Fig. 2. Further, EIS measurements suggest that the charge-transfer kinetics of the cathode contributes significantly to the overall cell impedance and poor rate capability. In contrast, a comparable cell possessing LiNiCoAlO$_2$ as the cathode, rather than the NMC-based material, displays much more facile lithium de-intercalation kinetics under similar conditions.
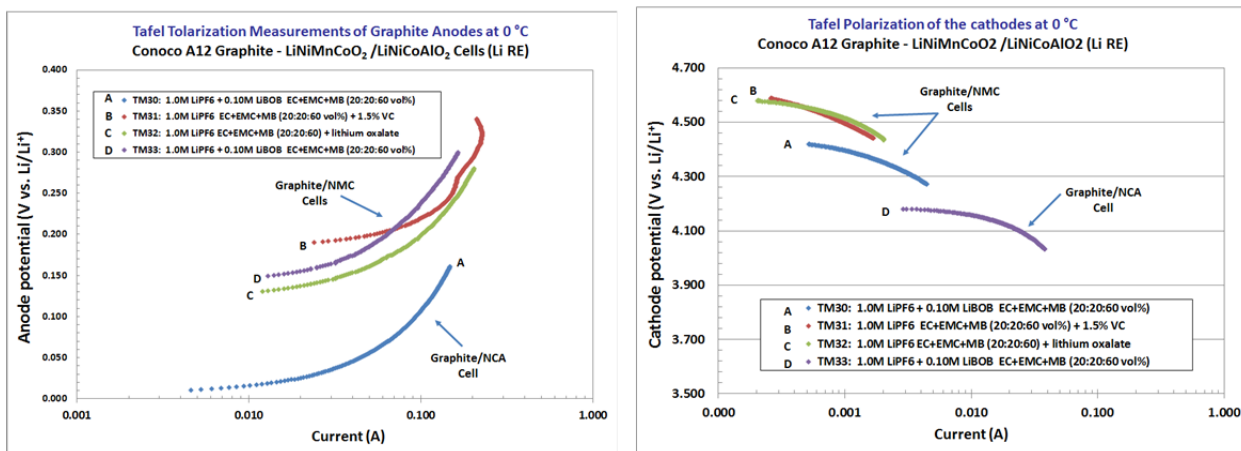
Figure 2: Tafel polarization measurements of Conoco A12 graphite anodes (Fig. 2A) and Toda HE 5050 LiNiCoMnO$_2$ (or NCA) cathodes (Fig. 2B) in contact with various methyl butyrate-based electrolytes at 0°C.

In general, we have observed good compatibility of the methyl butyrate-based electrolytes with this high voltage system. Cells containing the electrolyte 1.20M LiPF$_6$ in EC+EMC+MB (20:20:60 vol %) + 0.10M LiBOB delivered improved low temperature capability compared with the baseline. The improved low temperature rate capability of the cells containing the electrolyte with methyl butyrate and LiBOB is primarily ascribed to improved cathode kinetics, as substantiated by the Tafel polarization measurements, and improved ionic conductivity.

We are also currently evaluating a number of low flammability electrolytes in cells consisting of Conoco graphite anodes and LiNi$_{1/3}$Co$_{1/3}$Mn$_{1/3}$O$_2$ cathodes (electrodes supplied by Sandia National Laboratory). These electrolytes were previously developed under a NASA-funded project and possess triphenyl phosphate (TPP) as a flame retardant additive (10 to 15%). As a result of interest that DOE has expressed, cells containing some of these low flammability electrolytes developed at JPL will ultimately be subjected to safety testing by collaborators at Sandia National Laboratory. As shown in Fig. 3, preliminary results suggest good capability with the TPP-containing electrolytes with the graphite/ and LiNi$_{1/3}$Co$_{1/3}$Mn$_{1/3}$O$_2$ system.

Future work will involve continuing the investigation of the use of additives in conjunction with ester-based, wide operating temperature range electrolytes evaluated with different electrode chemistries, with a focus upon (i) assessing other candidate additives, (ii) studying the high temperature and cycle life degradation modes, (iii) correlating electrochemical trends with performance, and (iv) identifying performance limiting aspects at extreme temperatures. Future work will also focus upon demonstrating these systems in prototype cells.
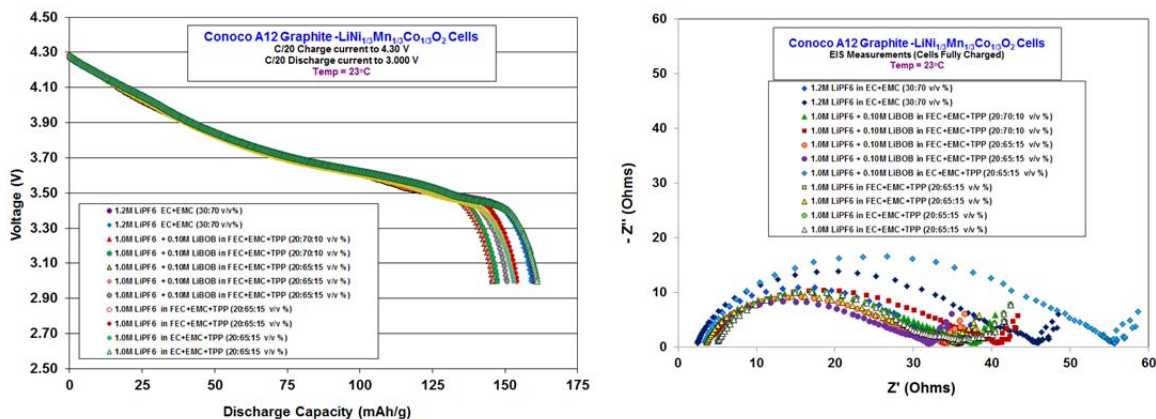
Figure 3: Discharge capacity of graphite/ and LiNi$_{1/3}$Co$_{1/3}$Mn$_{1/3}$O$_2$ coin cells after formation cycling (Fig. 2A) and Electrochemical Impedance Spectroscopy measurements performed at 23°C after formation cycling (Fig. 2B).

Publications:

1. M. C. Smart, B. L. Lucht, S. Dalavi, F. C. Krause, and B. V. Ratnakumar, "The Effect of Additives upon the Performance of MCMB/LiNiCoO$_2$ Li-Ion Cells Containing Methyl Butyrate-Based Wide Operating Temperature Range Electrolytes", J. Electrochem. Soc., **159 (6)**, A739-A751 (2012).
2. S. DeSilvan, V. Udinwe, P. Sideris, S. G. Greenbaum, M. C. Smart, F. C. Krause, K. A. Smith and C. Hwang, "Multinuclear NMR Studies of Electrolyte Breakdown Products in the SEI of Lithium-Ion Batteries", *ECS Trans.*, (2012) in press.
3. M. C. Smart, M. R. Tomcsi, C. Hwang, L. D. Whitcanack, B. V. Ratnakumar, M. Nagata, V. Visco, and H. Tsukamoto, "Improved Wide Operating Temperature Range of LiNiCoAlO2-Based Li-ion Cells with Methyl Propionate-Based Electrolytes", 221st Meeting of the Electrochemical Society, Seattle, WA, May 6-10, 2012.
4. N. Leifer, M. C. Smart, G. K. S. Prakash, L. Gonzalez, L. Sanchez, P. Bhalla, C. P. Grey, and S. G. Greenbaum, "^{13}C Solid State NMR Study of SEI Formation in Carbon Lithium Ion Anodes Cycled in Isotopically Enriched Electrolytes Suggests Unusual Breakdown Products", *J. Electrochem. Soc.*, **158 (5)**, A471-A480 (2011).
5. M. C. Smart and B. V. Ratnakumar, "Effect of Cell Design Parameters on Lithium Plating in Lithium-Ion Cells", *J. Electrochem. Soc.*, **158 (4)**, A379-A389 (2011).

TASK 1
Battery Cell Materials Development

Project Number: ES027   **Reporting Period:** FY 2012 Q2

Project Title: Novel Phosphazene Compounds for Enhancing Electrolyte Stability and Safety of Lithium-ion Cells

Project PI, Institution: Kevin L. Gering, INL

Collaborators (include industry): Michael T. Benson (INL), Mason K. Harrup (INL), Harry W. Rollins (INL), Sergiy V. Sazhin (INL), Khalil Amine (ANL), Chris Orendorff (SNL), Princess Energy Systems, Dow Chemical

Project Start/End Dates: Jan. 2009/Ongoing

Objectives: Our focus is to understand stability of our new classes of phosphazene materials and to establish viability for their use in lithium-ion cell electrolytes, considering both conventional voltage ranges (4.2V) and higher voltage electrode couples (4.5-5V). Comprising this overall work are the following focus areas:

♦ Synthesize novel solvents for Li-ion cells that are safer alternatives to volatile organics.
♦ Gain understanding of molecular-scale interactions between phosphazenes and other electrolyte components.
♦ Determine what phosphazene structures are more tolerant to high and low voltage, and to high temperatures.
♦ Determine the effect of phosphazenes on SEI films, cell performance, and cell aging in general, using ABR-relevant electrode couples.
♦ Synthesize and engineer novel phosphazene polymers that would serve as safe and robust alternatives to carbon-based anodes. Linked with our electrolyte research, this enhances overall compatibility of cell chemistry.

This collective effort will enable us to engineer advanced materials for more robust lithium-ion cells and move us closer to the overall goal of a carbon-reduced cell chemistry.

Approach: The INL is leveraging this work based on interdepartmental synergy between a well-established battery testing program and its foremost experts in phosphazene chemistry that are producing new classes of novel compounds for use in lithium-ion batteries. As such, the INL is strongly positioned to approach primary targets for ABR electrolyte development while maintaining historical knowledge of phosphazene chemistry and related applications.

This work is split under four primary tasks: solvent synthesis, characterization, DFT modeling, and lithium-ion cell testing. Upfront issues are

♦ voltage stability (CV)   ♦ temperature stability
♦ flammability (flash point)   ♦ lithium salt solubility
♦ transport properties (viscosity, conductivity)
♦ chemical compatibility with the cell environment
♦ molecular interactions (solvent-ion)

Coin cell testing covers issues of formation, interfacial impedance, polarization testing, and aging, using our compounds as electrolyte additives (1-10%). In previous quarters we investigated our electrolytes with ABR electrode couples LNMO/LTO, NMC(3M)/Carbon, and HE5050/Carbon. We test our novel polymeric anodes against ABR-relevant cathodes such as NMC. For most coin cell testing the general protocol is: formation cycling (C/10 @ 3), EIS, followed by a matrix of C/10, C/3, C/1, and 3C, all at 30 °C. Testing concludes with 3C cycling at 45-55 °C to determine electrolyte effect on high temperature tolerance. Final EIS is optional.

Milestones (cumulative over FY 2011-2012):

	= Activity completed in reporting period

Milestone	Status	Date
a. Synthesis of Fluorinated Phosphazene series (FM1,2,3)	completed	March 2011
b. Synthesis of Gen1 Ionic Liquid Phosphazene (PhIL-1)	completed	Feb. 2011
c. Synthesis of newer SM series (SM 5,6,7)	completed	October 2010
d. Development of improved voltammetry techniques for SEI characterization.	completed	December 2010
e. DFT simulations of selected phosphazenes regarding interaction with lithium ions	completed	Feb./March 2011
f. Thermal stability testing of blends with SM6 and SM7	completed	March 2011
g. Cell testing using LNMO/LTO and NMC/Carbon* couples: characterization of capacity and impedance attributes	completed	March 2011
h. Cell testing using LNMO/LTO and NMC/Carbon* couples: aging studies	completed	October 2011
i. Phase 1 concept validation for alternative anode materials	completed	October 2011
j. Cell testing using HE5050/Carbon couple: characterization of capacity and impedance attributes	completed	December 2011
k. DFT study on complete FM Series (fluorinated cyclics)	completed	February 2012
l. Cell testing using HE5050/Carbon couple: aging studies	completed	March 2012
m. Phase 2 concept validation for alternative anode materials	completed	March 2012
n. Initial PALS measurements of alternative anode materials	completed	March 2012
o. Synthesis of newer FM series and second-generation Ionic Liquid Phosphazenes	In Progress	
p. Abuse testing of INL electrolyte additives at SNL	In Progress	
q. Collaboration with ANL regarding scale-up of INL electrolyte compounds	In Progress	
Various supporting characterization and cell testing will be ongoing throughout FY 2012.		

PROGRESS TOWARD MILESTONES

(a, b) Completed 2011 Q2.

(c) Completed 2011 Q1.

(d) Completed 2011Q1.

(e) Completed 2011 Q2.

(f) Completed 2011 Q2.

(g) Completed 2011 Q2.

(h) Completed 2012 Q1.

(i) Completed 2012 Q1.

(j) Completed 2012 Q1.

(k) An extensive DFT analysis of our FM series was completed, looking in particular at solvent-lithium binding energy (BE). Modeling was done using Gaussian03, B3LYP/6-311++G(d,p). Structures are true minima (no imaginary frequencies). BE is seen to decrease linearly with fluorination of pendant groups, likely due to increasing electron withdrawing effect as more CF_3 groups are added (**Fig. 1**). This also leads to molecular distortion and slightly weakened coordination to Li^+. Lower BE translates to lesser solvation of Li^+ and a more efficient charge transfer process.

(l) We completed coin cell testing from (j) at 45 °C and a 3C rate to determine if the phosphazene compounds prolong cell life at these mildly abusive conditions. Capacity data indicates that the phosphazenes act to prolong cell life at elevated temperature, particularly our FM-2 and SM-6 compounds which in some cases promote capacity retention beyond that of the baseline (additive free) electrolyte 1.2M $LiPF_6$ + EC-EMC (2:8, wt.).

(m) We completed the Phase 2 matrix of our alternative anode materials investigation, using a polymeric approach (**Fig. 2**). Successful testing to 5V was achieved. Capacities are approaching that of conventional carbon systems, and we conclude that enhancing the electronic conductivity of these materials will allow us to improve capacity to achieve competitive levels. We are also seeing correlations between polymer type and lithium uptake, indicating further information regarding the 3D framework of these materials.

(n) Positron Annihilation Spectroscopy (PAS) was used to characterize surface features of our novel polymer-based anode materials. These measurements show consistent surface homogeneity, while detecting differences in electronic structure of the materials.

PAS and PALS are critically important tools for characterizing structural details of solids down to the nano-level. Through these tools we can look at defect attributes (dislocations), micro-porosity, and particle fracturing over aging.

(o) Synthesis targets are being used to generate newer generations of FM and phosphazene-based ionic liquid (PhIL) compounds. Synthetic efforts continued to produce a series of related phosphazene-based ionic liquid electrolyte solvents. Voltammetry studies clearly show that our phosphazene compounds can triple the voltage window of the baseline electrolyte (**Fig. 3**) while at moderate levels (20%); we will confirm and quantify such benefit for lesser amounts of our compounds. Other work focused on the synthesis of PhIL-3 (and later variants) which had initial stability issues, but an alternate synthetic route was discovered and PhIL-3 was successfully produced. We continue to explore optimal synthesis routes for the sake of compound purity, stability, and economy of manufacture. These compounds will also be tested with our novel electrode materials in (m) to further enhance cell voltage stability at 5V.

(p) Abuse testing (ARC) of INL Phosphazene compounds at SNL started January 2012, using 18650 cells containing the NMC (3M)/carbon (A10) couple. INL additives include FM-2, SM-6, and PhIL-2 at one and three percent levels. The focus of this work is to determine how INL additives help mitigate (delay) the onset of thermal runaway. Initial results from this work indicate overall benefit of INL phosphazene additives in terms of thermal stability (**Fig. 4**), in the order of {SM-6 > PhIL-2 > FM-2}. For example, at 3% levels SM-6 decreases the peak heating rate by over 100 degrees C per minute, while PhIL-2 cuts the gas evolution to one-third that of the baseline system. ARC and flammability testing is expected to conclude in Q3.

(q) We have continued our efforts to collaborate with ANL regarding the synthesis of INL phosphazene electrolyte compounds in the ANL materials scale-up facilities. The top candidate for scale-up will be the best compound(s) that emerges from the final results of the SNL abuse testing, which are not yet available as of this writing.

Publications, Reports, Intellectual property

- M. K. Harrup, K. L. Gering, H. W. Rollins, S. V. Sazhin, M. T. Benson, D. K. Jamison, C. J. Michelbacher, T. A. Luther , "Phosphazene Based Additives for Improvement of Safety and Battery Lifetimes in Lithium-Ion Batteries", ECS Transactions from the 220th Meeting of the Electrochemical Society (Oct. 2011, Boston, MA).
- A full patent application was filed in this quarter: ELECTRODES INCLUDING A POLYPHOSPHAZENE CYCLOMATRIX, METHODS OF FORMING THE ELECTRODES, AND RELATED ELECTROCHEMICAL CELLS, Inventors Kevin L. Gering, Frederick F. Stewart, Aaron D. Wilson, Mark L. Stone.
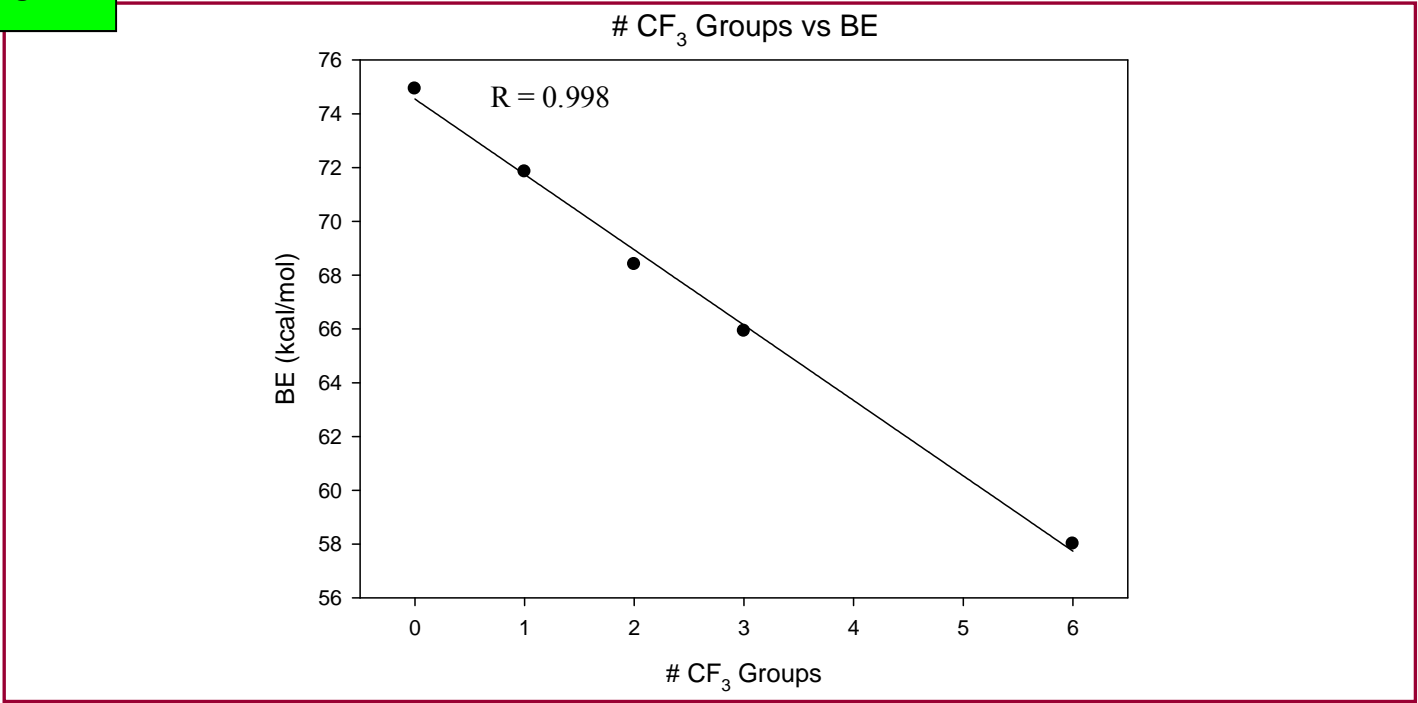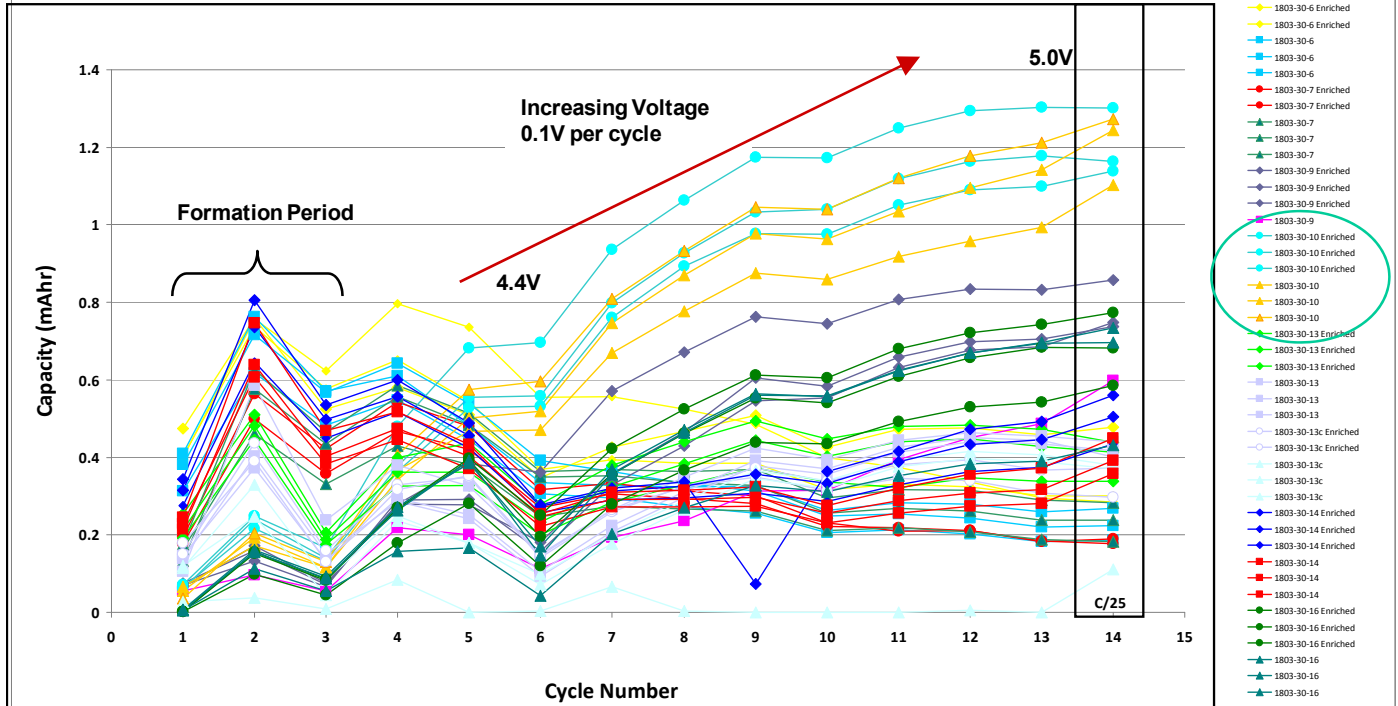
Fig. 1

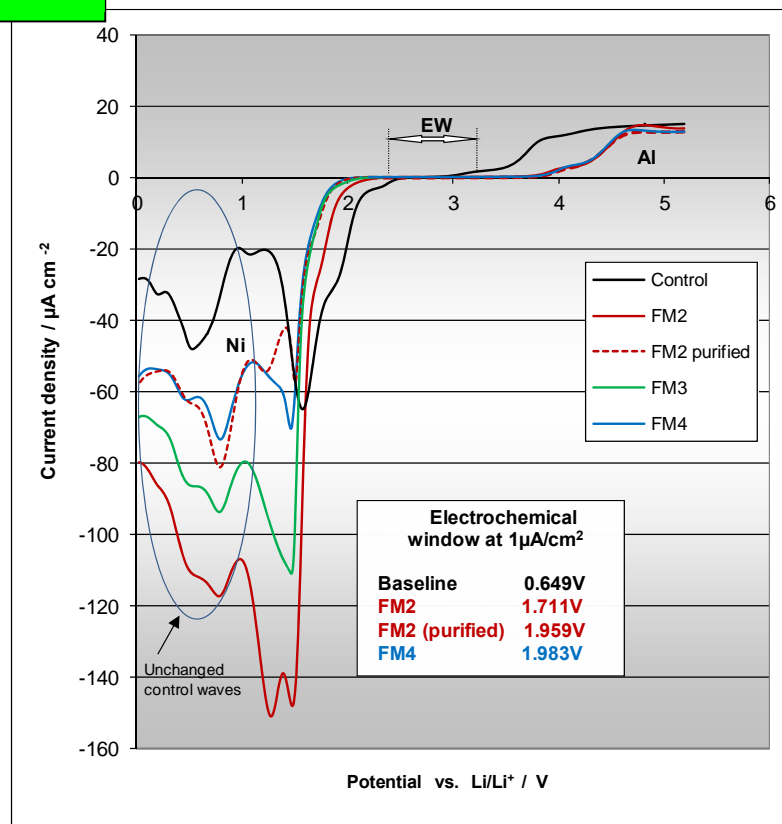# CF$_3$ Groups vs BE

R = 0.998

Fig. 2

Phase 2 Study:
C/10 discharge cycling with no taper charges.

Higher capacity is attained at lower voltages, compared to Phase 1 materials. Distinct differences in polymeric chemistry result in differences in energy storage. We can utilize such correlations to engineer finely tuned materials.
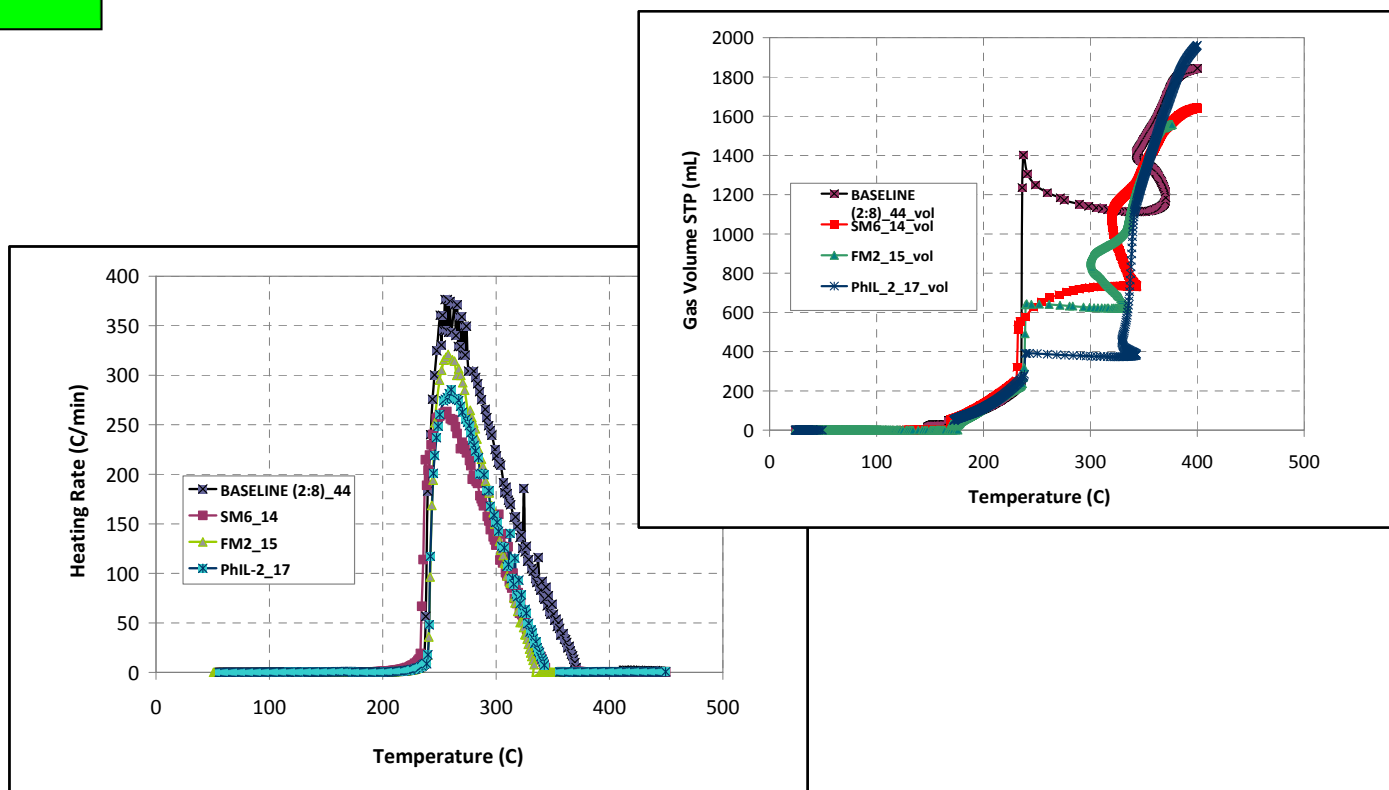
Fig. 3

- **Phosphazenes increase electrochemical window at negative and positive ends.**
- **Purification* of phosphazenes increase electrochemical window and reduce current at negative end.**
- **All the windows are less than operating voltage of Li-ion cells. At potentials beyond the electrochemical window, passivation does occur forming SEIs.**
- **Properties of passivating layers need to be measured quantitatively.**

*US Patent 5849429. Purification process for lithium battery electrolytes. S. Sazhin, M. Khimchenko, Y. Tritenichenko.

Electrochemical window at 1µA/cm²

Baseline	**0.649V**
FM2	**1.711V**
FM2 (purified)	**1.959V**
FM4	**1.983V**

Electrolytes: Baseline (1.2M LiPF₆ EC:MEC (2:8)) and blends of 20% phosphazene with 80% baseline.

Fig. 4

TASK 1
Battery Cell Materials Development

2nd Quarter Report, Jan. ~ Mar. 2011

Project Number: 1.1E (ES028)

Project Title: Streamlining the Optimization of Lithium-Ion Battery Electrodes

Project PI, Institution: Wenquan Lu, Argonne National Laboratory

Collaborators (include industry):
Qingliu Wu, Argonne National Laboratory
Khadija Yassin-Lakhsassi, Argonne National Laboratory
Miguel Miranda, Argonne National Laboratory
Dennis Dees, Argonne National Laboratory
Jai Prakash, Illinois Institute of Technology

Project Start/End Dates: October 2008 / September 2012

Objectives:
To establish the scientific basis needed to streamline the lithium-ion electrode optimization process.
- To identify and characterize the physical properties relevant to the electrode performance at the particle level.
- To quantify the impact of fundamental phenomena associated with electrode formulation and fabrication (process) on lithium ion electrode performance.

Approach:
The initial focus of this effort will be on optimizing the electronic conductivity of the electrode. The factors affecting the distribution of binder and conductive additive throughout the composite matrix will be systematically investigated at the particle level, as well as their effect on overall electrode performance. Modeling simulations will be used to correlate the various experimental studies and systematically determine their impact on the overall electrode performance.

Milestones:
(a) Modeling work on electrode optimization was initiated.
(b) Electrode conductivity and impedance measurement of $LiFePO_4$ electrode.

Financial data: $300K carryover fund

PROGRESS TOWARD MILESTONES

(a) Summary of work in the past quarter related to milestone (a).

The objective of the modeling work is to look at the effects of Active Material (AM)/Carbon/Binder composition on electrode performance. The model is built upon the COSMOL platform. As shown in Figure 1, we expect to locate the optimum composition zone through this exercise with knowing only the physical properties of every cell component, such as particle size, particle density, and electronic conductivity, etc.

As the cathode material with lowest electronic conductivity, $LiFePO_4$ was chosen for this model. Other high energy material will be investigated once the model is validated. First, the electrode properties, electrode conductivity and electrode porosity, were calculated using particle density model given the physical properties of every single electrode component. Then, the electrochemical performance was calculated using the COMSOL electrochemical model. at last, the optimum composition was then located according to the calculated local current density.
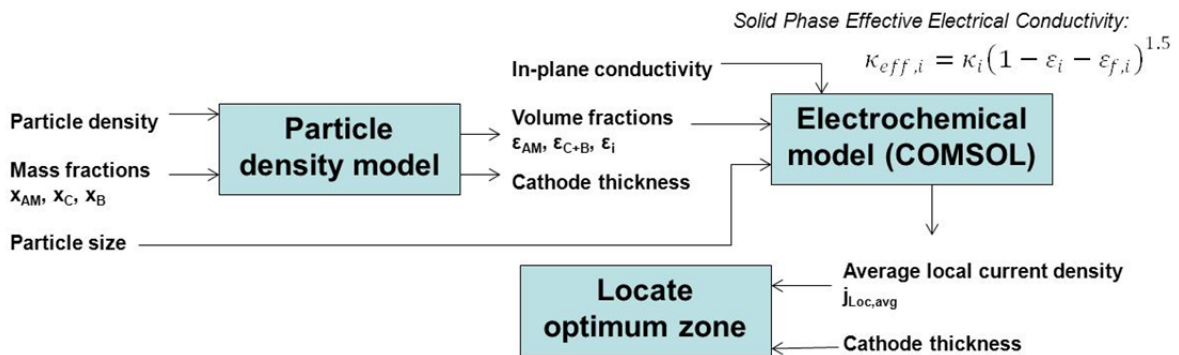

Figure 1. Diagram of optimization model

(b) Summary of work in the past quarter related to milestone (b).
The experimental work was also conducted to investigate how the related factors of $LiFePO_4$/Carbon Black/PVDF electrode affect its electrochemical performance and identify the predictability of the proposed model. Figure 2 shows the design of the mixtures of the electrode formulation. The low binder and carbon composition was limited to 5wt% due to mechanical integrity. The electrical conductivity and electrochemical performance will be conductive to correlate the optimum zone discovered by both modeling and experimental work.
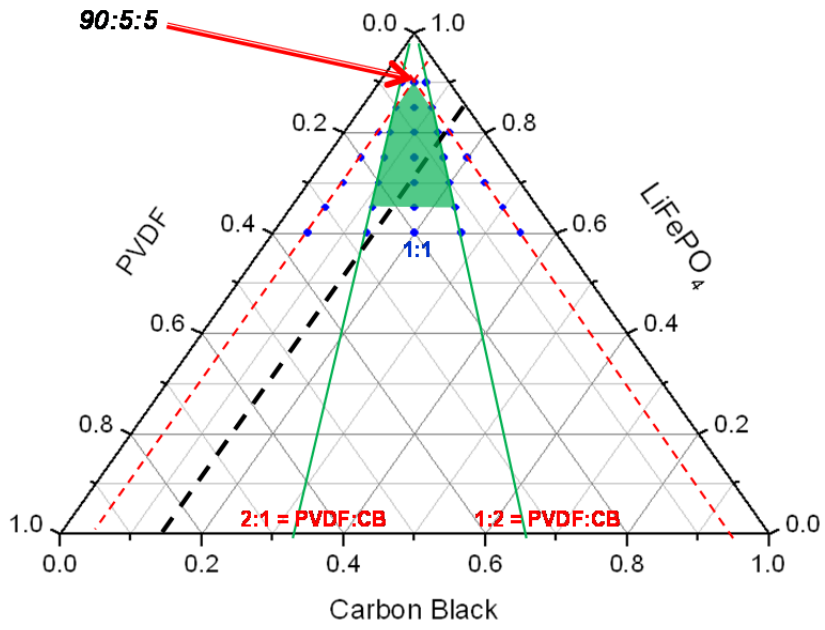
Fig. 2. Design of mixtures at different mass fractions

Publications, Reports, Intellectual property or patent application filed this quarter.

TASK 1
Battery Cell Materials Development

2nd Quarter Report, Jan. ~ Mar. 2011

Project Number: 1.3 (ES028)

Project Title: Screen Electrode Materials, Electrolytes, and Additives

Project PI, Institution: Wenquan Lu, Argonne National Laboratory

Collaborators (include industry):
Qingliu Wu, Argonne National Laboratory
Khadija Yassin-Lakhsassi, Argonne National Laboratory
Miguel Miranda, Argonne National Laboratory
Thomas K. Honaker-Schroeder, Argonne National Laboratory
Bryant Polzin, Argonne National Laboratory
Andrew Jansen, Argonne National Laboratory
Dennis Dees, Argonne National Laboratory
Jai Prakash, Illinois Institute of Technology
Harold Kung, Northwestern University
James Banas, JSR Corporation

Project Start/End Dates: October 2008 / September 2014

Objectives:
- To identify and evaluate low-cost cell chemistries that can simultaneously meet the life, performance, abuse tolerance, and cost goals for Plug-in HEV application.
- To enhance the understanding of advanced cell components on the electrochemical performance and safety of lithium-ion batteries.
- Identification of high energy density electrode materials is the key for this project.

Approach:
Based upon the battery design model developed by Argonne, the specific capacities of cathode and anode materials should be above 200mAh/g and 400mAh/g, respectively, to meet PHEV requirements set by USABC.

Since there is no commercial available electrode materials can meet PHEV energy requirements, the electrode material candidates will be required from both battery materials companies and research institutes. The promising materials will be evaluated under the controlled process and standard test procedures derived from the "Battery Test Manual for Plug-in Hybrid Electric Vehicles" by INL 2010. In addition, thermal properties of the electrode materials will be studied.

Other battery components for lithium ion batteries, such as electrolyte and additives, separators, binder, conductive additives, and other relevant materials, will also be investigated accordingly.

Milestones:
Materials have been investigated in 1st Quarter:
  a) Complete screening on silicon composite from Northwestern University
  b) Complete screening of $Li_{1+x}Ni_{1/3}Co_{1/3}Mn_{1/3}O_2$ (NCM-111) from BASF
  c) Complete screening of Nippon Denko's lithium manganese spinel

Financial data: $450K

PROGRESS TOWARD MILESTONES
Several materials, silicon composite, $Li_{1+x}Ni_{1/3}Co_{1/3}Mn_{1/3}O_2$, and $LiMn_2O_4$, have been investigated and the test results were delivered to customers. A couple of new composite materials developed at Argonne National Laboratory were received from developers. They are under screening process. Other than active materials, some work was conducted on additives and separators. The positive effect on silicon and high energy composite materials - LMR-LMO was observed.

(a) Summary of work in the past quarter related to milestone (a).
Silicon composite anode developed by Prof. Kung at Northwestern University was received and its electrochemical performance was investigated using both half cells and full cells. The silicon electrode prepared at Northwestern University has no binder, no current collector. In the half cells, the reversible capacity at C/10 rate is around 1500mAh/g when cycled between 20mV and 1.5V. Its electrochemical performance in full cell, coupled with lithium manganese spinel, was also investigated. The effect of fluorinated carbonate additive on silicon based electrode was also studied. The electrochemical performance was significantly improved.

(b) Summary of work in the past quarter related to milestone (b)
$Li_{1+x}Ni_{1/3}Co_{1/3}Mn_{1/3}O_2$ (NCM-111) cathode material was received from BASF. The excessive lithium is intended to improve the rate and cycle performance of the metal oxide. The NCM 111 electrode consists of 5wt% carbon and 8wt% PVDF. The electrochemical properties of NCM 111 were characterized using half cells. The NCM-111 was tested between 4.3V and 3.0V. At C/10 rate, 158mAh/g capacity was obtained, which is equivalent to 571 Wh/kg. The irreversible capacity loss during the first cycle was 10%. Low ASI result during HPPC test and good rate performance were also obtained in the half cell configuration. The information was delivered to CFF group for electrode preparation and cell fabrication.

(c) Summary of work in the past quarter related to milestone (c)
Electrochemical performance of lithium manganese spinel from Nippon Denko was studied for modeling group. This manganese material delivers about 105 mAh/g capacity at C/10 rate between 4.4V and 3.5V. The irreversible capacity loss during first cycle in half cell is only about 2%. When coupled with graphite, this material showed

excellent rate performance. For this electrochemical couple, more than 20% capacity fading was observed after 50 cycles. However, there was almost no capacity loss in 100 cycles when the spinel was coupled with lithium titanate.

Publications, Reports, Intellectual property or patent application filed this quarter. (Please be rigorous, include internal reports--invention records, etc.)

Electrochemical Investigation of LiMn2O4 Nippon Denko, Jan 2012.

Electrochemical Characterization of Si composite, Feb 2012.

SBR Binder from JSR, Mar. 2012.

TASK 1
Battery Cell Materials Development

Project Number: 1.2.2 Electrode Material Development (ES029)

Project Title: Scale-up and Testing of Advanced Materials from the BATT Program

Lead PI and Institution: Vince Battaglia, Lawrence Berkeley National Laboratory

Support PI and Institution: None

Barrier: Cost is too high (energy density needs to be increased.)

Specific Objectives: (*i*) Identify materials in the BATT Program that are ready for enhanced screening diagnostics, (*ii*) Procure *ca*. 10 grams of new material to make laminates for coin cell or pouch cell testing, (iii) Work with BATT researchers to improve their materials by identifying shortcomings.

General Approach: Work with BATT PIs in deciding what materials are ready for scale-up and enhanced testing and diagnostic evaluation in full cells.   Once materials are identified, decide on the best approach for increasing the quantity of the material to approximately 10 g. Make laminates of the material and test in coin cells against Li. Based on initial test results, decide on best automotive application for material, design the electrodes for the application, and perform long-term cycling tests. Provide a comparison to state-of-the art materials and cells.

Current Status as of October 1, 2011: Eight materials were identified for scale-up and further testing. Three of the materials showed significant problems during preliminary testing: two exhibited large first-cycle irreversible capacity losses, and the other displayed low specific capacity. Four materials continue on long-term cycling, and one material has recently begun preliminary testing. This last material, from MIT, was scaled-up and its claimed high-rate capability has been confirmed.

Expected Improvement by September 30, 2012: Will have identified at least three more BATT Program materials that should undergo further testing. Will have developed some basic principles for the optimal scale-up of the MIT material.

Schedule and Deliverables: Attend review meetings and present interim results on the scale-up of BATT Program materials (November 2011, February 2012, August 2012.)

Deliverable: Battery design, performance, and cycling characteristics of three BATT materials will be reported on at the DOE Merit Review (May 2012.)

Quarter 2 Report

This quarter, Ni-spinel high-voltage materials from the University of Texas (Prof. Manthiram) and MIT (Prof. Ceder) were received and evaluated at LBNL. Of particular interest are the voltage profile (not shown) and the rate performance (provided in Figure 1.). According to in-depth analyses performed in the BATT Program, the voltage profile provides an indication of the level of Mn^{3+} in the sample and the level of ordering of the Ni/Mn cations. These characteristics are important because Mn^{3+} contributes to an increase in electronic conductivity and ordered materials exhibit slower Li transport properties than their less-ordered counterparts.

Of all the materials tested in our group, the spinel from MIT showed the flattest potential in the 4.7 V region and the smallest Mn^{3+} signature. Its x-ray diffraction data also indicated that this material is ordered. Thus, as predicted by mathematical models, the MIT material shows the poorest rate capability, especially for a ~1 hr discharge.

The next steps are to evaluate the materials in full cells wherein the rate and cycle capabilities will be evaluated

Electrolyte additives from the University of Rhode Island (Lucht) were also received and tested in full cells, along with VC, an often-used Li-ion battery additive. Of the four additives tested, the addition of FEC to 1 M $LiPF_6$ in EC:DEC 1:2 resulted in the highest capacity retention as a function of charge rate. Close examination of the voltage data indicated smaller impedance rise in cells with FEC; hence the cell can reach greater capacities at high charge rates. These preliminary results suggest that good cell performance will require a combination of properly engineered cathode materials and electrolytes in order to achieve high rates, high available capacities, and long cycle life.
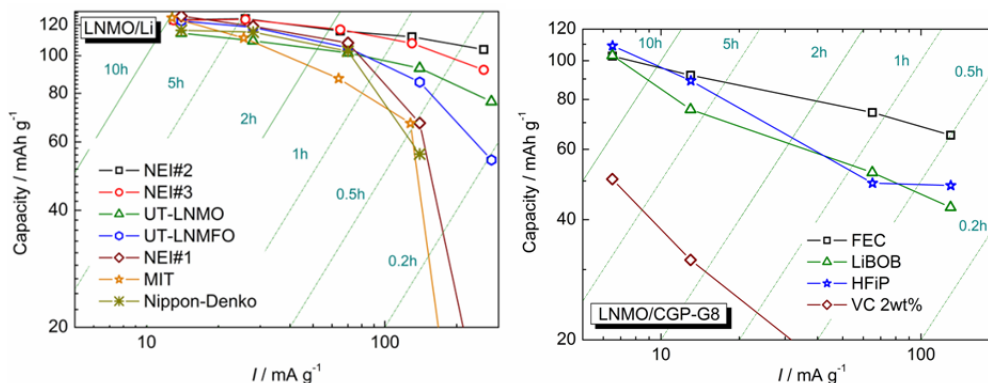

Figure 1. Left – A comparison of the rate performance of several materials in half-cells. Right – A comparison of the rate performance of full cells with different electrolyte additives.

TASK 1
Battery Cell Materials Development

Project Number: 1.2C (ES112)

Project Title: Mechanism of LTO Gassing and Potential Solutions

Project PI, Institution: Yan Qin, Zonghai Chen and Khalil Amine, Argonne National Laboratory

Collaborators (include industry):
EnerDel
University of Colorado

Project Start/End Dates: October 2010 / February 2012

Objectives: The objective of this work is to investigate the gassing mechanism of $Li_4Ti_5O_{12}$ and to develop advanced technologies to solve this problem.
– Identify gassing mechanism.
– Identify and develop advanced technologies to eliminate the gassing issue.

Approach: In-situ x-ray diffraction spectroscopy technique (XRD), has been applied to observe the $Li_7Ti_5O_{12}$ phase change during aging at 60^oC. Correlated with previous in-situ XANES data, we can further confirm that at 60^oC, lithiated LTO is experiencing phase change from $Li_7Ti_5O_{12}$ toward $Li_4Ti_5O_{12}$. Surface coating through Atomic Layer Deposition shows positive effect in reducing the gassing.

Milestones:
(a.) Self-discharge of the $Li_7Ti_5O_{12}$ during high temperature aging has been linked to gassing evolution. (On schedule)
(b.) Surface coating through atomic layer deposition technique shows positive effect in reducing the gassing. (On schedule)

Financial data: $300K

PROGRESS TOWARD MILESTONES

Gassing mechanism has been further understood through in-situ XANES study of the Ti valence state change and in-situ XRD study of the LTO phase change during aging at elevated temperatures. As we proposed, the first step is the self-discharge of $Li_7Ti_5O_{12}$, which releases lithium ion and electrons and causes the Ti valence change from Ti^{3+} to Ti^{4+}. The in-situ XRD study further confirms that at 60^oC aging, the LTO is undergoing phase transition from $Li_7Ti_5O_{12}$ to $Li_4Ti_5O_{12}$. Evolution of the gas is the sequent reaction involving the electrons released from the self-discharge. Surface passivation of LTO has been proposed in order to cut off the direct electron transfer pathway through which the

electron is shuttled to participate the gassing reaction. Besides additives demonstrated previous, surface coating of LTO particles through atomic layer deposition technique also shows positive effect by reducing gassing.

(a) Summary of work in the past quarter related to milestone (a).

Previously, we have directly witnessed the Ti valence state change during aging at various high temperatures by applying in-situ XANES technique. Now, with in-situ XRD data, it further proves that the lithiated LTO is undergoing phase transition from $Li_7Ti_5O_{12}$ to $Li_4Ti_5O_{12}$. Such phase transition can be demonstrated by the peak shift shown in Fig 1 and 2. Fig 1 shows the phase (844) peak shift to left as aging. At the same time, the peak broadening was also observed, which is the sign of the co-existence of two phases ($Li_7Ti_5O_{12}$ / $Li_4Ti_5O_{12}$). The same phenomena, peak shifting and broadening, was also observed in Fig. 2 for phase 840. After about 2 ½ hrs aging, the shifted peak is getting close to the one in $Li_4Ti_5O_{12}$ phase, but does not overlap with it. This means that in the giving time period, such phase transition from $Li_7Ti_5O_{12}$ to $Li_4Ti_5O_{12}$ couldn't complete. This is consistent with the real experiments, the gassing is happening over days instead of hours as shown in Fig.3.

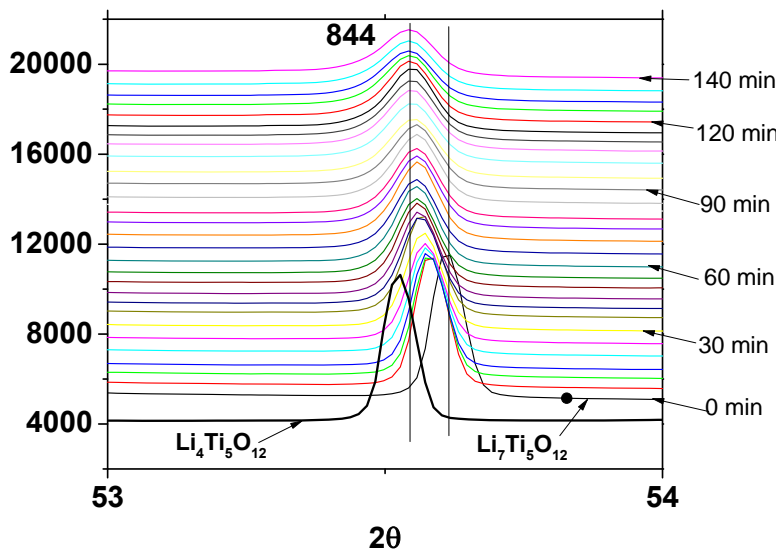**Fig 1** shows the peak (844) shifting when $Li_7Ti_5O_{12}$ was aging at $60^{\circ}C$ with electrolyte 1.2M LiPF6 in EC:EMC=3/7. After about 2 ½ hours aging, the peak is getting close to but not overlap with phase $Li_4Ti_5O_{12}$.

Fig 2 shows the peak (840) shifting when $Li_7Ti_5O_{12}$ was aging at $60^{\circ}C$ with electrolyte 1.2M $LiPF_6$ in EC:EMC=3/7. After about 2 ½ hours aging, the peak is getting close to but not overlap with phase $Li_4Ti_5O_{12}$.


68
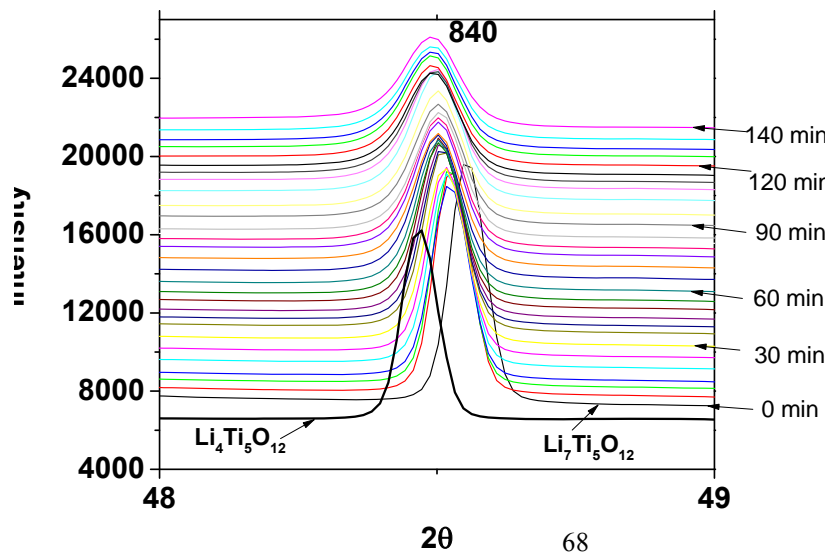
(b) Summary of work in the past quarter related to milestone (b)

Since the charged LTO surface is the place the reaction taking place, passivation of the LTO surface might be able to cut off the reaction pathway. Previously, we demonstrated that certain additives can form effective passivation film on the surface of the LTO electrode, hence to reduce the gas generation.

Besides that, direct surface coating of the protection film also shows positive effect in reducing gassing. Fig. 3 shows the gas evolution with time. With ALD coated Al_2O_3 on the surface of LTO particles, the amount of gas generated is reduced. Thicker coating (ALD 5 cycles) has better performance in reducing gassing than thinner coating (ALD 3 cycles) in the first 30 days. After that, the difference is getting smaller.

Fig 3 shows the effect of surface coating through ALD in reducing the gas. With Al_2O_3 coating on the surface of LTO particles, the generated gas volume is reduced.
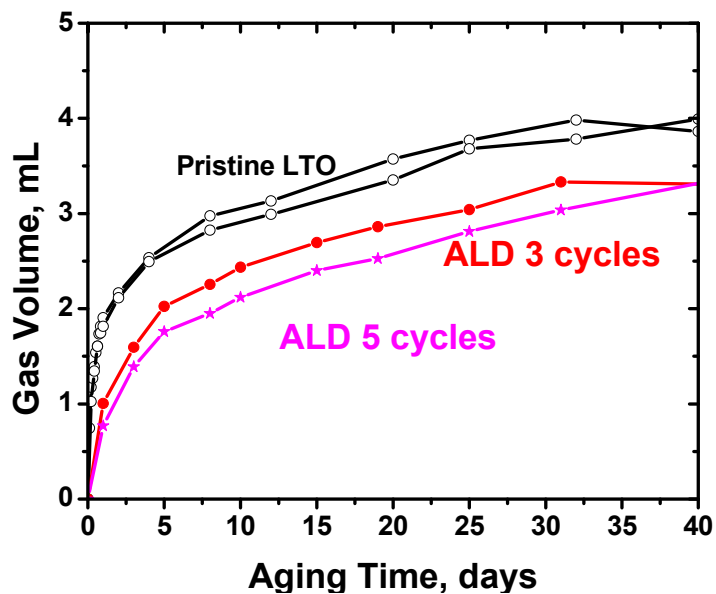
Publications, Reports, Intellectual property or patent application filed this quarter. (Please be rigorous, include internal reports--invention records, etc.)

No publications, reports, or patents were submitted this quarter.

TASK 1
Battery Cell Materials Development

Project Number: 1.1L (ES113)

Project Title: Development of High Voltage Electrolyte for Lithium Ion Battery (High Voltage Electrolyte for Lithium Batteries)

Project PI, Institution: Zhengcheng Zhang, Khalil Amine, Argonne National Laboratory

Collaborators (include industry):
Libo Hu, Argonne National Laboratory
Huiming Wu, Argonne National Laboratory
Wei Weng, Argonne National Laboratory
Kevin Gering, Idaho National Laboratory
Daikin Industry

Project Start/End Dates: October 2010 / September 2014

Objectives: The objective of this work is to develop an electrolyte with wide electrochemical window that can provide stable cycling performance for cathode materials that can charge above 4.5 V.

FY12's objective is to enable the LNMO/LTO and LNMO/graphite cell using fluorinated electrolyte solvents as high voltage electrolyte.

Approach: Investigate new solvents as high voltage electrolyte applications. Based on the theoretical calculation, the introduction of electron-withdrawing group on the will increase the oxidation stability. We will continue the fluorinated carbonate based electrolyte study in the new fiscal year. We will also design and synthesize new solvents to further explore other possibilities for high voltage application. Exploring a hybrid electrolyte made of the mixture of the above solvents is the general approach.

Milestones:
(a.) Material evaluation in the graphite cell system, December, 2012 (Complete)
(b.) New material synthesis and purification, March, 2012 (Complete)
(c.) Physical properties of the new high voltage electrolyte candidates (March, 2012 (Complete)
(d.) Complete evaluation of high voltage electrolyte using LNMO/LTO and LNMO/Graphite chemistries, September 2012 (On schedule)

Financial data: $300K

PROGRESS TOWARD MILESTONES

(a) Summary of work in the past quarter related to milestone

Fluorinated carbonates were synthesized and purified. Their oxidation/reduction potentials were calculated by DFT method. As shown in Table 1, the fluorinated carbonate showed improved oxidation stability over the non-fluorinated carbonates. Experiment data are consistent with the theoretical calculation results.

Table 1. Theoretical Oxidation and Reduction Potential of Some Fluorinated Carbonate Solvents.
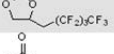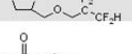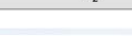
| Code Name	Chemical Structure	$P_{ox}{}^a$ / V	P_{red} / V
EC		6.91	1.43
PC		6.80	1.35
EMC		6.63	1.30
A8		6.97	1.69
A9		7.02	-
FEC		7.16	1.63
HFEEC		6.93	1.50
F3		7.10	1.58
D2		7.29	1.82

Figure 1 is the summary of the leakage current in a floating test using Pt/Li/Li electrochemical cell. At each potential from 5.0V to 6.4V, fluorinated carbonate electrolyte showed much smaller leakage current than Gen2, the traditional electrolyte, indicating the improved voltage tolerance.
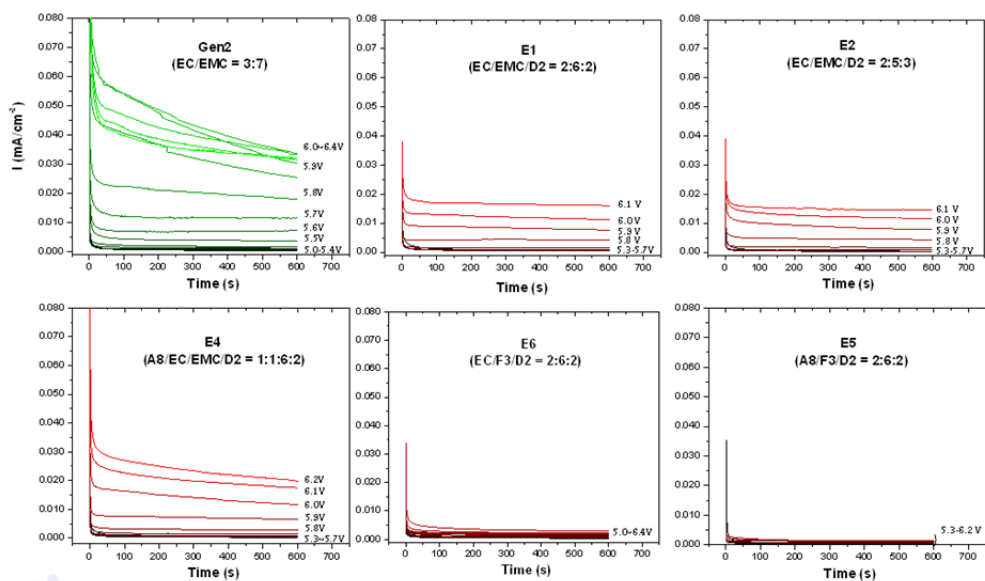
* Three-electrode electrochemical cell with Pt as working electrode and Li as reference and counter electrode.

Figure 1. Gen2 electrolyte and fluorinated electrolyte leakage currents at various potentials with Pt/Li/Li cell.

To further confirm the improved voltage stability, a real high voltage cell (LNMO/Li) was used to conduct the floating test and the test results are summarized in Figure 2. At 5.3V, the leakage current of fluorinated electrolyte is only about 25% of that of Gen2 electrolyte. This test is agreed well with LNMO/LTO cell performance reported in last quarter.
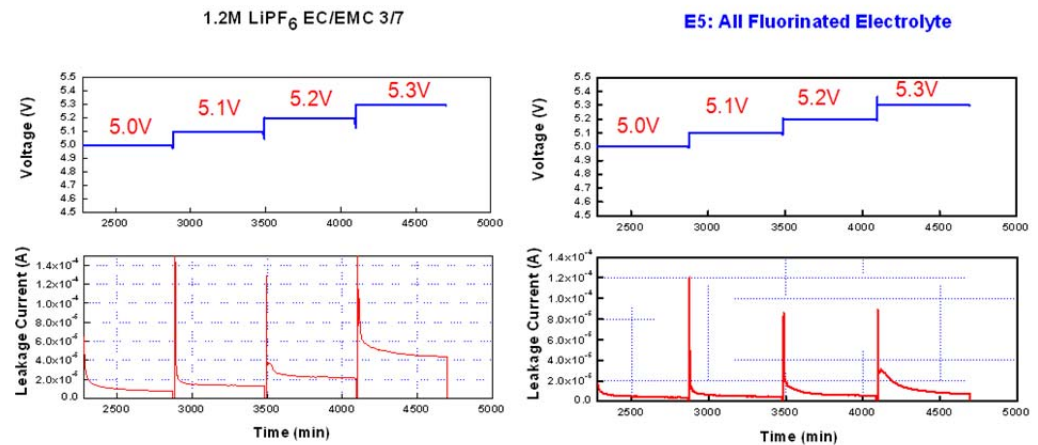
* (1) Working electrode: $LiNi_{0.5}Mn_{1.5}O_4$ /Carbon Black/Binder: 84%/8%/8% in weight
  (2) Electrode disc area: 1.6cm^2
  (3) Reference electrode: Li metal
  (4) CC-CV charge the LNMO/Li cell with C/10 rate to 5.0V, 5.1V, 5.2V and 5.3V, respectively. Maintain at each voltage for 10h to observe the leakage current.

Figure 2. Gen2 electrolyte and fluorinated electrolyte leakage currents at various potentials with LNMO/Li cell.

(b) Summary of work in the past quarter related to milestone

The first cyclic voltammetry scan of LNMO/graphite cell with new formulated fluorinated electrolytes is shown in Figure 3. Electrolyte E1 and E4 showed more symmetrical redox curves than electrolyte E2 and E5, indicating the different SEI formation process.
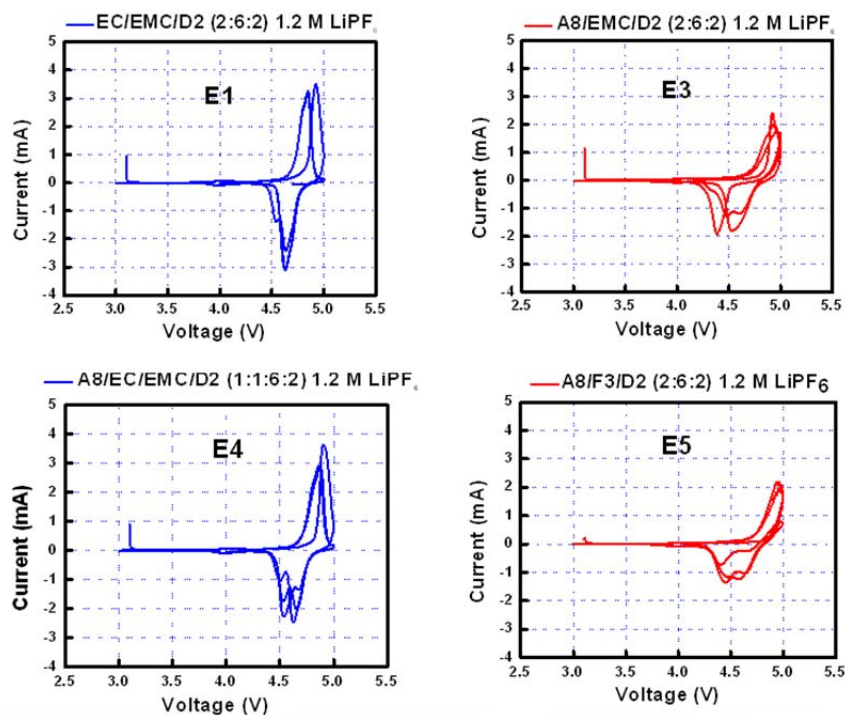

Figure 3. Cyclic voltammetry profiles of LNMO/Li cells using fluorinated electrolytes.

As evidenced from the cycling data shown in Figure 4 (a), electrolyte E5 has a very low initial charge and discharge capacity and a fading cycling performance indicating a poor SEI formation with continuous Li consuming side reaction occurring on the graphite abode. Among the fluorinated electrolytes, E1 showed the best compatibility with 5V LNNO and graphite electrode (Fig.3). It is speculated that EC component in E1 electrolyte formulation accounts for the SEI formation while D2 provides voltage stability and surface wetting. This formulation also cycles better than Gen2 electrolyte at room temperature (Figure 4(b)).
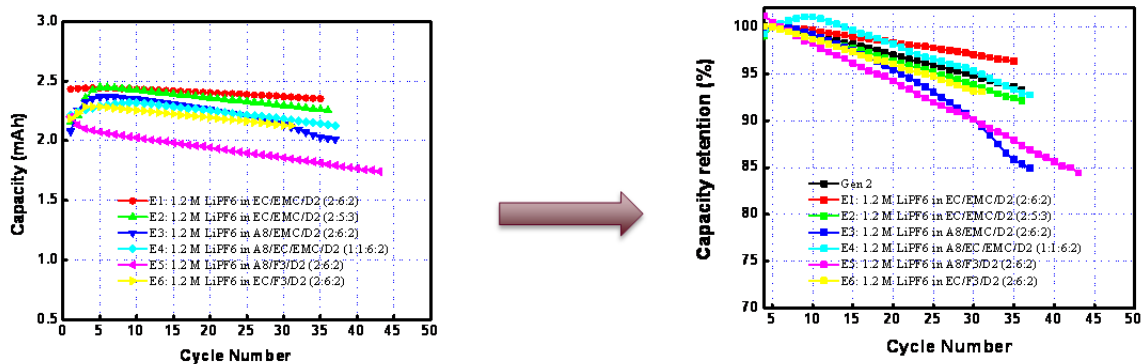
Figure 4. LNMO/Graphite cell cycling profiles at room temperature (a) and the cycling performance using fluorinated electrolytes (b) Normalized capacity retention of fluorinated electrolyte and Gen2. Cycling rate is C/10, cutoff voltage is 3.5-4.9 V.

(c) Summary of work in the past quarter related to milestone

The ambient cycling performance of the E1, E2, E4 fluorinated electrolytes showed improved cyclability, however at high temperature, their performance getting worse, indicating the instability of the SEI layers. E4's formulation includes EC, which is good for SEI formation, and A8, F3 and D2, which are all high voltage solvent and additives. This quarter's research clearly indicates that we need to develop the integrated SEI formation additive for this new electrolyte system.

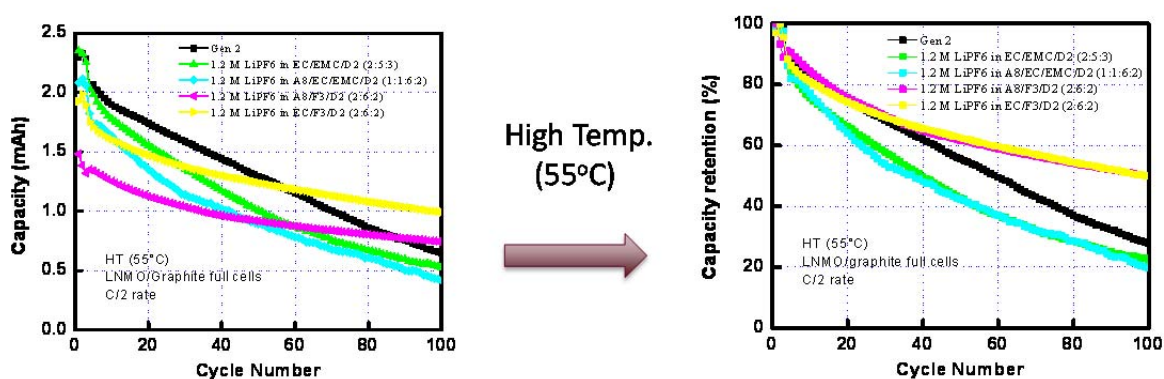

Figure 5. LNMO/Graphite cell cycling profiles at 55°C(a) and the cycling performance using fluorinated electrolytes (b) Normalized capacity retention of fluorinated electrolyte and Gen2. Cycling rate is C/10, cutoff voltage is 3.5-4.9 V.

74

Publications, Reports, Intellectual property or patent application filed this quarter. (Please be rigorous, include internal reports--invention records, etc.)

Argonne-Daikin Joint Workshop on High Voltage Electrolyte, Feb. 25, 2012

Electrolyte for electrochemical cells. US patent application ANL-IN-09-039.

Recent development of high voltage electrolytes, oral presentation on USABC-ABR-BATT Electrolyte Workshop, Aug.18-19, 2011, Southfield, MI, US.

Advanced Electrolyte and Electrolyte Additive for lithium ion batteries, invited talk on 4th International Conference on Advanced Lithium Batteries for Automotive Application (ABAA-4), Sep. 20-23, 2011, Beijing, China.

Advanced Battery Materials for EV Applications, invited talk on EV Battery Tech: 5th Global Cost Reduction Initiative, Feb. 28-29, 2012 London, United Kingdom

TASK 1
Battery Cell Materials Development

Project Number: 1.2D (ES114)

Project Title: High Capacity Composite Carbon Anodes Fabricated by Autogenic Reactions

Project PI, Institution: Vilas G. Pol, Argonne

Collaborators (include industry): Michael M. Thackeray (Co-PI, Argonne), ConocoPhillips, Superior Graphite

Project Start/End Dates: 1 October 2011/30 September 2012

Objectives:
The objectives of this project are to evaluate *high capacity*, spherically-shaped carbon particles, combined with lithium-alloying elements as anode materials for HEVs, PHEVs and EVs and to compare their electrochemical behavior with commercial carbon-composite electrode materials.

Approach:
1) Exploit autogenic reactions to prepare spherical carbon quickly, cost-effectively and reliably;
2) Collaborate with industry to access high-temperature furnaces to increase the graphitic component in spherical carbon;
3) Increase the capacity of the carbon spheres by combining them with lithium alloying elements to form carbon-composite anode materials;
4) Study and compare the electrochemical, chemical, physical and thermal properties of Argonne's carbon-composite products with commercially available carbon-composite materials;
5) Optimize processing conditions and evaluate the electrochemical properties of pristine and carbon-composite materials in collaboration with industry;

Milestones:
(a) Consolidate industrial collaboration for this project (January 2012);
(b) Prepare carbon samples for industrial partner for heat-treatment; prepare carbon-composite samples from Argonne's carbon materials and from industrial products (April 2012);
(c) Evaluate and optimize the electrochemical properties of carbon-composite samples in lithium half cells and full cells (September 2012);
(d) Determine the chemical, physical and thermal properties of Argonne's carbon-composite anodes with commercial carbon-composite materials (September 2012);

Financial data: $300K/year

PROGRESS TOWARD MILESTONES

Milestone (a). Consolidate industrial collaboration for this project

Industrial collaborations were strengthened during this quarter by company visits and information exchange. Batches of carbon spheres were prepared autogenically and shipped to an industrial collaborator, ConocoPhillips, for high temperature treatment at 2400 °C/8h and at 2800 °C/2h under inert conditions. Previously heat-treated carbon spheres (2400 °C/1h, Superior Graphite) were combined with lithium alloying elements to form carbon-composite materials to increase the reversible capacity of the carbon sphere electrodes. Commercial carbon products are being sent to Argonne for similar treatment with lithium alloying elements to increase their capacity and for comparative electrochemical evaluations.

Milestone (b). Prepare carbon samples for industrial partner for heat-treatment; prepare carbon-composite samples from Argonne's carbon materials and from industrial products

Pure spherical carbon electrodes typically offer a stable rechargeable capacity of 250 mAh/g. To further enhance their electrochemical properties, carbon microspheres, heated at 2400 ºC for one hour were used as a support to decorate Sn nanoparticles by sonochemical surface modifications. In a typical synthesis, heat-treated carbon spheres were first dispersed in ethanol, and subjected to ultrasonic irradiation [40% intensity] for one minute. The appropriate amount of $SnCl_2$, as a tin precursor, was then added to the carbon spheres-ethanol dispersion. Sonication of the slurry was carried out with high-intensity ultrasonic irradiation for seven minutes by direct immersion of a titanium horn (40% intensity, 20 kHz, 20W/cm^2) in a glass sonication cell under flowing argon gas. After removing the ethanol, the product was dried at 100 ºC and further heated under an inert argon atmosphere at 500 ºC for 3 hours. Intermediate products of carbon spheres coated with Sn-containing precursors, and the final heat-treated, Sn-coated carbon sphere products were evaluated for their morphological, compositional, structural and electrochemical properties.

Milestone (c). Evaluate and optimize the electrochemical properties of carbon composite samples in lithium half cells and full cells

Electrochemical evaluations were carried out in coin cells using a lithium metal foil electrode, a Sn-decorated carbon sphere counter electrode, and an electrolyte consisting of 1.2M $LiPF_6$ in a 3:7 mixture of ethylene carbonate (EC) and ethylmethyl carbonate (EMC). Figure 1 (left panel, inset) shows the discharge/charge behavior of a typical cell during the first two cycles between 1.5 to 0.01 V at a current density of 136 mA/g (about C/2.7 rate). The first-cycle charge and discharge capacities of the Sn-carbon composite electrode were 454 mAh/g and 293mAh/g, respectively, reflecting a first-cycle irreversible capacity loss of 35%. Thereafter, the cell demonstrated stable cycling; it delivered a steady reversible capacity of approximately 340 mAh/g at a C/2.7 rate for 100 cycles (Figure 1, left panel), which is considerably higher than that delivered by the

carbon spheres alone (about 250 mAh/g). By increasing the current rate to 1.5C and 2C, respectively, electrode capacities of approximately 320 mAh/g and 160 mAh/g were achieved. Efforts to increase the capacity above 400 mAh/g by tailoring the loading of lithium-alloying elements on the surface of the carbon spheres are in progress.

Milestone (d). Determine the chemical, physical and thermal properties of Argonne's carbon-composite anodes with commercial carbon-composite materials

Scanning and transmission electron micrographs of the Sn-coated carbon spheres (Figure 1, right panel) and energy dispersive X-ray analysis indicated that the surface of the carbon particles were uniformly covered by <10nm diameter Sn nanoparticles (~10 wt.%) that were identified by X-ray powder diffraction as metallic Sn with a tetragonal unit cell. Although it was apparent that no crystalline SnO_2 was formed during the sonication or heating processes under inert conditions, the Sn nanoparticles oxidized readily if exposed to air.

This project is a work-in-progress and is being extended to investigate the effects of sonochemical deposition of Sn and other alloying materials on industrially-prepared and commercially available carbon products. Preliminary results of Sn-coated carbon samples from industry have been obtained; these data will be presented in a subsequent report, once the results have been discussed with our industrial partner.
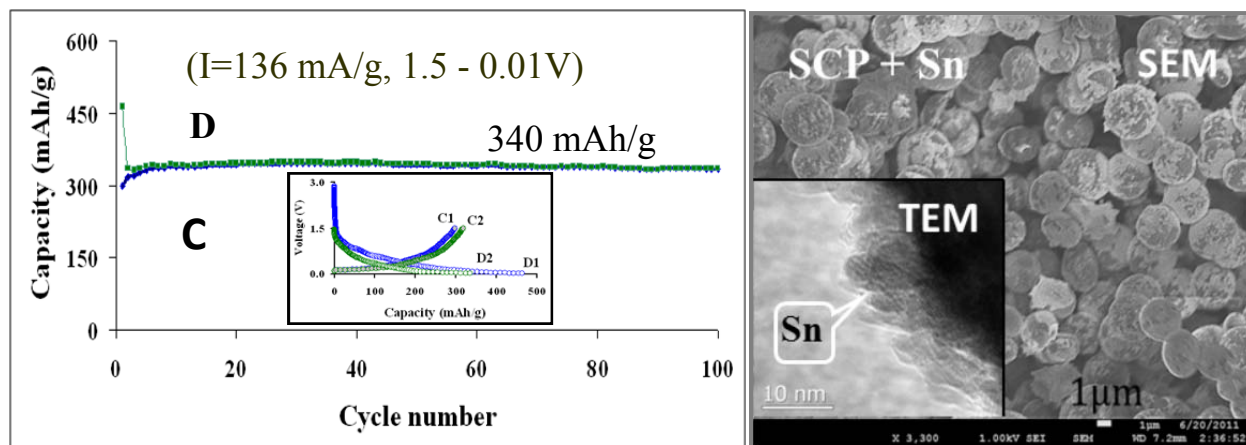

Figure 1. Left panel: First and second discharge-charge- profiles (inset) and capacity vs. cycle number plot of a lithium half cell with Sn-carbon sphere electrodes between 1.5 V and 0.01 V at a C/2.7 rate; Right panel: SEM and TEM (inset) of Sn-coated carbon spheres.

Publications, reports, talks, invention reports, patent applications.

1) V.G. Pol and M. M. Thackeray, *Thermal Treatment, Structural Evolution and Electrochemical Performance of Carbon Spheres Prepared by Autogenic Reactions*, MRS Spring Meeting, San Francisco, 9-13 April (2012).

2) V. G. Pol and M. M. Thackeray, *Spherical Carbon Particles: Synthesis, Characterization and Electrochemical Performance*, ConocoPhillips, Houston, 18 January (2012).

3) V. G. Pol and M. M. Thackeray, *Spherical Carbon Anodes Fabricated by Autogenic Reactions*, 2011 DOE Annual Peer Review Meeting Presentation, Washington DC, 9-13 May (2011).

TASK 1
Battery Cell Materials Development

Project Number: 1.1V (ES115)

Project Title: Synthesis and Development of High-Energy and High-Rate Cathode Materials from Ion-Exchange Reactions (Novel Composite Cathode Structures)

Project PI, Institution: Christopher Johnson, Argonne National Laboratory

Collaborators (include industry):
Michael Slater, Argonne National Laboratory
Donghan Kim, Argonne National Laboratory
Shawn Rood, Argonne National Laboratory
Eungje Lee, Argonne National Laboratory
Wenquan Lu, Argonne National Laboratory
Stephen Hackney. Michigan Technological University

Project Start/End Dates: October 2010 / September 2016

Objectives: Ion-exchange reactions are used to make new cathode materials with high-energy and high-rate. The objective is to produce an optimized material that shows an improvement over the drawbacks of Argonne high-energy cathodes. These ion-exchange cathodes should thus demonstrate <10% irreversible capacity in the first cycle, > 200 mAh/g at a C rate, no alteration in voltage profile during cycling, lower cost, and improved safety.

Approach: We will synthesize, characterize, and develop new cathode materials that exploit the difference in sodium versus lithium cation radii and their respective coordination properties. Cathodes will be derived from layered sodium transition metal oxide precursors that contain modest amounts of lithium in the transition metal (TM) layer. The sodium in the precursor materials is then ion-exchanged with lithium to form layered composite oxide cathodes for lithium batteries. We will focus on electrode materials that contain redox active Ni, and low cost Mn and Fe transition metals

Milestones: Materials will be produced and tested that will show progressively improved properties as the project moves forward.
(a) Synthesize new materials, September 2011, (completed)
        - Optimize ion-exchange reaction conditions, April 2012 (on-going)
(b) Characterize electrochemical properties of synthesized materials, March 2012, (on-going)
        - Demonstrate high-rate of 205 mAh/g @ 2C rate, March 2012, (completed)
(c) Characterize structure of materials, April 2012, (on-going)
        - Examine morphology of starting materials, and ion-exchange products, June 2012, (on-schedule)

(d) Continue optimization of Na, Li and transition metal content ratios in materials, September 2012, (on-schedule)

(e) Initiate measurement of thermal properties of charged cathode materials that have been compositionally optimized using DSC, September 2012, (on-schedule)

Financial data: $500K; $50K subcontracted to Prof. S. Hackney (Michigan Technological University)

PROGRESS TOWARD MILESTONES

(a) The ion-exchange reaction used to make the composite-structured Li-ion cathode from the precursor material ($Na_{1.0}Li_{0.2}(Ni_{0.25}Mn_{0.75})O_y$) is continually being optimized. After electrochemical analysis, it appears that the best route to date is refluxing methanol with LiBr and where the precursor was made originally from a sol-gel route (Fig.1). More synthesis work using similar reaction conditions will be conducted next.
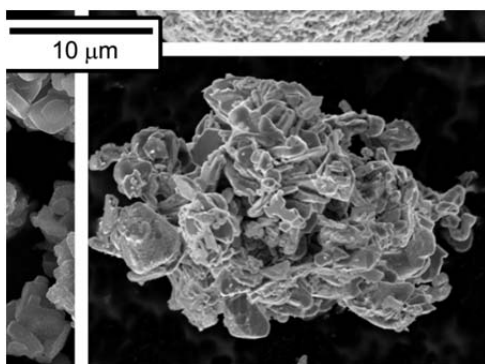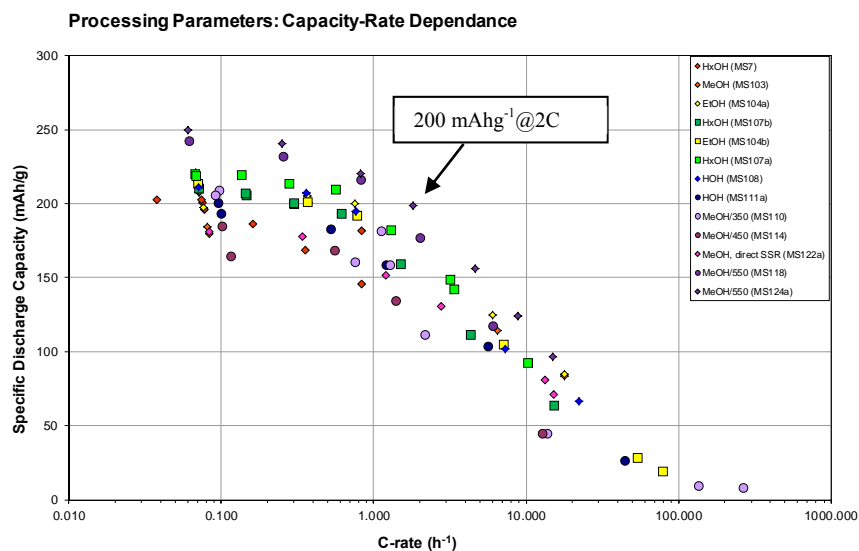

Fig. 1. SEM of sodium-based sol-gel precursor ($Na_{1.0}Li_{0.2}(Ni_{0.25}Mn_{0.75})O_y$) used for ion-exchange reaction to make the lithium cathode material with approximate composition of $Li_{1.05}Na_{0.02}Ni_{0.21}Mn_{0.63}O_2$.

Fig. 2. Rate capabilities of various lithium cathode materials with approximate composition of $Li_{1.05}Na_{0.02}Ni_{0.21}Mn_{0.63}O_2$. Legend lists the type of solvent used and heat-treating conditions.

Processing Parameters: Capacity-Rate Dependance

200 mAhg^{-1}@2C

Legend:
- HxOH (MS7)
- MeOH (MS103)
- EtOH (MS104a)
- HxOH (MS107b)
- EtOH (MS104b)
- HxOH (MS107a)
- HOH (MS108)
- HOH (MS111a)
- MeOH/350 (MS110)
- MeOH/450 (MS114)
- MeOH, direct SSR (MS122a)
- MeOH/550 (MS118)
- MeOH/550 (MS124a)

(y-axis) Specific Discharge Capacity (mAh/g)
(x-axis) C-rate (h^{-1})

(b) Various Li half cells for cathode testing made from ion-exchange materials were built. The numerous ion-exchange reaction conditions are listed in Fig. 2.

More tests are continuing, particularly on full cells. From the electrochemistry performance, it appears that the best performing cells have a chemically-integrated 5 V spinel ($LiNi_{0.5}Mn_{1.5}O_4$) component incorporated likely at the surface of the particles. The 5 V spinel will no only aid in the rate capability due to the 3D nature of its crystal structure, but also, the higher voltage contributes to a higher average voltage in the cathode material (Fig. 3).
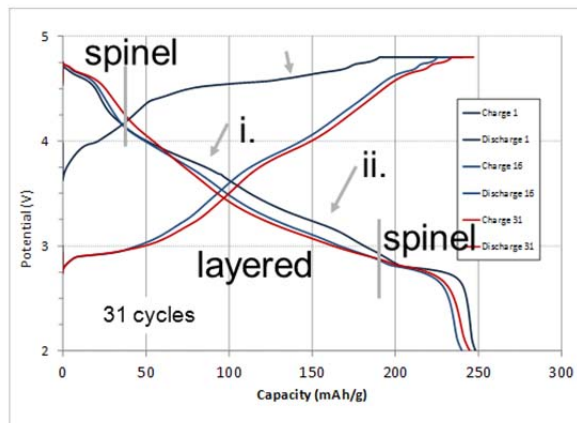

Fig. 3. Voltage profiles of $Li/Li_{1.05}Na_{0.02}Ni_{0.21}Mn_{0.63}O_2$ cell showing the layered and 5 V spinel signature.

(c) TEM analysis of the composite active material ($Li_{1.05}Na_{0.02}Ni_{0.21}Mn_{0.63}O_2$) was done. The layered component ($LiMO_2$) shows strain, and there are defects at the edge of the layers. Finally, the Li_2MnO_3 monoclinic layered-rock salt component has been positively identified in the composite active materials.

(d) The Mn/Ni ratio continues to be varied; we are working on $Na(Ni_{0.5}Mn_{0.5})O_2$ type precursor phase now with and without Li in the material. This will be reported in the next quarter.

(e) Thermal properties of the charged materials in milestone (a) are on schedule. Coatings may be evaluated in this task since they are known to belay the heat output.

Publications, Reports, Intellectual property or patent application filed this quarter.

<u>Posters</u>
- **"Composite Sodium-Lithium-Transition-Metal Oxides As Cathodes In Alkali-Ion Batteries"** <u>**Michael Slater**</u>**, Shawn Rood, Aaron DeWahl, Stephen Hackney, and Christopher Johnson, Gordon Research Conference: Batteries, 4 March 2012**

<u>Oral Presentations</u>
- **"Composite Sodium-Lithium-Transition-Metal Oxides As Cathodes In Alkali-Ion Batteries",** <u>**Michael Slater**</u>**, Aaron DeWahl, Victor Maroni, Stephen Hackney, Christopher Johnson, University of Illinois Postdoctoral Research Symposium, 27 January 2012.**

Battery Cell Materials Development

Project Number: ES038

Project Title: High Energy Density Ultracapacitors

Project PI, Institution: Patricia Smith, NAVSEA-Carderock

Collaborators: Thanh Tran and Thomas Jiang (NAVSEA-Carderock), Michael Wartelsky (SAIC), Deyang Qu (University of Mass., Boston)

Project Start/End Dates: FY09 to FY12

FY12 Objectives: Assess safety and electrochemical performance of LIC technology. Improve low-temperature energy density of lithium ion capacitor (LIC) by 25% (in comparison to 1st generation LIC cells).

Approach:

Identify candidate high-performance electrolyte compositions via technical discussions with battery/capacitor manufacturers, DOE investigators and from literature reports. Evaluate most promising systems by fabricating and cycling pouch cells in the temperature range from $25^{o}C$ to $-30^{o}C$. Investigate the effect of negative electrode carbon graphitization on cell performance and thermal stability. Identify optimal carbon pore size for low temperature performance. Evaluate the thermal stability of electrode materials, electrolytes, and cell design using differential scanning calorimetry (DSC) and accelerating rate calorimetry (ARC). Evaluate the effect of temperature and discharge rate on experimental LIC cell performance.

Milestones:

(a) Safety and performance evaluation of 1st generation LIC cell technology (March 2011). Status: Complete
(b) Identification of negative electrode material that exhibits high reversible capacity, high power capability, and good low temperature performance. (September 2012). Status: Initiated
(c) Identification of high-performance, low-temperature electrolyte (July 2011). Status: Complete
(d) Safety and performance evaluation of 2nd generation LIC cell technology (September 2011). Status: Complete
(e) Evaluation of the effect of temperature and discharge rate on the electrochemical performance of 1,000F experimental cells (January 2012). Status: Complete
(f) Evaluation of the self-discharge behavior of LIC cells. Comparison to lithium ion batteries and electrochemical double layer capacitors (June 2012). Status: Initiated

Financial Data: Project budget/year, amount subcontracted if appropriate
Funding Expensed 2Q FY12: $97,000

Progress Toward Milestones:

Although preliminary reports indicate that the energy density of the LIC (10-15 Wh/kg, 25 Wh/L) is superior to that of a conventional EDLC (4-6 Wh/kg, 5 Wh/L) at room temperature, the LIC performance at low or high temperatures has not been explored adequately. During this period, the electrochemical performance of two experimental 1,000F lithium ion capacitor cell designs was assessed over the temperature range of -30°C to 65°C. One design utilized $LIPF_6$ in ethylene carbonate (EC), propylene carbonate (PC) and diethyl carbonate (DEC). This electrolyte is referred to as generation 1 (Gen-1). The other cell's electrolyte, referred to as generation 2 (Gen-2), contained $LIPF_6$ in a similar, although not identical, carbonate mixture. Gen-2 electrolyte was shown to be approximately 65% more conductive than Gen-1 electrolyte at -20°C. As shown in Figures 1 and 2, cells containing Gen-2 electrolyte displayed better low temperature performance than Gen-1 cells while Gen-1 cells displayed better high temperature performance.
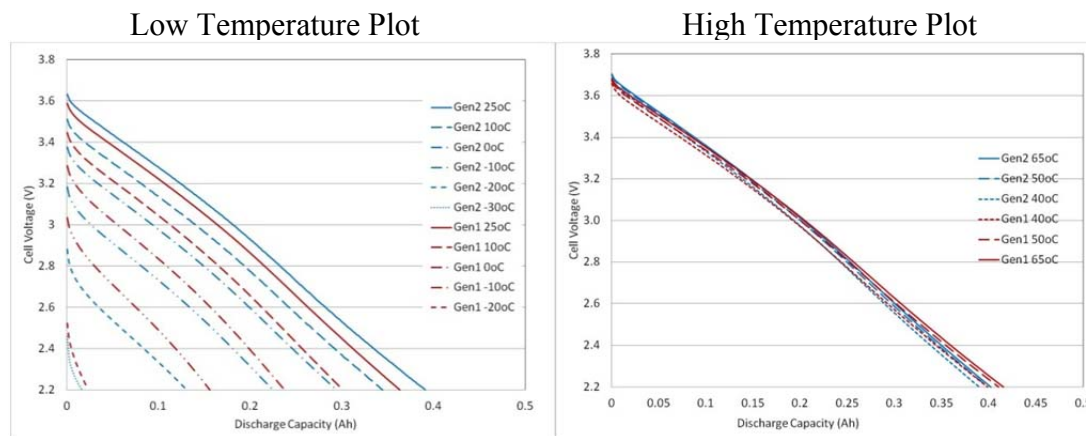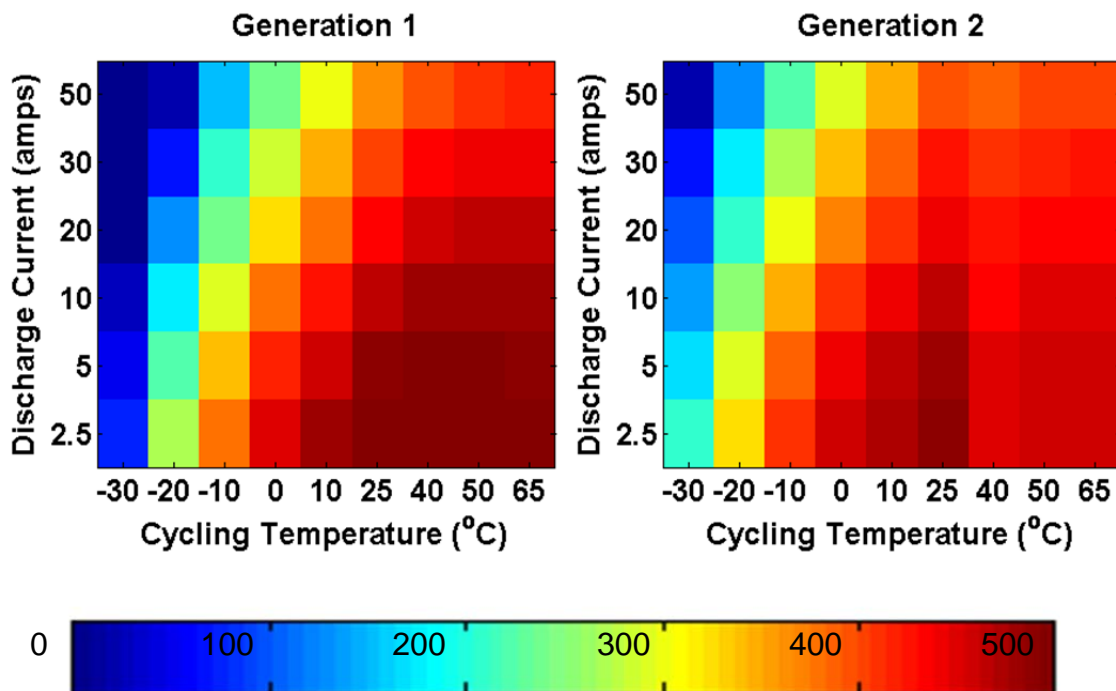

Figure 1. The effect of temperature on 1,000F experimental LIC cell discharge performance. Cells were cycled at the 100C rate (50A) from 3.8V to 2.2V. Gen-1 cells contained $LIPF_6$ in EC/ PC/ DEC, while Gen-2 contained a similar carbonate electrolyte.

Figure 2. Color plot showing the discharge capacities of two experimental LIC cell designs that were cycled at various temperatures and currents.

Publications, Reports, Intellectual Property or Patent Application Filed this Quarter.

None during this period

<h1 style="text-align:center">TASK 1
Battery Cell Materials Development</h1>

Project Number: 1.1Y (ES163)

Project Title: Transition Metal Precursors for High Capacity Cathode Materials

Project PI, Institution: Ilias Belharouak, Argonne National Laboratory

Collaborators (include industry): D. Wang, Argonne National Laboratory.

Project Start/End Dates: January 1, 2011-September 30, 2014

Objectives: Develop a better correlation between the electrochemical properties of a high capacity material and its structural, morphological, and physical properties.

Approach: Carbonate is developed to prepare the precursors that will serve to produce high capacity cathode materials $Li_{1+t}(Ni_xCo_yMn_z)_{1-t}O_2$ ($t \geq 0$, $x+y+z=1$). A comparative study using the three routes (carbonate, hydroxide, and oxalate) will be made at the level of the materials morphology, physical characteristics, and electrochemical properties.

Milestones:

a) Synthesis of ($Ni_{0.25}Mn_{0.75}CO_3$) carbonate precursor using a continuous stirred tank reactor (CSTR) continued. (Completed).
b) Structural, physical, and chemical characterizations of ($Ni_{0.25}Mn_{0.75}CO_3$). (Completed).
c) The electrochemical performance of the final lithiated cathode materials is investigated (Completed).

Financial data: $300K/year, $250K received in FY11.

PROGRESS TOWARD MILESTONES

This report is the continuation of the study initiated in the first quarter.

Figure 1 compares the primary particle size of the samples sieved below 20 μm (Fig. 1a), between 20 μm and 38 μm (Fig. 1b), and above 38 μm (Fig. 1c). After calcination, the primary particles of all samples shared polyhedral facets and had an average particle size between 100 and 300 nm. Also, we observed porosity between the primary particles, which could be useful for facilitating the penetration of electrolyte into the inner core of the secondary particle and, therefore, improve the overall electrochemical performance of the samples. Based on these observations, the lithium diffusion rate into the primary particles is expected to be more or less the same for all sieved samples.

Thereafter, EDXS (Fig. 2) was performed on cross-sectioned particles of $Ni_{0.25}Mn_{0.75}CO_3$ and $Li_{1.42}Ni_{0.25}Mn_{0.75}O_{2+\gamma}$ along the diameters of the samples sieved below 20 μm (Fig. 1a), between 20 μm and 38 μm (Fig. 1b), and above 38 μm (Fig. 1c). This experiment was conducted primarily to check the manganese and nickel compositions across the secondary particle of both the precursor and lithiated compounds after sieving. Nickel and manganese atomic percentages are shown as green and red lines, respectively, in Fig. 1. For all samples, we observed small fluctuations around the nominal atomic percentages (25% Ni and 75% Mn). This finding indicates that the chemical composition was relatively homogeneous for the precursors and cathode materials within the composition analysis limits of EDXS. One of the interesting observations was a "core-shell" type morphology in both the precursor and cathode materials, which was manifested as concentric circular rings for larger particles (Fig. 2). The interfaces between these layers can be distinguished by darker contrasts in the case of the precursors, whereas, in the case of cathode samples, the interfaces evolved into clear voids separating the nearby layers. The number of concentric rings increased with the increase in secondary particle size. Indeed, for particles below 20 μm, only one interface could be observed separating a core of about 15 μm and a thinner shell. For the particles larger than 38 μm, up to 10 rings could be found. The solid core and subsequent rings of the cathode sample are clearly visible in the high-magnification SEM image in Fig. 3. The cohesion between the adjacent dense rings is ensured through the continuity between the dendritic particles grown on each side of the rings. The high porosities observed between the dense rings could be useful for electrolyte impregnation across the layers. However, because the dense character of the rings could lead to the blockage of electrolyte, lithium diffusion between the outer and inner rings and the core of the particles could be inhibited.
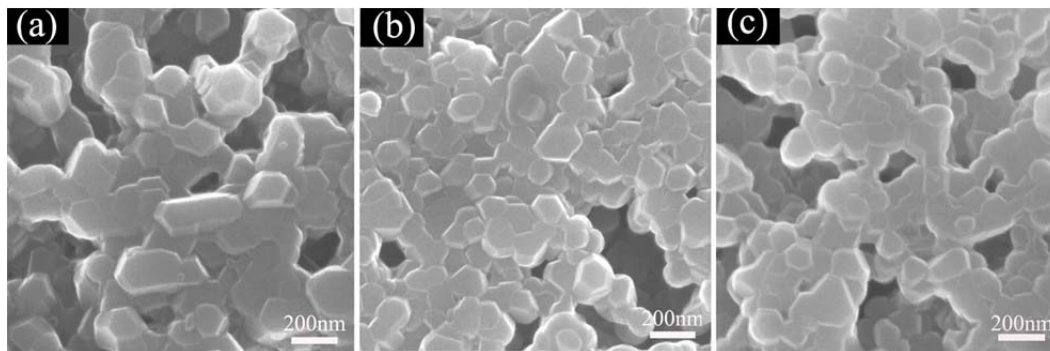

Fig. 1. SEM images of cathode materials with different secondary particle sizes: (a) less than 20 μm, (b) 20-38 μm, and (c) larger than 38 μm
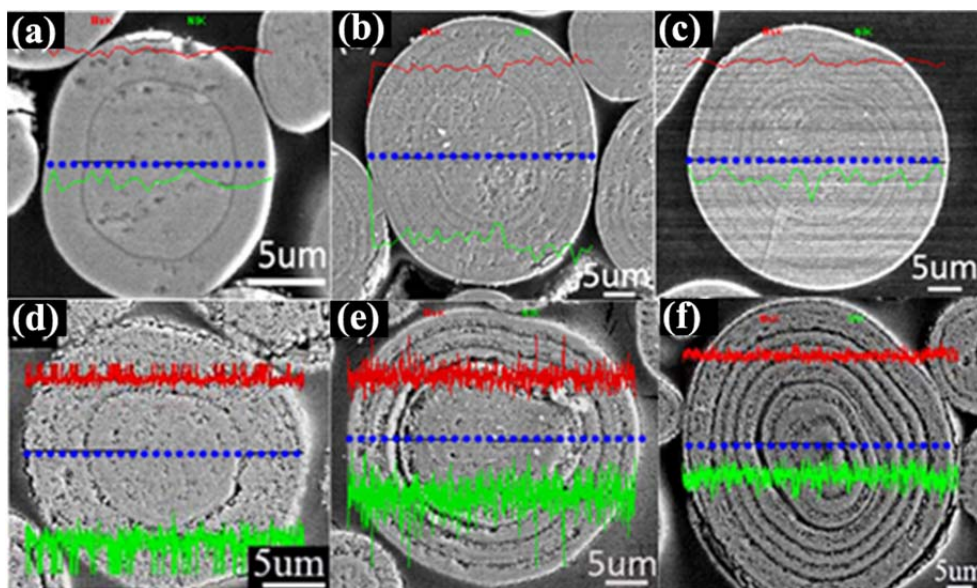
Fig. 2. EDXS curves superimposed on SEM images of bisected precursors with particle sizes of (a) <20 µm (b) 20-38 µm, and (c) 38-75 µm and cathode materials with particle sizes of (d) <20 µm (e) 20-38 µm, and (f) 38-75 µm
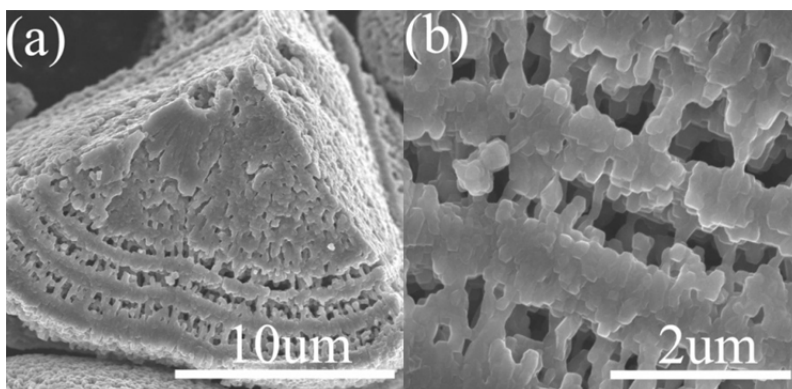

Fig. 3. SEM images of cathode materials with core-shell like features: (a) low magnification image and (b) higher magnification image of local area

Because of the secondary particles with different sizes, we suspected that, during calcination with lithium carbonate, the cathode sample particles may have different degrees of lithiation, depending upon their sizes. To investigate this hypothesis, high-energy XRD and ICP were used to characterize the structure and chemical composition of the lithiated samples after sieving. The XRD patterns of all samples are shown in Fig. 4. All of the cathodes with different particle sizes can be mainly indexed to the R3m space group, and matched well with the diffraction pattern of $LiNi_{0.5}Mn_{0.5}O_2$ reference material. The small additional peaks between 20 and 23° (2θ) are usually assigned to Li^+ and Mn^{4+} order in the manganese layer of the Li_2MnO_3 component in this material. Essentially, we did not notice a measurable difference between the diffraction patterns for the samples sieved below 20 µm,

between 20 μm and 38 μm, and above 38 μm. In fact, the calculated cell parameters obtained using Rietveld refinements (Table 1) were found to be similar for the different samples. Furthermore, the ICP results presented in Table 2 do not reveal any significant deviation in the Mn/Ni atomic ratio among the samples. However, the compositions in all samples were slightly lean in nickel, possibly due to the incomplete precipitation of nickel during the co-precipitation process. This point was discussed in our previous report.

In the next report we will provide details on the electrochemical properties on these compounds.
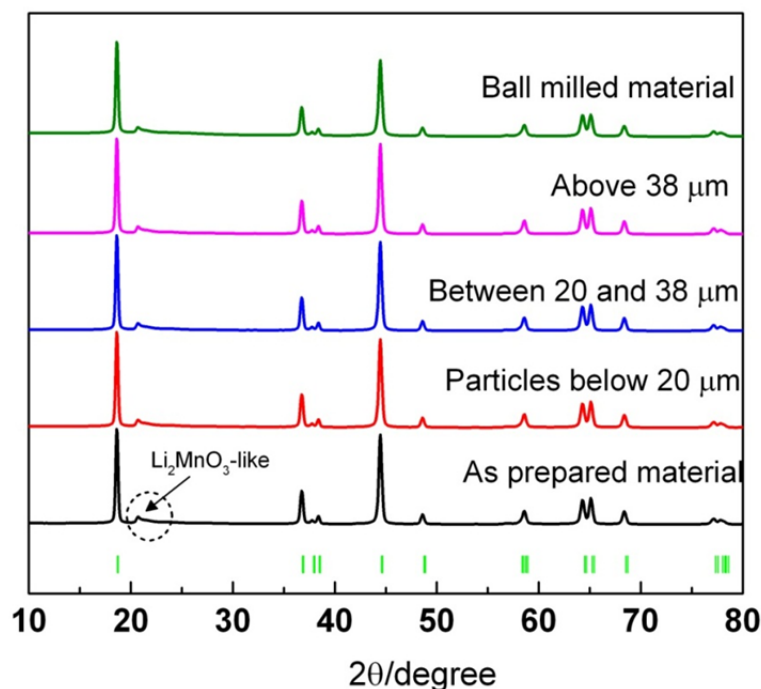

Fig. 4. High-energy XRD patterns for cathodes with different particle sizes

Sample	a (Å)	b (Å)	c (Å)	Cell Volume (Å^3)	c/a
Pristine	2.862(8)	2.862(8)	14.267(2)	101.266(7)	4.98(3)
>38um	2.862(7)	2.862(7)	14.266(9)	101.259(6)	4.98(3)
20-38um	2.862(9)	2.862(9)	14.268(2)	101.279(7)	4.98(3)
<20um	2.862(7)	2.862(7)	14.268(8)	101.274(4)	4.98(4)

Table 1. Cell parameters after GSAS refinement

Sample	Mn (atomic %)	Ni(atomic%)	Mn/Ni(atomic)	Li/(Mn+Ni) (atomic)
<20um	75.6±5.3	24.380±1.7	3.10±0.22	1.49±0.11
20-38um	75.9±5.4	24.111±1.7	3.14±0.22	1.52±0.11
>38um	75.9±5.4	24.065±1.7	3.15±0.22	1.50±0.11

Table 2. ICP result of cathode materials with different particle sizes

TASK 1
Battery Cell Materials Development

Project Number: FY12 New Start (ES164)

Project Title: Overcoming Processing Cost Barriers of High Performance Lithium Ion Battery Electrodes

Project PI, Institution: David Wood, Oak Ridge National Laboratory

Collaborators: Argonne National Laboratory, Sandia National Laboratories

Project Start/End Dates: 10/1/11 to 9/30/14

Objectives: Electrode suspensions for lithium ion batteries are currently formulated using expensive polyvinylidine fluoride (PVDF) binder and toxic, flammable n-methylpyrrolidone (NMP) solvent. It is desirable to replace these components with water and water-soluble binders, but methods of mass production of these suspensions are currently underdeveloped. The major problems with aqueous electrode dispersions are: 1) agglomeration of active phase particles and conductive carbon additive; 2) poor wetting of the dispersion to the current collector substrate; and 3) cracking of the electrode coating during drying. NMP based processing also has the inherent disadvantages of high solvent cost and the requirement that the solvent be recovered or recycled. Initial projections of the minimum cost savings associated with changing to water and water-soluble binder are 70-75%, or a reduction from \$0.210/Ah to \$0.055/Ah. The objective of this project is to transform lithium ion battery electrode manufacturing with the reduction or elimination of costly, toxic organic-solvents.

Approach: Fabrication of composite electrodes via organic (baseline) and aqueous suspensions will be completed. A focus will be placed on the effect of processing parameters and agglomerate size on the aqueous route cell performance and microstructure of the composite electrode. Several active anode graphite and cathode (NMC, $LiFePO_4$, etc.) materials will be selected with various water-soluble binders. The conductive carbon additive will be held constant. Rheological (viscosity) and colloidal (zeta potential) properties of the suspensions with and without dispersant will be measured with a focus on minimization of agglomerate size. These measurements will show the effects of agglomerate size and mixing methodology on suspension rheology and help determine the stability (i.e. ion exchange processes across the surfaces of various crystal structures) of active materials in the presence of water. Composite electrodes will be made by tape casting and slot-die coating, and the drying kinetics of the electrodes will be measured by monitoring the weight loss as a function of time and temperature. Solvent transport during drying will also be monitored as a method to control electrode morphology, porosity, and tortuosity. Electrode microstructure and surface chemistry will be characterized and correlated with cell performance. Electrochemical performance of electrode coatings made from the various suspensions

will be supplied to ORNL's strategic industrial partners for external validation in large cell formats.

Improved cell performance with reduced processing and raw material cost will be demonstrated using pilot-scale coatings. At ORNL coin cells will be tested and evaluated for irreversible capacity loss, AC impedance, capacity vs. charge and discharge rates, and long-term behavior through at least 500 charge-discharge cycles. Half cells, coin cells, and pouch cells will be constructed and evaluated. The coin cells will be used for screening and coarse evaluation of different suspension chemistries and coating methodologies. A fine tuning of these research areas will be completed using ORNL pouch cells and large format cells with ORNL's industrial partners. Electrode coatings will be produced on the ORNL slot-die coater and supplied in roll form to the industrial partners for assembly into large format cells.

Electrode morphology will be characterized by scanning electron microscopy (SEM) and TEM. The bulk structure and surface of the active materials will be characterized using XRD and XPS, respectively. In addition, in-situ TEM will be performed to investigate real-time SEI layer formation as a function of the different suspension chemistries.

Milestones:
  a) Development of an aqueous formulation for cathodes (March 2012); complete.
  b) Development of an aqueous formulation for anodes (May 2012); on schedule.
  c) Coating technique and drying protocol for anodes and cathodes (July 2012); on schedule.
  d) Development of porosity control in thin electrodes (September 2012); on schedule.
  e) Match cell performance in terms of initial capacity, irreversible capacity loss, and cyclability through 100 cycles of aqueous suspension and water-soluble binder to NMP/PVDF based suspensions (Sept. 2012); on schedule.

Financial data: $300k/year for FY12

PROGRESS TOWARD MILESTONES

Summary of work in the past quarter related to milestones (a) and (b).
All anode and cathode active and inactive materials were received in February 2012 from SNL and ANL, and electrode processing work was started. Currently, we have finished identification and verification of CMC as a dispersant for both NCM 523 and A12 graphite for aqueous processing. We have also completed the baseline coatings with NMP as the solvent, and the long-term performance of NCM 523 and A12 graphite is being obtained. Based on these results, a second set of baseline coatings will be made with necessary solid loading adjustments for electrode balancing.

1. Aqueous processing — selection of dispersant

Zeta potential was measured for dispersant selection for both $LiNi_{0.5}Mn_{0.3}Co_{0.2}O_2$ (NCM 523, Toda America) and A12 graphite (ConocoPhillips) using a ZetaPALS instrument (Brookhaven Instrument Coporation). Carboxymethyl cellulose (CMC) has been reported to be an effective dispersant for graphite and was selected for this work as a starting point. According to the zeta potential results in Figure 1, the isoeletric point (IEP) of A12 graphite was pH≈3. The addition of 1 wt% CMC (Fisher Scientific, MW = 250,000 g/mol, DS = 0.7) shifted the IEP to lower pH. More importantly, the zeta potential range of A12 with 1 wt% CMC was more negative compared to that of A12 and close to -30 mV at the natural pH of the A12 dispersion (pH≈6). Generally, dispersed particles with a surface charge more positive than 30 mV or more negative than -30 mV are considered to be stably dispersed. Thus, the stability of the A12 graphite dispersion with 1 wt% CMC was improved over that without CMC addition.
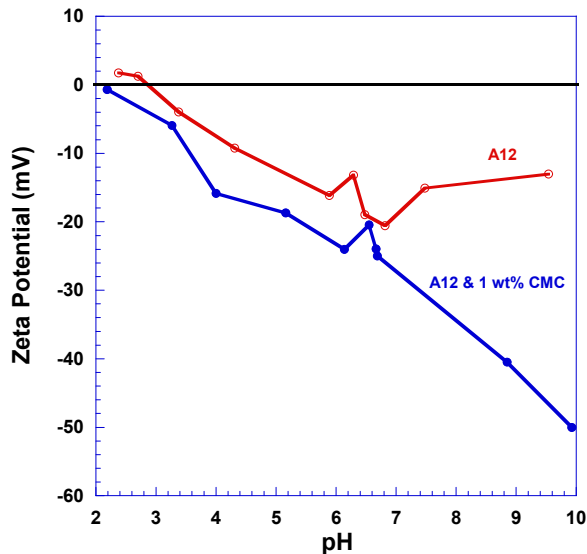

Figure 1. Zeta potential of A12 graphite with and without CMC; the addition of 1 wt% CMC resulted in a more negative charge on the A12 surface.
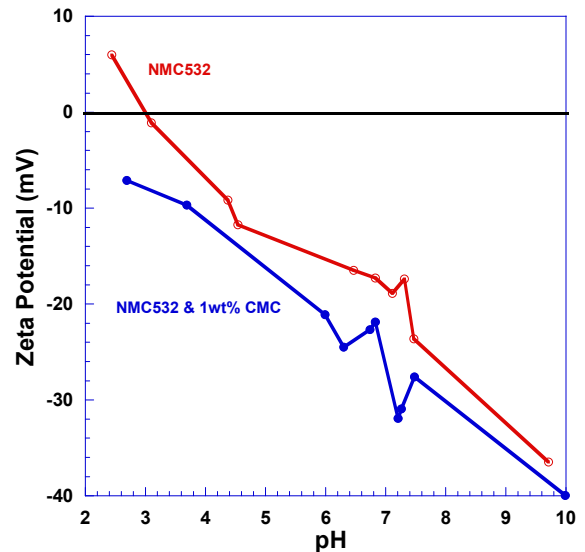
Figure 2. Zeta potential of NCM 523 with and without CMC; the addition of 1 wt% CMC resulted in a more negative charge on the NCM 523 surface.

Similarly, zeta potentials of NCM 523 with and without CMC were also investigated. The addition of 1 wt% CMC shifted the IEP to pH<2, and the zeta potential with CMC was more negative than -30 mV at the natural pH of NCM 523 (pH≈7.2). Therefore, CMC was also effective in improving the stability of the NCM 523 aqueous dispersion.

2. Organic system processing — baseline coating

A NCM 523 dispersion consisting of 50.7 wt% solids (NCM 523/Denka carbon black/Solvay 5130 PVDF=90/5/5 wt fraction) and 49.3 wt% NMP was prepared by first mixing NCM 523 with 5132 PVDF in NMP solution, followed by dispersing the Denka carbon black. An A12 graphite dispersion was prepared composed of 45 wt% solids

(A12/super P Li carbon/Kureha 9300 PVDF=92/2/6 wt fraction) and 55 wt% NMP. Super P Li carbon was first dispersed in the Kureha 9300 PVDF and NMP solution. Then A12 was mixed into the resulting dispersion with a high shear mixer (model 50, Netzsch). The rheological properties of both dispersions were measured using a Rheometer (AR-G2, TA Instrument). The dispersions were coated using a slot-die coater and the wet electrode was pre-dried when it passed through seven convection ovens with temperatures ranging from 150°F to 270°F.

Half cells were assembled inside an Ar-filled glove box with Li metal as the counter electrode, and Celgard 2325 was used as the separator. The electrolyte was 1.2 M LiPF$_6$ in ethylene carbonate: diethyl carbonate (3/7 wt ratio, Novolyte). The solid loadings for NCM 523 and A12 graphite were 17.0 mg/cm^2 and 14.0 mg/cm^2, respectively. These half cells were cycled using a VSP potentiostat (BioLogic) between 3.0 V and 4.2 V (for NCM 523), and 0.5 mV to 2.0 V (A12 graphite), respectively.

2.1 Rheological properties of NCM 523 and A12 graphite dispersions

Figure 3 shows the rheological properties of the NMP-based NCM 523 dispersion. The dispersion exhibited shear shinning behavior as shown in Figure 3a, and it was further verified by the shear stress results shown in Figure 3b, which was fitted with Herschel−Bulkley (H−B) model. The H−B equation is one of the most utilized models for situations where a nonlinear dependence exists for shear stress on shear rate. It is described by a power law equation:

$$\tau = \tau_0 + K\dot{\gamma}^n \quad \text{if } \tau > \tau_0$$
$$\dot{\gamma} = 0 \quad \text{if } \tau \leq \tau_0 \qquad (1)$$

where τ, τ_0, K, $\dot{\gamma}$ and n are the shear stress, yield stress (stress needed to initiate the flow), consistency index, shear rate and power-law index, respectively. If n = 1, this function reduces to the classical Bingham plastic equation. If $\tau_0 = 0$ and n = 1, this function describes Newtonian
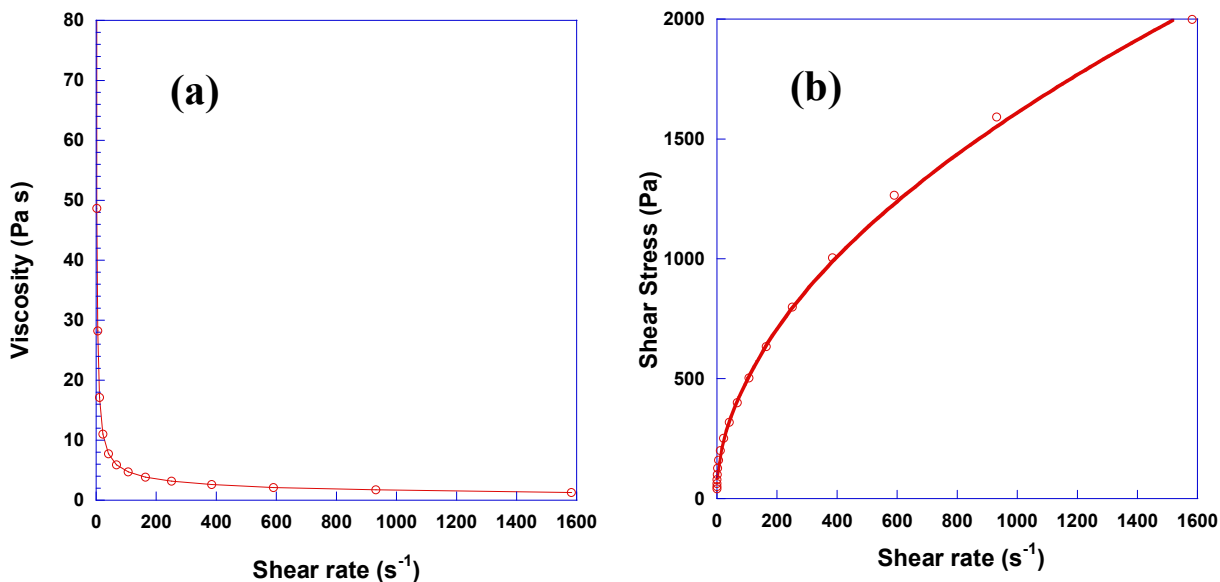
Figure 3. Rheological properties of the NCM 523 dispersion; a) viscosity vs. shear rate and b) shear stress vs shear rate.
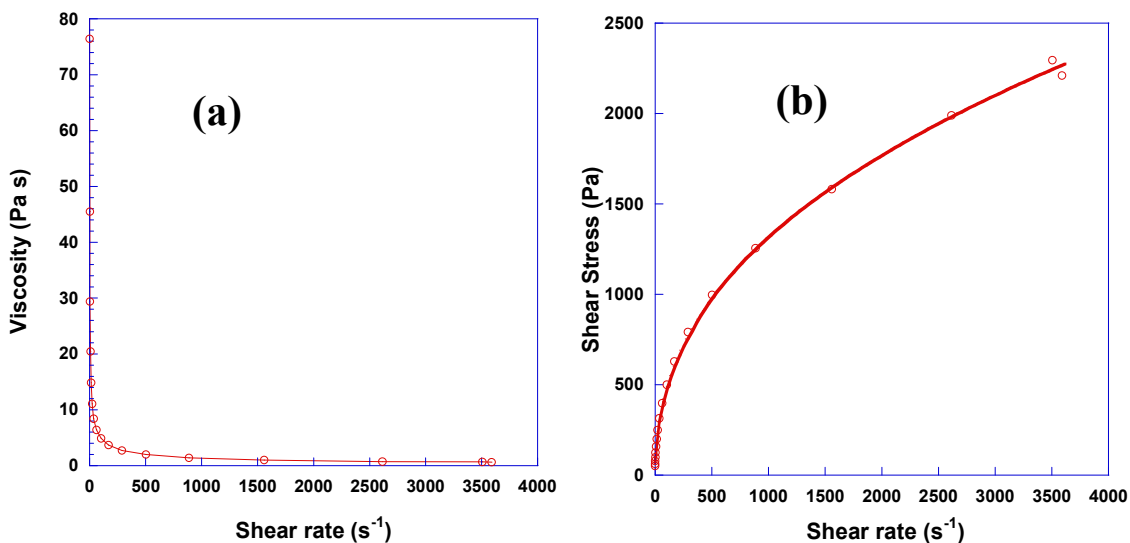

Figure 4. Rheological properties of A12 graphite dispersion; a) viscosity vs. shear rate and b) shear stress vs shear rate.

behavior. The power-law index for the NCM 523 dispersion was n=0.53, indicating shear shinning behavior. The rheological properties of the NMP-based A12 graphite dispersion is shown in Figure 4, and it also exhibited shear shinning behavior with n=0.42.

2.2 NCM 523 performance

NCM 523 cells are being evaluated by charging and discharging at C/5 for 50 cycles, and rate performance was investigated by charging at C/5 and varying the discharge rates. C-rate was calculated based on a theoretical capacity of 160 mAh/g for NCM 523. As shown in Figure 5a, NCM 523 demonstrated excellent first charge and discharge capacity of 172.1 and 170.0 mAh/g, respectively, with 2.1 mAh/g irreversible capacity loss (ICL). The discharge capacity after 25 cycles was 165.7 mAh/g, with retention of 97.5%. C-rate effect was plotted in Figure 5b and excellent capacity at C/10 and C/5 was obtained – higher than 165 mAh/g. The capacity dropped from ~165 mAh/g to ~140 mAh/g when the C-rate was increased from C/5 to 2C and the capacity decrease was much smaller subsequently – only dropping from ~140 mAh/g to ~134 mAh/g when C-rate was further increased from 2C to 10 C. This rate behavior indicates a well-produced electrode.
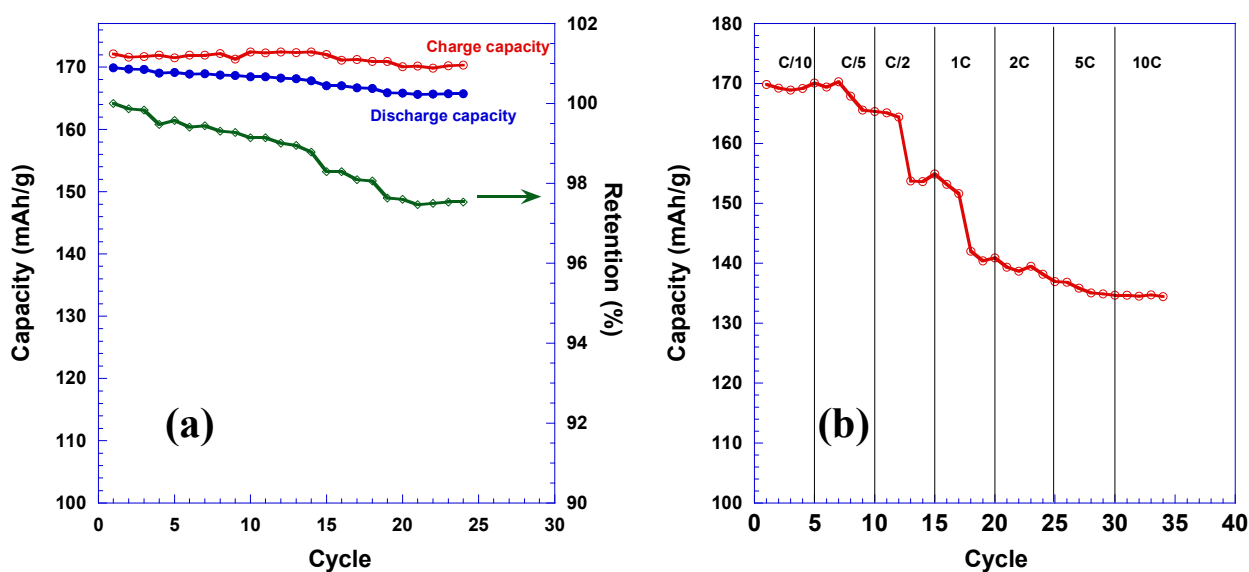

Figure 5. Performance of NCM 523 cathodes; a) 25 cycles discharged at C/5 and b) rate performance.

Publications, Reports, Intellectual property or patent application filed this quarter.

1. J. Li, C. Rulison, J. Kiggans, C. Daniel, and D.L. Wood, "Superior Performance of LiFePO$_4$ Cathode Dispersions via Corona Treatment and Surface Energy Optimization," *Journal of The Electrochemical Society*, Under Review, 2012.

TASK 1
Battery Cell Materials Development

Project Number: ES162

Project Title: Development of Industrially Viable Battery Electrode Coatings

Project PI, Institution: Robert Tenent and Anne Dillon (co-PI), NREL

Collaborators (include industry): Chunmei Ban (NREL), Steven George (University of Colorado, Boulder), Chris Orendorff (Sandia National Laboratory)

Project Start/End Dates: December, 2012 – September, 2016

Objectives: (1) Demonstration of Al_2O_3-based Atomic Layer Deposition coatings for improved cycling durability and abuse tolerance using standard electrode materials currently employed within the ABR program. (2) Design of an in-line atmospheric pressure atomic layer deposition (AP-ALD) system to demonstrate a process that may easily and inexpensively be integrated into the existing industrial Li-ion electrode fabrication lines.

Approach: Previously obtained results indicate that atomic layer deposition (ALD) can be used to form thin and conformal coatings on electrode materials that lead to both increased cycling lifetime, especially at high-rate, as well as abuse tolerance (e.g. stable cycling at high temperature and/or high voltage). This project will initially focus on using existing deposition capabilities to demonstrate an Al_2O_3-based ALD protective coating process for materials that are already commercially available at large-scale or are under advanced study within the VTP-EERE programs. This will include both anode and cathode materials in order to facilitate full cell testing and abuse studies. Initially, testing will be performed at the coin cell level to establish a stable baseline for comparison to existing data. In a later phase of the project larger format electrodes will be coated for testing in both pouch and 18650 cells. Coatings will be demonstrated on electrode materials produced at NREL as well as from outside parties. Finally, testing will be conducted both at NREL as well as within collaborating laboratories via a "round robin" process to ensure quality of data and the development of robust and transferrable processes.

In addition to small-scale exploratory research on various possible coating/electrode combinations, design work will be conducted for the development of a deposition system that will allow in-line coating at atmospheric pressure using an "ALD-like" process. The ultimate goal is to demonstrate a process that can be inexpensively integrated into existing industrial Li-ion battery electrode fabrication lines.

Milestones:

a) Demonstration of an Al_2O_3 ALD coating showing improved durability and abuse tolerance performance for a commercially viable cathode material
Due: May, 2012
Status: On Schedule

b) Design and initiate construction of a deposition system capable of in-line AP-ALD on commercially relevant substrate sizes.
Due: September 2012
Status: On Schedule

Financial data: Current Funding $300K/year

PROGRESS TOWARD MILESTONES

(a) Formed electrodes of Toda NMC 111 and A10 graphite were received from Sandia National Laboratories. A modified rotary ALD reactor was used to coat these electrodes with 2 cycles of ALD alumina. 18650 cells were then constructed using various combinations of coated and uncoated electrodes and subjected to thermal testing at Sandia. Data for ARC measurements comparing two cells is shown below. One cell was formed from an ALD coated anode and
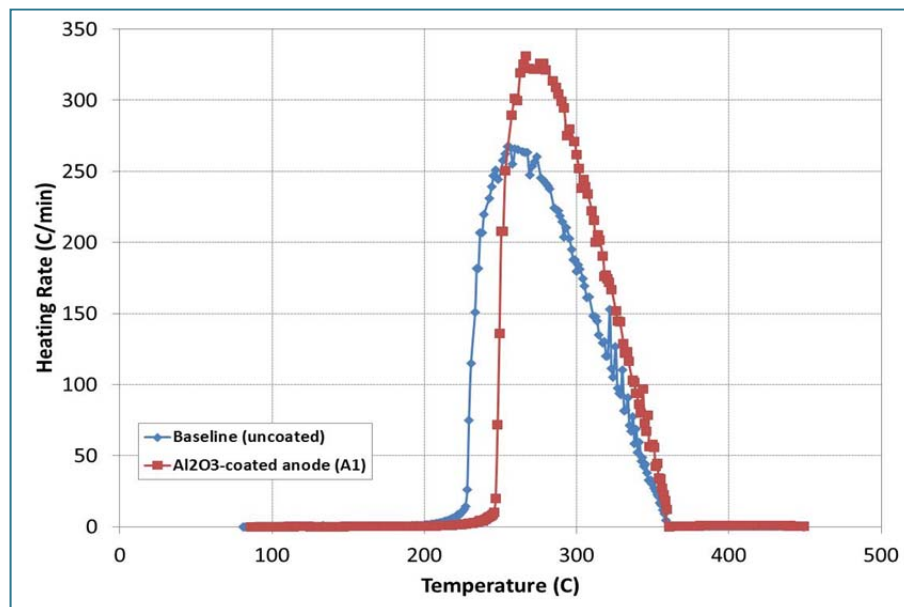
uncoated cathode. The second sample was a control device with no electrode coatings. The anode coated cell appears to show an approximately 20°C increase in on-set temperature for high rate thermal runaway. The higher anode decomposition suggests that thermal runaway can be suppressed by the presence of the ALD coating. Additional samples are currently under test, specifically coated cathode samples and results are expected shortly.

(b) Several meetings were held with collaborators at the University of Colorado-Boulder (CU) to discuss design parameters for the in-line ALD deposition system. CU has previously demonstrated a small scale prototype in-line ALD system and has obtained preliminary results with that system. Performance of that system and follow on units were discussed in detail including the addition of computational flow dynamics calculations to assess design performance. It has been decided to leverage the existing work from CU by hiring a post-doctoral researcher to continue efforts on the in-line ALD design with specific focus on the battery application. NREL representatives also visited a vendor (SierraTherm, Inc.) site to observe deposition systems that could be made capable of in-line ALD processing. These systems are presently used for coating glass and silicon samples using a similar method. Negotiations are currently underway for SierraTherm to supply a baseline system to NREL that will be used for on-line coatings. Furthermore, SierraTherm and their parent company are planning to visit NREL and discuss possibly further collaborations in the energy storage area. Anne Dillon also spoke regarding this project at the recent Gordon Conference on lithium-ion batteries and was approached by multiple vendors, including Advanced Materials about possible collaboration.

Publications, Reports, Intellectual property or patent application filed this quarter. (Please be rigorous, include internal reports--invention records, etc.)

Anne Dillon, Gordon Conference on Lithium-Ion Batteries, Jan, 2012

TASK 2
Calendar & Cycle Life Studies

Project Number: 2.1B (ES030)

Project Title: Fabricate PHEV Cells for Testing & Diagnostics in Cell Fabrication Facility

Project PI, Institution: Andrew Jansen and Bryant Polzin, Argonne National Laboratory

Collaborators (include industry):
Dennis Dees, Argonne National Laboratory
Steve Trask, Argonne National Laboratory
Wenquan Lu, Argonne National Laboratory
Chris Orendorff, Sandia National Laboratory
Claus Daniel and David Wood, Oak Ridge National Laboratory

Project Start/End Dates: October 2008 / September 2014

Objectives: The objective of this work is to speed the evaluation of novel battery materials from the ABR and BATT programs, as well as from universities and the battery industry. The main objective in FY12 is to fabricate in-house pouch and 18650 cells in Argonne's new dry room facility using advanced energy storage materials.

Approach: Promising new exploratory materials are often developed in small coin cells, which may or may not scale up well in large PHEV battery designs. For this reason, pouch cells or rigid cells such as 18650's will be used for proofing of new battery materials in the capacity range of 0.4 to 2 Ah.

Pouch cells will be used for initial evaluations of long-term exploratory materials. Pouch cells are an efficient method of determining the stability of a cell system during calendar and cycle life aging. If the chemistry is not stable, it is likely that gassing will occur inside the cell. This will result in the pouch cell bulging or rupturing if the gassing is significant. More established materials and chemistries (or those that pass the pouch cell evaluation) will be used in rigid cells (e.g. 18650s).

Milestones:
(a.) Optimize electrode slurry process using new Ross Mixer, March, 2012 (Completed)
(b.) Evaluate materials from MERF scale-up of Argonne's cathode, May, 2012   (On schedule)
(c.) First cell build using 18650 cell making equipment, June 2012   (On schedule)

Financial data: $1,100K

PROGRESS TOWARD MILESTONES

(a) Summary of work in the past quarter related to milestone (a)

The ability to make cells with long cycle life and good electrochemical performance is dependent on making high quality electrodes. Key to this is the ability to make homogenously dispersed electrode slurries with intimate contact between active particles and conductive additives. To accomplish this step, a high energy/shear planetary mixer was purchased from Ross with a 2 liter chamber capacity. This relatively small capacity size is ideal for the typical electrode builds made with the pilot scale coater, where supply of novel materials is often limited. Installation of this mixer was completed in October, 2011.


Numerous slurry batches were made using ConocoPhillips CGP-A12 graphite and Toda' high energy cathode material HE5050 ($Li_{1.2}Ni_{0.15}Co_{0.10}Mn_{0.55}O_2$) to gain experience with the mixer and to optimize the mixing parameters and process steps. It was estimated that the minimum slurry volume is near 300 mL; below that amount resulted in insufficient mixing due to splatter from the high shear blade and not fully engaging the high shear blade.   Single-sided and double-sided electrodes were made with both anode and cathode slurries.

Efforts were then spent in the making of xx3450 pouch cells using these electrodes, and with electrodes made with a small supply of an exploratory high-energy NMC cathode ($Li_{1.2}Ni_{0.3}Mn_{0.6}O_{2.1}$) made by Argonne researchers in several batches.

A quick summary is provided here of the cell build using A12 graphite and Toda HE5050. After formation and characterization cycles were conducted, the pouch cells were placed on a cycle life profile, which consisted of repeated units of 40 cycles at C/2 rate followed by an HPPC test at the 5C discharge pulse. Based on earlier Diagnostic results, the upper voltage was limited to 4.4 V to enhance life. These cells have achieved nearly 300 cycles and are still under test (at 30°C).
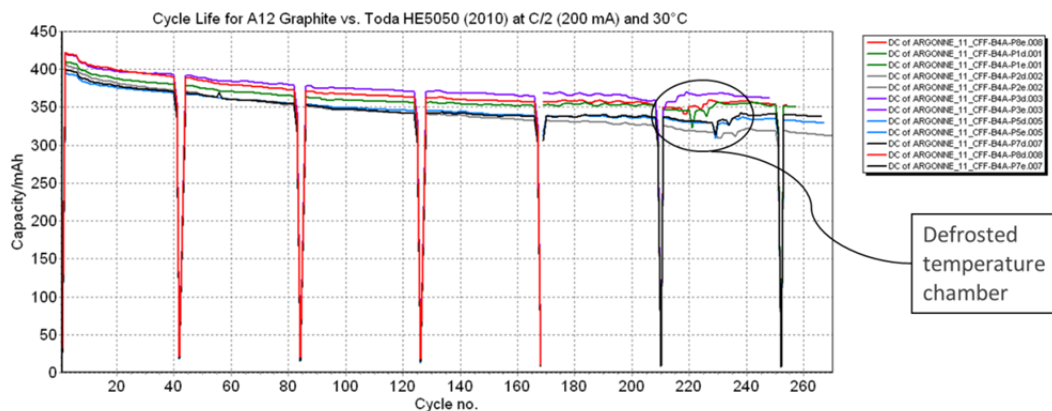

The following chart on the left shows the HPPC discharge ASI over 220 cycles of a typical cell from this cell build. From this data it can be determined that the ASI

increases significantly before cycle 50 and then gradually rises with cycling. The following chart on the right shows the 1-hour rest open circuit voltage from the HPPC tests over 220 cycles. Some evidence of voltage fading below 40% DoD is observed early in the life of the cells.
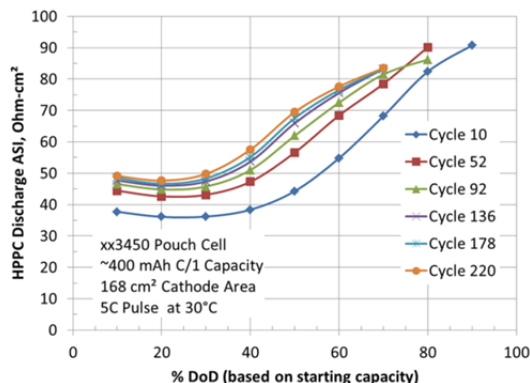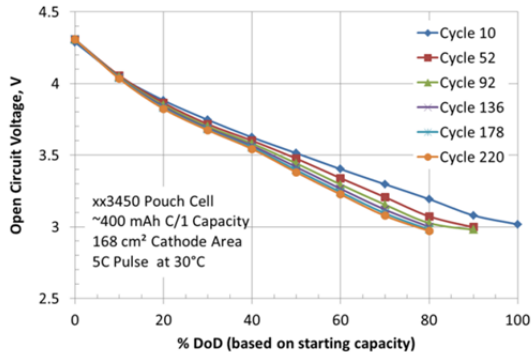
A summary of the rate capability for the first four pouch cell builds using high energy cathodes is shown in the table at right. Cell builds 1 and 4 used Toda HE5050 as the cathode, while cell builds 2 and 3 used small batches of R&D made cathode materials. Cell builds 3 and 4 were made with the new Ross mixer. The significant improvements in performance between cell builds 1 and 4, which have identical compositions, shows the level of expertise gained from repeated cell builds. Note that no electrolyte additives were used in these cell builds, which was done so that a baseline could be established

Rate	Capacity of Cell Builds (mAh/g cathode)			
	1	2	3	4
C	146	196	150	198
C/2	163	205	193	213
C/3	172	209	203	217
C/5	183	217	215	227

for each class of materials. Future cell builds with these materials will include additives and variations in formation process and test conditions.

(b) Summary of work in the past quarter related to milestone (b)

The Materials Engineering Research Facility (MERF) has scaled up their capability to make tens of kilograms of advanced cathode materials in their 20 L reactor – many of these cathode materials were discovered by researchers in the ABR Program. In fact, the first cathode material MERF is scaling up is a high-energy NMC cathode ($Li_{1.2}Ni_{0.3}Mn_{0.6}O_{2.1}$) developed by Argonne researchers, and referred to here as ABR1. They had great success in earlier scaling up this cathode to hundreds of grams using their 4 L reactor, and have now been successful in scaling up the process in their 20 L reactor. The MERF made a 10 kg cathode batch that was validated in initial testing at the coin cell level. One kg of this batch was then delivered to CFF in early March. Efforts are now centered on making electrodes and pouch cells with it.

(c) Summary of work in the past quarter related to milestone (c)

Effort was directed toward fabricating 18650 cells with commercially available materials and exploratory materials. It is anticipated that making 18650 cells will require significantly more material than pouch cell fabrication. For this reason, a commercial source was sought willing to supply openly at least 20 kg of advanced NCM material. Toda Kogyo agreed to supply Argonne with 40 kg of their NCM 5:2:3 cathode ($Li_{1.1}(Ni_{0.5}Co_{0.2}Mn_{0.3})_{0.9}O_2$). This material arrived in March of 2012 and was shared with Sandia and Oak Ridge for their cell builds. The first cell build in the 18650 format is expected to begin in May.

Publications, Reports, Intellectual property or patent application filed this quarter. (Please be rigorous, include internal reports--invention records, etc.)
None in this quarter.

TASK 2
Calendar & Cycle Life Studies

Project Number: 2.2B (ES031)

Project Title: Model Cell Chemistries (Electrochemistry Cell Model)

Project PI, Institution: Kevin Gallagher, Argonne National Laboratory

Collaborators (include industry):
Dennis Dees, Argonne National Laboratory
Daniel Abraham, Argonne National Laboratory
Andrew Jansen, Argonne National Laboratory
Wenquan Lu, Argonne National Laboratory
Bryant Polzin, Argonne National Laboratory
Kevin Gering, Idaho National Laboratory

Project Start/End Dates: October 2008 / September 2014

Objectives: The objective of this work is to correlate analytical diagnostic results with the electrochemical performance of advanced lithium-ion battery technologies for PHEV applications.
  – Link experimental efforts through electrochemical modeling studies.
  – Identify performance limitations and aging mechanisms.

Approach: Electrochemical modeling studies are utilized to elucidate transport, reaction, and thermodynamic phenomena in advanced lithium-ion cell chemistries. This work builds on earlier successful characterization and modeling studies in extending efforts to new PHEV technologies. The challenges center on expansion of the data base and enhancement of the modeling capabilities.

Milestones:
(a.) Complete initial parameter estimation of high-energy LMR-NMC/graphite system. September 2012, (On schedule)
(b.) Advance development of PHEV focused electrochemical models in support of programmatic goals. September 2014, (On schedule)
(c.) Complete integration of new differential algebraic equation solver package with enhanced capabilities and complete conversion of existing models to newly adopted package. September 2012, (On schedule)
(d.) Complete implementation and initial testing of full SEI growth model. December 2012, (Delayed)

Financial data: $400K/year

PROGRESS TOWARD MILESTONES

(a) Summary of work in the past quarter related to milestone (a)
The Electrochemical Impedance Spectroscopy (EIS) cell model[1] was used to examine the impedance characteristics of the LMR-NMC positive electrode. The fit of the model to positive electrode EIS data is given in Figure 1. The experimental results were obtained from diagnostic EIS studies conducted on LMR-NMC positive/graphite negative micro-reference electrode cells. As can be seen in Figure 1, the impedance is dominated by a high frequency interfacial arc associated in the model with the electronic contact resistance between the oxide active material and the conducting carbon additive. Similar to previous positive electrode EIS modeling studies, multiple particle fractions of oxide active material were utilized in the electrochemical model to improve the fit of the low frequency Warburg diffusional impedance.
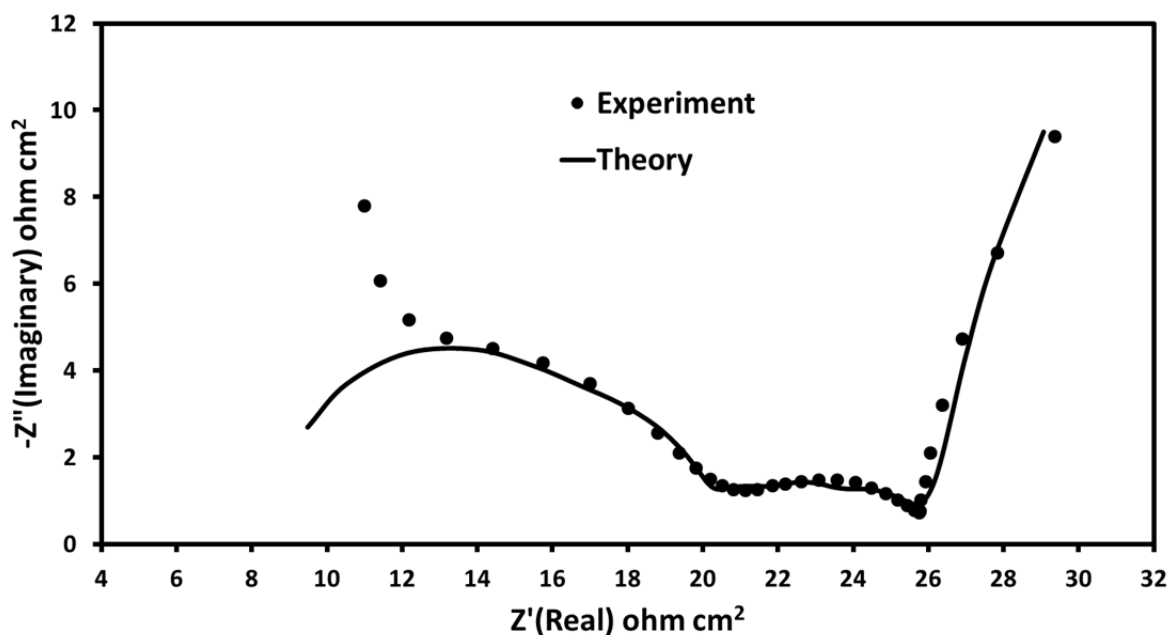

Figure 1. EIS model simulation of LMR-NMC positive electrode impedance data (100 kHz-10 mHz) taken at a cell voltage of 3.75 volts and 30°C.

A comparison of the LMR-NMC positive electrode impedance model parameters to earlier positive electrode studies is given in Table 1. All three electrodes examined have similar formulations and oxide particle size (secondary 9-12 μm average diameter), but vary in active material and loading:

NCA: Active Loading 8 mg/cm^2, BET 0.39 m^2/g, Electrode Thickness 35 μm
NMC: Active Loading 10.4 mg/cm^2, BET 0.41 m^2/g, Electrode Thickness 55 μm
LMR-NMC: Active Loading 6.4 mg/cm2, BET 2.63 m^2/g, Electrode Thickness 35 μm

The electrochemical model is capable of accounting for the differences in the electrodes, which allows for a more direct comparison of the material performance. In the model, the LMR-NMC active material is assumed to have thicker SEI film thickness (100 vs. 40 nm) than the other two oxides, because it operates at higher voltages using the same

electrolyte. Conversely, the oxide surface layer thickness is assumed to be thinner than the one measured for the NCA electrode (5 vs. 10 nm). The conventional NMC [Li(Li$_{0.1}$(Ni$_{1/3}$Mn$_{1/3}$Co$_{1/3}$)$_{0.9}$)O$_2$] electrode was assumed to not have an oxide surface layer. Diagnostic studies are underway to examine these assumptions.

From Table 1 it can be seen that the lithium diffusion coefficient in the LMR-NMC active material is an order-of-magnitude lower than that of the conventional NMC material. Also, the LMR-NMC positive electrode has a high electronic contact resistance (σ_P). However, the difference is accentuated because the model uses the electrochemically active area to establish the contact area. As seen below, it would be better to use a mass specific resistance (MSR) rather than an area specific resistance (ASR) for this parameter. Ideally, some measure of the electronic contact area would be optimal. In general, the LMR-NMC positive electrode's interfacial characteristics are somewhat worse than the other oxides, but are offset by the higher surface area.

Parameter	Active Material Surface Layer				SEI Film on Active Material			Electronic Contact Resistance	Kinetic and Capacitance			
	a	D_{si}	D_{sb}	K_s	D_+	κ_f	c_+	σ_p	i_o	C_c	C_d	C_f
	cm^{-1}	cm^2/s			cm^2/s	Ω^{-1}cm^{-1}	M	Ωcm^2	mA/cm^2	μf/cm^2		
NCA	8900	10^{-10}	10^{-10}	5	10^{-9}	10^{-7}	10^{-2}	0	1	0	40	0.3
NMC	7700	10^{-11}	10^{-11}	1	10^{-9}	10^{-7}	10^{-2}	170	0.1	0.06	100	0.5
LMR-NMC	48000	10^{-12}	10^{-12}	6	10^{-8}	10^{-8}	10^{-3}	1500	0.1	0.005	20	0.1

Table 1. Positive electrode electrochemical model parameters for NCA, NMC, and LMR-NMC electrodes.

As shown in Figure 2, the electrochemical modeling studies indicate a correlation between the measured powder electronic conductivity of active materials (i.e. conductivity of the dry powder in a pressed bed of only active material) and their particle contact resistance (i.e. σ_P ASR number from model converted to MSR) in the cell. The NMC electrode active material's lower electronic conductivity make them more challenging to obtain stable high-performance electrodes. On the positive side, limited electrode formulation optimization studies suggest that it is possible to significantly reduce the contact resistance associated with the NMC materials.
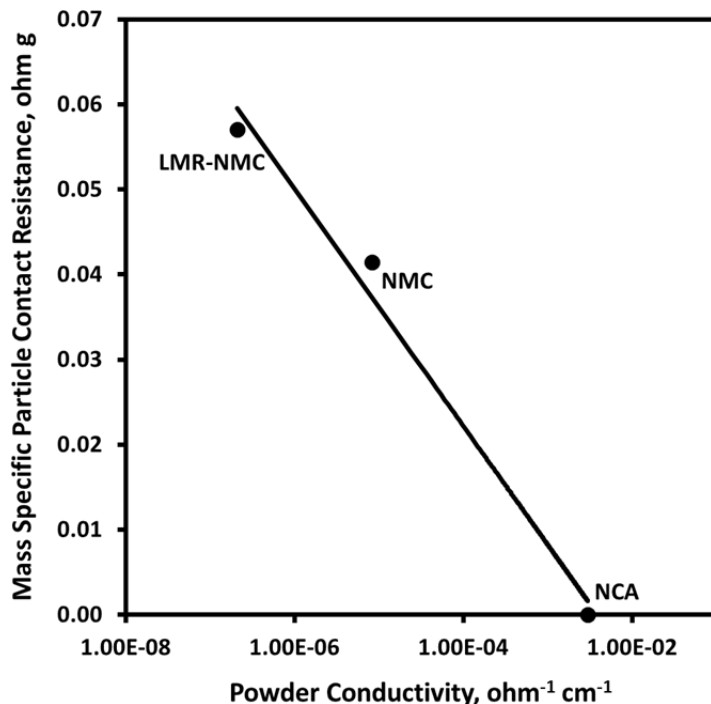
Figure 2. Mass specific particle contact resistance determined by electrochemical model for NCA, NMC and LMR-NMC electrodes compared to the dry powder's particle conductivity

(b) Summary of work in the past quarter related to milestone (b).
The discussion in the previous quarterly focused on the hysteresis observed in the open circuit voltage curve for the LMR-NMC materials (see Figure 4). The data was obtained using the Galvanostatic Intermittent Titration Technique (GITT) on LMR-NMC electrodes in half-cells (i.e. with a lithium counter electrode). As can be seen in Figure 3, DC electrochemical model[2] simulation, assuming a standard intercalation active material, of a typical GITT polarization/relaxation curve from a LMR-NMC half-cell is complicated by a very slow relaxation process not accounted for in the model. This slow relaxation phenomenon begs the question of whether the hysteresis is truly a thermodynamic phenomenon, or it is related to the slow relaxation of the electrode. This is fundamental question that has a significant impact on the model development for these LMR-NMC materials. A set of experiments were conducted to address this question. First, a fully discharged LMR-NMC half-cell was charged to 3.7 volts and held at constant voltage for a week, then discharged fully. Second, a fully charged LMR-NMC cell was discharged to 3.7 volts and held at constant voltage for a week, then discharged fully. As can be seen in Figure 4, there is a significant difference in capacity (i.e. lithium content in the LMR-NMC material) between the two experiments, even though they were both held at the same voltage for a week. This stable path dependence suggests that the physical process that generates the hysteresis appears to be thermodynamically stable. From the discussion above in part (a) both the slow relaxation and the hysteresis phenomena do not have a major impact on our ability to model the EIS phenomena. This is mostly related to the frequency range for the EIS data, which only went down to 10 mHz.
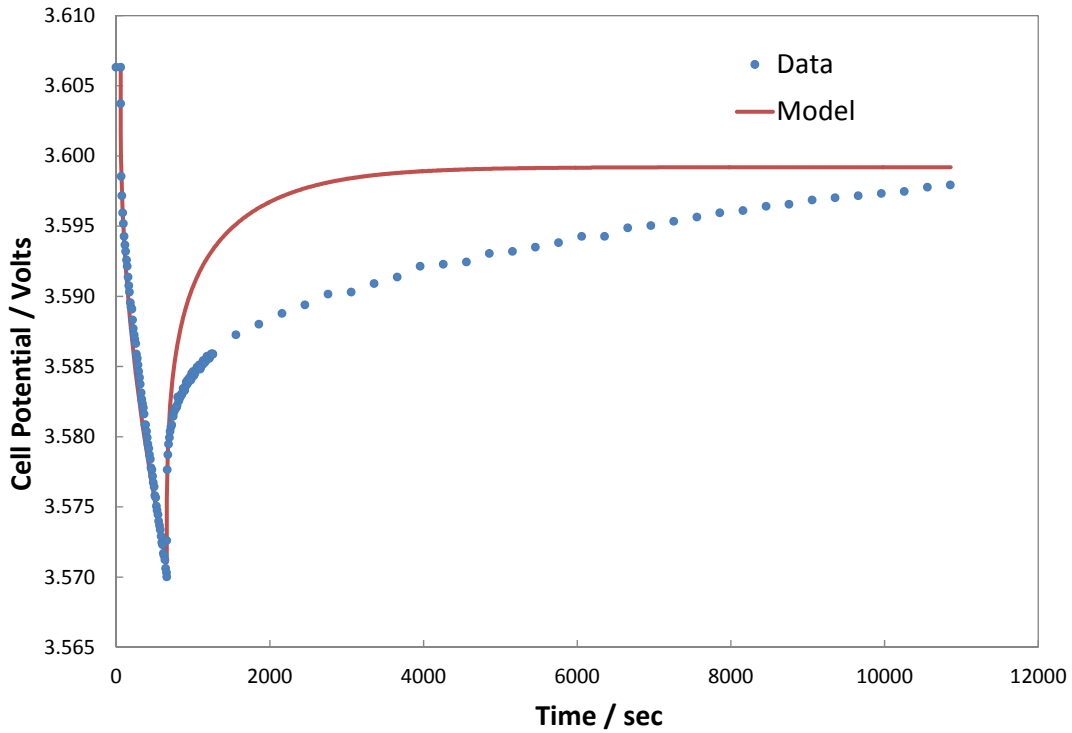
Figure 3. Typical DC electrochemical model fit of GITT studies conducted on LMR-NMC half-cell. Model assumes LMR-NMC material behaves as a standard intercalation active material.
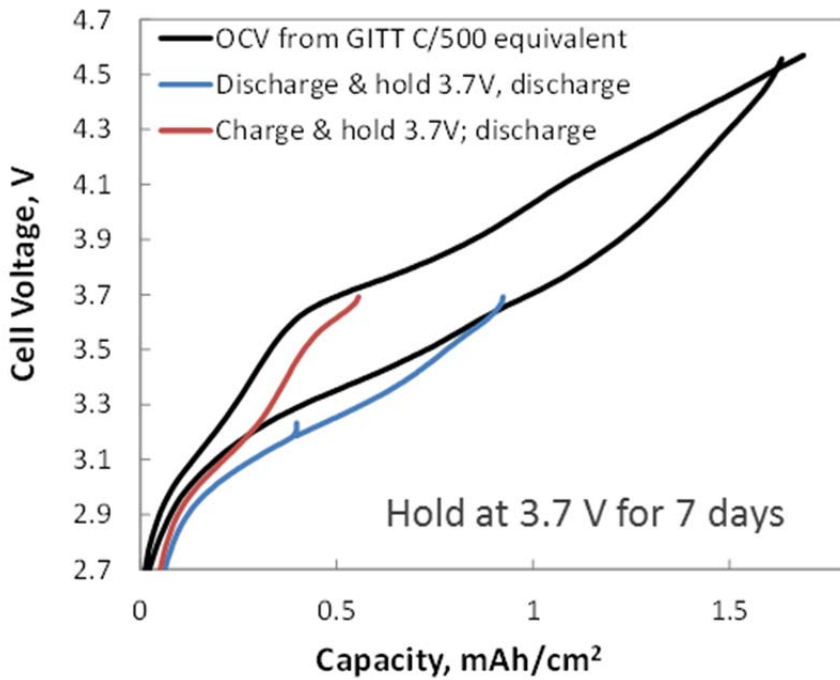

Figure 4. LMR-NMC half-cell data showing hysteresis of OCV curve between charge and discharge (black curves) compared to two other experiments, one starting with a

discharge to 3.7 volts and the other starting with a charge to 3.7 volts (not shown). The cell in both experiments is held at 3.7 volts for a week before fully discharging (red and blue curves).

(c) Summary of work in the past quarter related to milestone (c)
This project has been continually challenged by finding efficient ways to solve increasingly complex electrochemical cell models. A new differential algebraic equation solver package (PSE gPROMS) is being adopted to solve a wide variety of cell studies at the required level of complexity. Parameter estimation is always a serious challenge when dealing with the complex phenomenological modeling being used in this project. Previous effort used a "hand-fit" approach where the modeler systematically varied parameters to find a "best-fit" to the eye of the user. The new software package being implemented has parameter estimation algorithms and statistical assessment of the solution. Efforts this period continue to focus on integrating and improving the phase change model for electrode active materials. The importance of including phase change into the electrochemical model for electrodes like graphite has been well established, and recent work on the LMR-NMC electrode material indicates that more complex models will be needed for that electrode also. Further, the parameter estimation capabilities for the DC model are continuing to be utilized and improved.

(d) Summary of work in the past quarter related to milestone (d)
Implementation of the SEI growth model for the negative graphite electrode has been deemphasized because of the challenges the high energy LMR-NMC positive electrode are presenting.

Publications, Reports, Intellectual property or patent application filed this quarter. (Please be rigorous, include internal reports--invention records, etc.)

No publications, reports, or patents were submitted this quarter.

1) D. Dees, E. Gunen, D. Abraham, A. Jansen, and J. Prakash, J. Electrochem. Soc., 152 (7) (2005) A1409.
2) D. Dees, S. Kawauchi , D. Abraham, and J. Prakash, J. of Power Sources, 189 (2009) 263–268.

TASK 2
Calendar & Cycle Life Studies

Project Number: 2.3A (ES032)

Project Title: Diagnostic Evaluations - Electrochemical

Project PI, Institution: Daniel Abraham, Argonne National Laboratory

Collaborators (include industry): M. Bettge, Y. Li, Y. Zhu, D. Dees, A. Jansen, Argonne National Laboratory; Prof. A. Wei, Purdue University; Prof. I. Petrov, University of Illinois

Project Start/End Dates: October 2011/September 2012

Objectives: Electrochemical couples containing various positive and negative electrodes are being examined in the ABR program. The baseline electrolyte in these cells is EC:EMC (3:7, by wt.) + 1.2M $LiPF_6$. The main objective of this study is to use electrochemical diagnostic tools to identify factors that determine cell performance and performance degradation (capacity fade, impedance rise) on long-term storage and on extensive deep-discharge cycling. The electrochemical data obtained from these measurements are used in ABR's phenomenological modeling studies. A secondary objective of this study is to recommend and implement solutions that improve the electrochemical performance of materials and electrodes so that the PHEV cells may meet their 15y life criterion.

Approach: Our electrochemical measurements are conducted in various cell configurations that include coin cells, pouch cells, and reference electrode (RE) cells. Our investigations are conducted both on as-prepared single-sided electrodes, and on double-sided electrodes harvested from pouch- and 18650- cells. Our research includes the following components: (i) Studies in Reference Electrode cells – Data from these cells help identify causes of impedance rise and concomitant capacity fade; this knowledge will help us target the development of solutions to reduce cell performance degradation; (ii) development of electrolyte additives – these form surface films that protect the electrode components from further degradation; (iii) development of electrode coatings – modification of the electrode-electrolyte interfaces by these coatings have been shown to improve cell life.

Milestones:
(a) Determine sources of impedance rise/capacity fade during extensive cycling of cells containing various electrochemical couples; September 2012 (on schedule)
(b) Identify at least one electrolyte additive that improves cell life by 50% at 30°C and 25% at 55°C; September 2012 (on schedule).
(c) Identify at least one electrode coating that improves cell life by 50% at 30°C and 25% at 55°C; September 2012 (on schedule)

Financial data: $450 K (subcontracted $30K to Purdue University)

PROGRESS TOWARD MILESTONES (1 page)

(a) Summary of work in the past quarter related to milestone (a).

The ABR-1 positive electrodes contain 86 wt% $Li_{1.2}Mn_{0.55}Ni_{0.15}Co_{0.1}O_2$ (HE5050), 4 wt% SFG-6 graphite (Timcal), 2 wt% SuperP (Timcal) and 8 wt% PVdF (Solvay 5130). The SFG-6 graphite and SuperP form the electron percolating network to improve electronic conductivity within the electrode; the PVdF binds the various coating constituents and makes the coating adhere to the Al current collector. The carbons (electron conduction additives) are generally considered inactive during electrochemical cycling; but are these components really inactive? To answer this question we prepared an SFG-based electrode that contained 90 wt% SFG-6 + 10 wt% PVdF (Solvay 5130) and a SuperP-based electrode that contained 80 wt% SuperP + 20 wt% PVdF (Solvay 5130); both coatings were on an Al current collector.

Figure 1 shows capacity-voltage plots for the SFG-6 based and Super-P based electrodes in cells with a Li counter electrode and Gen2 electrolyte. The cells were cycled at 30°C between 3.4 and 5V vs. Li/Li^+ at rates indicated in the figures. Figure 2 shows the corresponding differential capacity plots.
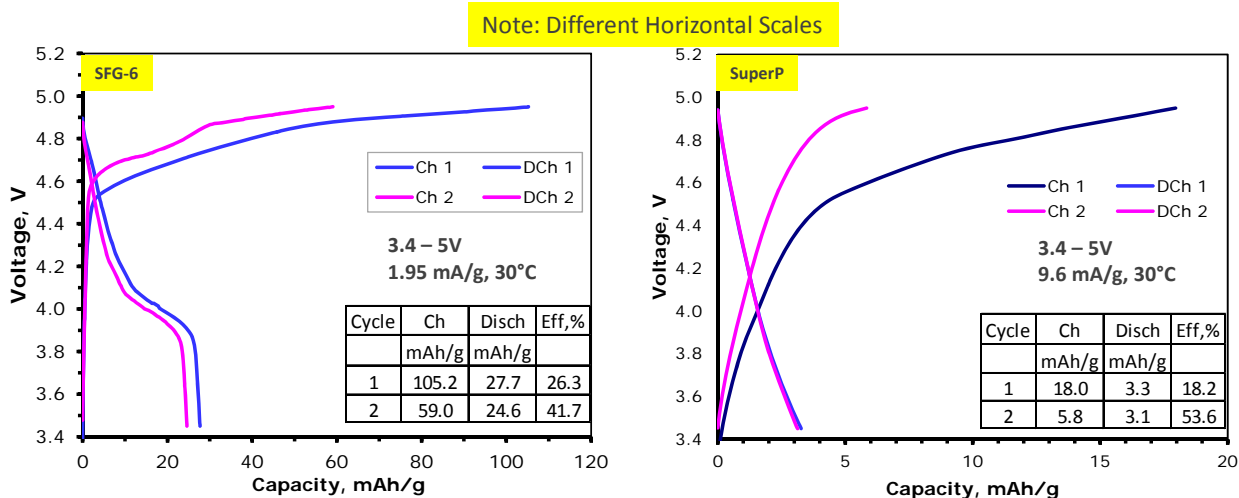

Fig.1. Capacity-voltage plots for the SFG-6 based and Super-P based electrodes in cells with a Li counter electrode and EC:EMC (3:7) + 1.2M $LiPF_6$ (Gen2) electrolyte.
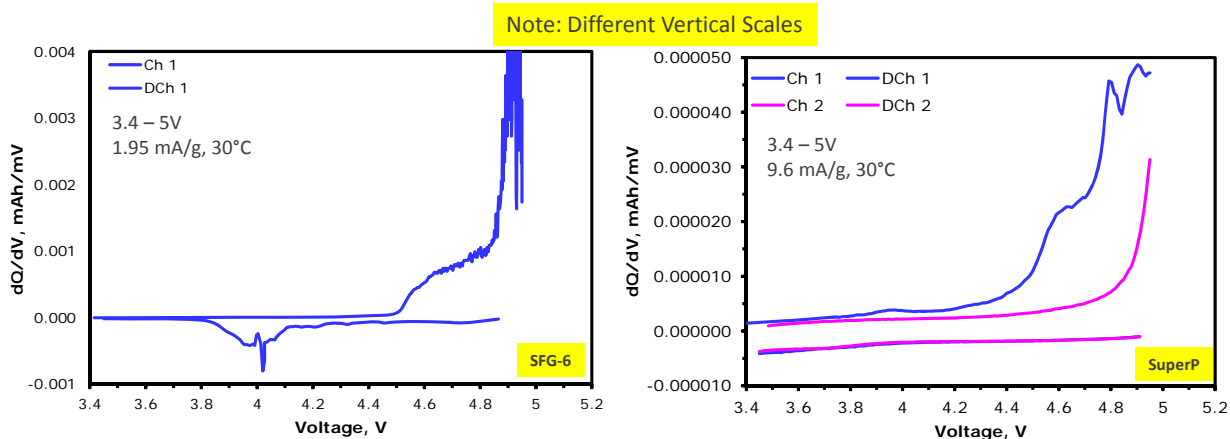
Fig.2. Differential capacity plots for the data shown in Fig. 1.Only the first cycle is shown for the SFG-6 based electrode, whereas first and second cycles are shown for the SuperP based electrode.

In Figure 1, the reversible capacity seen for the SFG-6 based electrodes is probably due to PF_6^- intercalation into the graphite; this reversible capacity increases with the upper cut-off voltage limit. Note that the coulombic inefficiency; i.e., the difference between charge and discharge capacities, suggests significant electrolyte oxidation on the graphite surface. On continued cycling, both the reversible and irreversible capacities decrease, but they do not go to zero, i.e., they maintain a finite value. PF_6^- intercalation is not expected to occur into the SuperP carbons; the reversible capacity of the SuperP-based electrodes is, therefore, small. The coulombic inefficiency is high, which again suggests significant electrolyte oxidation on the carbons. All capacities decrease on cycling but remain finite, especially the charge capacities.

In Figure 2, for the SFG-6 based electrode, on charge the area under the dQ/dV vs. V plot has two contributions: PF_6^- intercalation into graphite and electrolyte oxidation. Significant PF_6^- intercalation appears likely only beyond 4.45V vs. Li/Li^+. The steep increase beyond 4.8V is probably due to significant electrolyte oxidation on the graphite surface. Note that the charge and discharge curves are asymmetric; the discharge peak at 4V vs. Li/Li^+ is probably due to PF_6^- deintercalation from graphite. For the SuperP based electrode, although distinct features are seen note that the vertical scale values are roughly 2 orders of magnitude lower than that for the SFG-6 plots. Also, the features are prominent only on the first charge. Electrolyte oxidation on the SuperP is expected to be very small and maybe a concern only beyond 4.8V. When the SFG-6 and SuperP data are plotted on the same scale (after normalizing for electrode surface area) the SuperP carbon features are indistinct and barely visible. We may, therefore, conclude that PF_6^- intercalation and electrolyte oxidation are not a significant concern for the SuperP (relative to SFG-6).

Based on the above data we recommend that SFG-6 (or other graphites) not be used for preparation of high-energy cathodes, wherein the electrode voltage is expected to exceed

4.5V vs. Li/Li$^+$. Graphites may be used as electron conducting agents in cathodes that are cycled at voltages lower than 4.4V vs. Li/Li$^+$.

(b) Summary of work in the past quarter related to milestone (b)

The tris_hexafluoro-*iso*-propyl_phosphate (HFiP) electrolyte additive has been shown to be effective in 5V spinel/Li cells (Cresce and Xu, JES 158 (2011), p. A337). This additive has been shown to participate in protective interphasial chemistry both on the transition metal oxide electrodes (~5V vs. Li) and the graphite electrodes (~ 0V vs. Li).

We examined the effect of HFiP in ABR-1 cells that contained $Li_{1.2}Mn_{0.55}Ni_{0.15}Co_{0.1}O_2$ (HE5050) -based positive electrodes, Graphite (A12)–based negative electrodes, Celgard 2325 separator, and EC:EMC (3:7, by wt.) + 1.2M LiPF$_6$ (baseline) electrolyte; small amounts of HFiP (1 and 2 wt%) were added to the baseline electrolyte. The capacity and impedance data are shown in Figures 3 and 4, respectively.
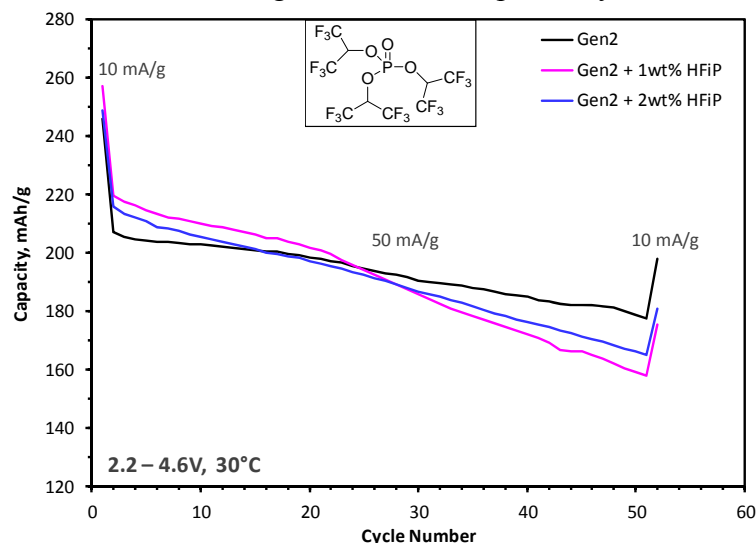

Fig.3. Capacity as a function of cycle number showing effect of 1 and 2 wt% HFiP additive in the baseline Gen2 electrolyte. The inset shows the composition of the HFiP compound.

Figure 3 contains capacity as a function of cycle number data showing the effect of 1 and 2 wt% HFiP added to the baseline electrolyte; the Gen2 electrolyte data is shown for reference. The first and last cycle in the plot were carried out with a 10 mA/g current, whereas the intermediate cycles were conducted with a 50 mA/g current. The cells with the HFiP additive show slightly higher initial capacity, but also faster capacity fade relative to the baseline Gen2 electrolyte. The faster fade may indicate that the SEI formed on the negative electrode is not stable.
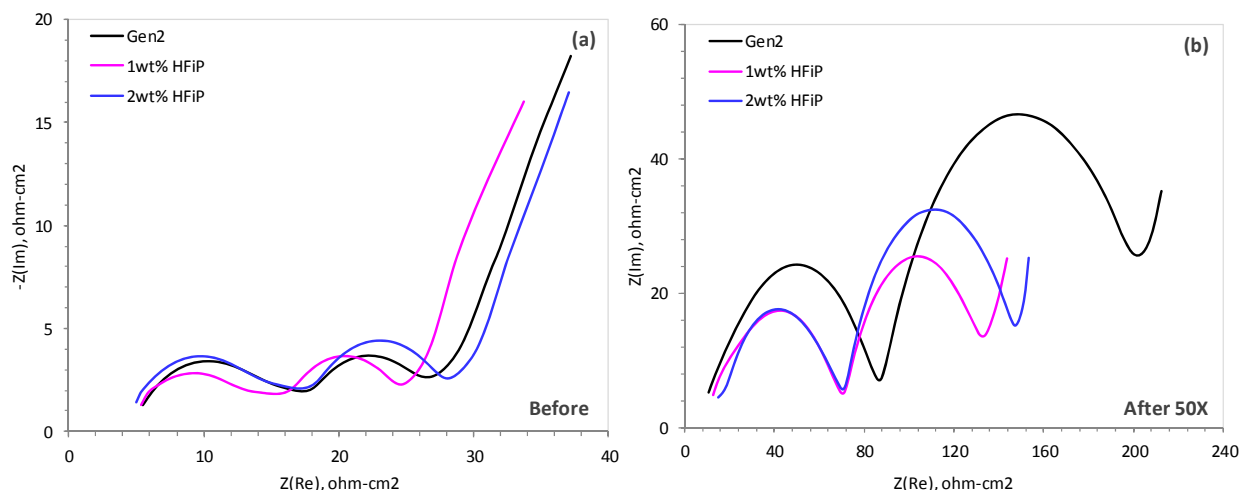
Fig.4. EIS data (3.75V, 30°C, 100 kHz-0.01 Hz) from full cells showing effect of HFiP additive.

Figure 4 contains EIS data from full cells containing the baseline Gen2 electrolyte, and with 1 and 2 wt% HFiP additive in the baseline electrolyte, (a) before (b) and after 50 cycles at 30°C in the 2.2 to 4.6V voltage window. The "before" data is after formation cycling, which includes 3 initial 2–4.1V cycles, followed by two 2-4.6V cycles. The impedance of the additive-containing cells is lower than that of the baseline cells. This observation may indicate that the HFiP forms partially protective films on the positive electrode (because previous reference electrode cell data have shown that impedance rise on cycling arises at the positive electrode).

(c) Summary of work in the past quarter related to milestone (c)
Modification of the positive electrode surface by Atomic Layer Deposition (ALD) coatings has been conducted. Initial data show significant improvement in cell performance, i.e., both capacity fade and impedance rise of the full cells decreases significantly. We will report on data from these tests at a later time.

Publications, Reports, Intellectual property or patent application filed this quarter. (Please be rigorous, include internal reports--invention records, etc.)
None

Project Number: 2.3B (ES032)

Project Title: Diagnostic Evaluations - Physicochemical

Project PI, Institution: Daniel Abraham, Argonne National Laboratory

Collaborators (include industry): M. Bettge, Y. Li, M. Balasubramanian, D. Miller, Argonne National Laboratory; Prof. I. Petrov, University of Illinois; Prof. B. Lucht, University of Rhode Island; Prof. P. Guduru, Brown University

Project Start/End Dates: October 2011/September 2012

Objectives: Various lithium-ion chemistries are being examined for use in cells for PHEV applications. The main objective of this study is to use physicochemical characterization tools and techniques to explain the electrochemical performance and performance degradation mechanisms of ABR cells. The physicochemical data are used to guide development of electrochemical models that relate material and electrode chemistry to observed changes in cell performance during cycling and accelerated aging. Determining degradation mechanisms is an important step towards modifying the cell chemistry to attain the 15y life goal for these cells.

Approach: Our physicochemical examinations employ a combination of spectroscopy, microscopy, diffraction, and chemical analysis techniques. Our investigations are conducted on components harvested from small cells (1 to 50 mAh), and from pouch and 18650 cells subjected to characterization and long-term aging. Our research includes the following three components: (i) studies of the electrode-electrolyte interface using various techniques that include X-ray photoelectron spectroscopy; (ii) electrode studies using techniques that include X-ray diffraction, X-ray absorption spectroscopy (XAS), and Electron Microscopy (AEM); and (iii) stress evolution studies using techniques that include the "wafer curvature method".

Milestones:
(a) Performance degradation mechanisms in HE5050(+)/A12(-) cells, September 2012 (on schedule)
(b) Initial information on performance degradation mechanisms in $Li_{1.14}Mn_{0.57}Ni_{0.29}O_2$ bearing cells, September 2012 (on schedule)
(c) Stress evolution data on oxide and graphite electrodes during electrochemical cycling, September 2012 (on schedule)

Financial data: $450 K (subcontracted $30K to Brown University; $50K to University of Illinois)

PROGRESS TOWARD MILESTONES

(a) Summary of work in the past quarter related to milestone (a).

X-ray absorption spectroscopy (XAS) studies were conducted on positive electrode samples harvested from ABR-1 FULL cells to examine the effect of cell aging on electrode degradation; the cells were discharged and held at 2V before electrode extraction. The experiments were performed in the PNC-XOR bending magnet beamline (20-BM) of the Advanced Photon Source at Argonne. XANES data at the Mn- and Ni-edges are shown in Figure 1; these data provide information on transition metal (TM) oxidation states in the samples.
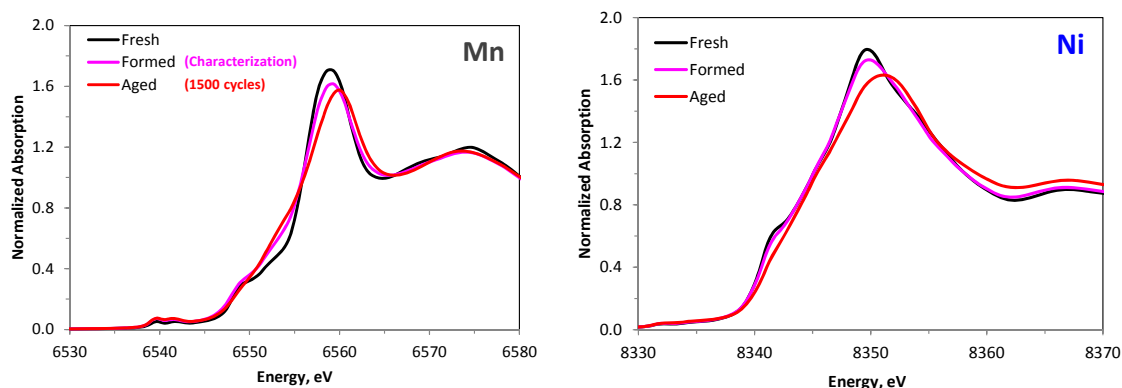
Figure 1: XANES data from ABR-1 positive electrode samples from FRESH (no exposure to electrolyte), FORMED (after initial characterization cycles), and AGED (after 1500 cycles) cells.

Formation cycling induces the biggest change in the Mn-edge data; the changes on further cycling are relatively small. These changes (seen in the FORMED sample data) are probably associated with loss of oxygen, which may preferentially occur around the Mn atoms. On further cycling/aging, there's relatively little change in the data. There is no obvious indication of changes in Mn oxidation states, i.e., the Mn-oxidation state in the discharged samples appears unchanged from 4+ on cycling/aging.

The average Ni oxidation state in the FRESH sample is slightly higher than 2+. A slight increase in oxidation state is seen for the FORMED sample. More Ni 3+ is present in the AGED sample. This shift is a result of Li-loss from the oxide; charge compensation, during lithium extraction from the oxide, is achieved through oxidation of the Ni.

(b) Summary of work in the past quarter related to milestone (b)
Electrochemical characterization of $Li_{1.14}Mn_{0.57}Ni_{0.29}O_2$-bearing cells is in progress. The performance degradation trends are very similar to those observed for the $Li_{1.2}Ni_{0.15}Mn_{0.55}Co_{0.1}O_2$ -bearing cells. The physicochemical data, and the mechanisms that govern cell performance degradation, are hence expected to be very similar.

(c) Summary of work in the past quarter related to milestone (c)
Real-time stress evolution in the ABR-1 negative-electrode during electrolyte wetting and electrochemical cycling was measured through the wafer-curvature method. The

ABR-1 electrode contains 90 wt% A-12 (ConocoPhilips) graphite, 4 wt% SuperP (Timcal) and 6 wt% PVdF (Kureha KF-9300). Upon electrolyte addition, the composite electrode rapidly developed compressive stress of the order of 1-2 MPa because of binder swelling. Upon continued exposure, the stress continued to evolve towards an apparent plateau (see Figure 2). The stress evolution on electrochemical cycling is shown in Figure 3.
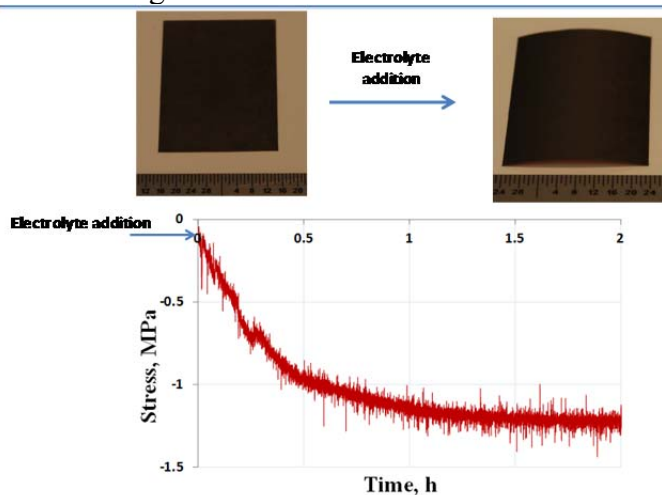

Fig. 2: Stress evolution in a graphite-based negative electrode upon exposure to electrolyte.
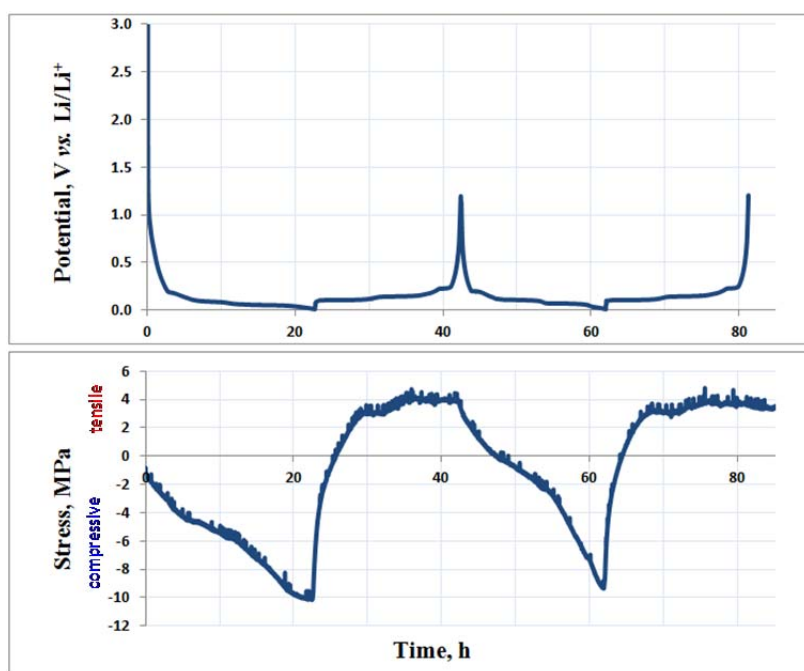
Fig. 3: Stress evolution in a graphite-based negative electrode upon electrochemical cycling.

During electrochemical intercalation at a slow rate, the compressive stress increases with the electrode's state-of-charge, reaching a maximum value of ~10 MPa. There appears to be an approximate correlation between the rate of (compressive) stress rise and the

staging behavior of the lithiated graphite. De-intercalation at a slow rate results in an initial decrease in electrode stress followed by the development of tensile stress in the electrode. In the 2nd intercalation cycle, the tensile stress decreases with increasing lithium content in the graphite, and eventually becomes compressive; extraction of lithium ions from the graphite results again in tensile stress development. The alternating tensile-compressive stress that results from electrochemical cycling can lead to mechanical degradation of the electrode that would be manifested as electrode capacity fade and impedance rise.

Publications, Reports, Intellectual property or patent application filed this quarter. (Please be rigorous, include internal reports--invention records, etc.)

None.

TASK 2
Calendar & Cycle Life Studies

Project Numbers: 1.1.1 and 2.4 (ES033)

Project Title: Strategies to Enable the Use of High-Voltage Cathodes (1.1.1) and Diagnostic Evaluation of ABRT Program Lithium Battery Chemistries (2.4)

Project PI, Institution: Robert Kostecki and Thomas Richardson, Lawrence Berkeley National Laboratory

Collaborators (include industry): None.

Project Start/End Dates: LBNL carried out diagnostics in the ATD Program since its 1999 inception, and the ABRT Program began October 2008.

Objectives: Task 1.1.1: To enable increased energy density by addressing the impact of high-voltage cathodes on the conducting carbon matrix. Task 2.4: (i) Determine the key factors that contribute to the degradation mechanism in the PHEV test cells and individual cell components. (ii) Characterize SEI formation on model electrode surfaces to improve understanding of key interfacial phenomena in PHEV cells.

Approach: Task 1.1.1**:** (i) determine the mechanisms for carbon damage and retreat at high potentials. (ii) Investigate mitigating treatments, additives, and procedures. Task 2.4: Use in situ and ex situ advanced spectroscopic and microscopic techniques in conjunction with standard electrochemical methods to characterize components harvested from fresh and tested PHEV cells, model thin-film cells, and special cells used to evaluate SEI formation processes.

Milestones: Determine interfacial degradation mechanism CBs in high-voltage cathodes (July 2012). On schedule. Synthesize a new type of CB with improved interfacial properties (September 2012). On schedule. Attend review meetings and present diagnostic results obtained in collaboration with ABRT Program participants. On schedule.

Financial data: FY 2012 funding $600K

<div align="center">PROGRESS TOWARD MILESTONES</div>

We have previously reported how a carbon dioxide treatment can improve the performance of carbon black conductive additives for high-voltage cathodes. The thermogravimetric behavior of a model sample (pyrolized polyimide) and commercial samples (Super P, Denka black) were investigated (Fig.1 a). The structural effect of CO_2 treatment was investigated using Raman spectroscopy. The area ratio of the D- to the G-band of pyrolized carbon changed from 0.71 for a sample treated under N_2 at 900°C to 0.65 for a sample processed under CO_2 for two hours at 900°C. The position of the D-band also shifted to lower wavenumbers, indicating a change in the surface structure. No significant difference between Raman spectra of samples treated for 1 and 2 hours was

observed. The surface structural change seems to be complete after 60 minutes and further treatment mainly increases the porosity of the carbon film.

A larger batch of a commercial carbon black powder (Super-P) was modified. This sample displayed a low electrochemical reactivity up to 4.5 V vs. Li/Li^+ and lower electrolyte decomposition currents over the whole potential range (Fig. 2). The electrode carbon mass loading was corresponds exactly to the amount of carbon additive present in a commercial composite electrode i.e., 0.75 mg/cm^2.
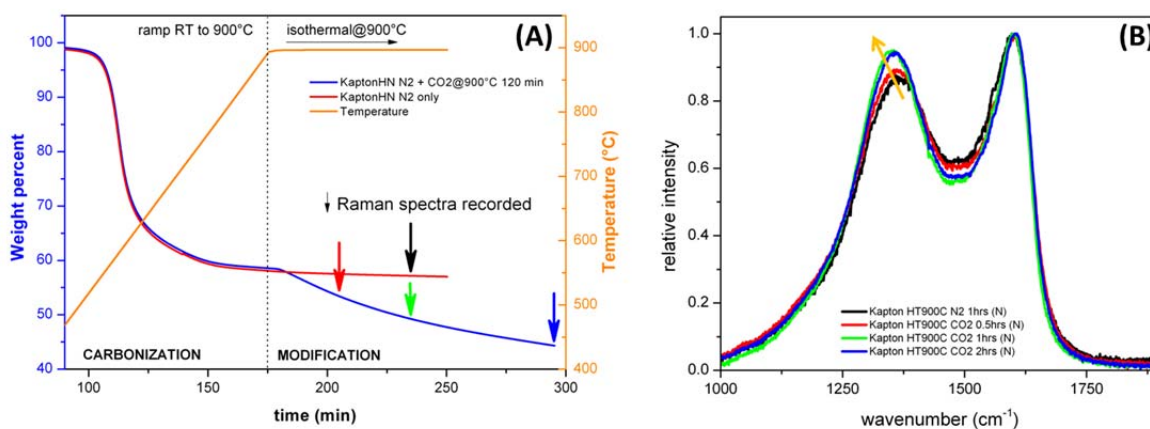
Fig. 1. TGA analysis (a) and Raman spectra (b) of Kapton HN with and without CO_2 treatment. Arrows in the TGA curve mark with corresponding colors the points where Raman spectra were obtained.

Ongoing investigations include the preparation of composite electrodes using various modified and unmodified carbon blacks. Furthermore, a controlled effort to optimize the temperature and time of the heat treatment will be undertaken and a correlation with the physical and electrochemical properties established.
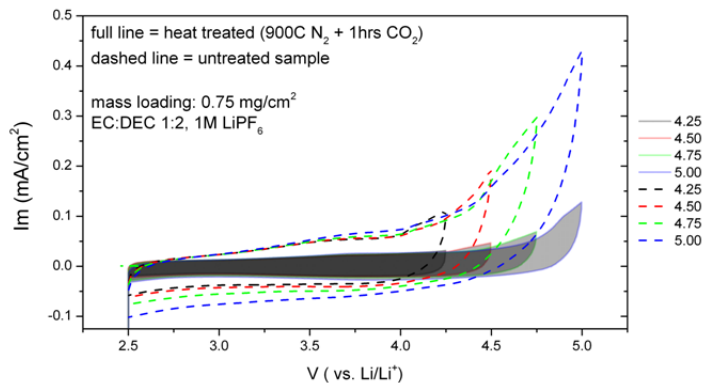

Fig. 2. Cyclic voltammogram of untreated and heat treated commercial Super-P samples (scan speed: 5mV/s).

Our second goal was to correlate the observed impedance growth on both negative and positive electrodes in cycled cells with a possible chemical cross-talk via soluble electrolyte decomposition products generated at the electrodes. Our previous report showed virtually no change in the impedance of graphite baseline electrodes cycled in symmetric cells. A similar experiment that employed the baseline positive electrode (lithium-nickel-manganese-cobalt oxide (Toda)) was carried out.

Two vacuum-dried baseline Toda disk composite electrodes of significantly different sizes (20 mm vs. 3 mm diameter) underwent formation cycling in the 1.2 M $LiPF_6$ in 3:7 EC:EMC electrolyte in two separate beaker cells. The large electrode was polarized to 4 V vs. Li/Li^+ (corresponding to the middle of the plateau) and the small electrode was brought to 4.7 V vs. Li/Li^+ (fully oxidized state). The electrodes were thoroughly washed in EMC and mounted against one another in a 2032 coin cell with a Cellgard® separator and 20 µl of the electrolyte. This cell was cycled between -1.5 V and 0.7 V, which corresponds to the galvanostatic polarization of the small electrode between 2.5 to 4.7 V vs. Li/Li^+ at a C/3 rate. The potential of the larger (oversized) counter electrode was virtually constant upon cycling. Every ten cycles an impedance spectrum was recorded in the discharged state (-1.5 V). No significant changes in the spectra were observed up to 1200 cycles (Fig. 4). All spectra were very similar in shape, and only a small offset along the ReZ axis was observed (spectra moving back and forth along this axis, without any specific pattern). The origin of that phenomenon will be a subject of further studies. We plan to pursue the analysis of cycled electrodes using synchrotron radiation, Raman spectroscopy and microscopy.

TASK 2
Calendar & Cycle Life Studies

Project Number: 2.4 and 3.3 (ES034)

Project Title: Life and abuse tolerance diagnostic studies for high energy density PHEV batteries
Task 2.4: Life Diagnostics, Task 3.3: Abuse Behavior Modeling and Diagnostics

PI, Institution: Kyung-Wan Nam and Xiao-Qing Yang, Brookhaven National Laboratory

Barrier: Calendar and cycling life, Abuse tolerance

Objectives: The primary objectives of the efforts at BNL are: to determine the contributions of electrode materials changes, interfacial phenomena, and electrolyte decomposition to cell capacity power decline, and abuse tolerance; to develop new diagnostic techniques (in situ and ex situ) for lithium-ion batteries; to help other ABR teams and the battery developers to understand the technical barriers by using these new techniques; to explore new techniques to improve the abuse tolerance.   The other objective is to design, synthesize and characterize new electrolyte for PHEV oriented lithium-ion and Lithium-air batteries with better performance and safety characteristics. Special attention will be given to the capabilities of electrolytes in improving the high voltage cycling of lithium-ion batteries.

Approach: Our approach is to use a combination of *in situ, ex situ* and time-resolved synchrotron based x-ray techniques to characterize electrode materials and electrodes taken from baseline ABR Program cells.   *Ex situ* soft X-ray absorption spectroscopy (XAS) will be used to distinguish the structural differences between surface and bulk of electrodes using both electron yield (EY) and fluorescence yield (FY) detectors. Time-resolved X-ray diffraction technique will also be used to understand the reactions that occur in charged cathodes at elevated temperatures in the presence of electrolyte.   In situ x-ray diffraction will be used to monitor the structural changes of the electrode materials during charge-discharge cycling at different conditions.   A combination of time resolved X-ray diffraction (XRD), in situ soft and hard X-ray absorption (XAS), in situ transmission electron microscopy (TEM) techniques during heating will be applied to study the thermal stability of the electrode materials. The atomic layer deposition (ALD) technique will be used for the surface modification of new cathode materials, which will be studied using time resolved X-ray diffraction (XRD) for the effects of surface modification on the thermal stability. These approaches developed at BNL will be available to other members of ABR projects through extended collaboration. We will continue to develop new synchrotron based x-ray techniques such as combined in situ x-ray diffraction and mass spectroscopy during heating for the thermal stability of cathode material studies. We will continue to develop TEM based in situ diagnostic tools to

study the structural changes at both surface and bulk of the electrode particles with high spatial resolution.

Milestones:
 (a) By April 2012, complete the study of thermal decomposition of charged $Li_xNi_{0.8}Co_{0.15}Al_{0.05}O_2$ (NCA) cathode materials during heating using combined Time-Resolved XRD and Mass Spectroscopy. **Completed.** (b) By April 2012, complete the Time resolved r-ray diffraction (TRXRD) studies of ALD coated Al_2O_3 on $Li_{1.2}Ni_{0.17}Co_{0.07}Mn_{0.56}O_2$ new cathode material during heating. **Completed.** (c) By September 2012, complete the study of charged $Li_xNi_{1/3}Co_{1/3}Mn_{1/3}O_2$ (NCM) cathode material for thermal decomposition during heating using combined Time-Resolved XRD and Mass Spectroscopy. **On schedule.** (d) By September 2012, complete the in situ XRD studies of $Li_{1.2}Ni_{0.15}Mno_{0.55}Co_{0.1}O_2$ (Toda HE5050) cathode material during charge-discharge cycling. **On schedule.**

Progress toward milestones for the 2nd quarter of FY2012:

(a) Summary of work in the past quarter related to milestone (a).
The work related to milestone (a) has been completed in the past quarter: In order to understand the thermal degradation of the electrodes in Li-ion cells, we have developed techniques using the combination of the *in situ* time resolved X-ray diffraction (TR-XRD) and mass spectroscopy to study the structural changes and gas evolution during the thermal decomposition of charged cathode materials. Our new studies on the structural changes of layered nickel based cathode materials (e.g., $Li_{1-x}NiO_2$ and $Li_{1-x}Ni_{0.8}Co_{0.15}Al_{0.05}O_2$) during thermal decomposition have been completed.

(b) Summary of work in the past quarter related to milestone (b)
The work related to milestone (b) has been completed in the past quarter:
The Time resolved r-ray diffraction (TRXRD) studies of atomic layer deposition (ALD) coated Al_2O_3 on the surface of $Li_{1.2}Ni_{0.17}Co_{0.07}Mn_{0.56}O_2$ new cathode material during heating are completed in the second quarter of 2012. As shown in Figure 1, at the fully charged state, when heated from room temperature to 600 °C, the uncoated $Li_{1.2}Ni_{0.17}Co_{0.07}Mn_{0.56}O_2$ sample went through a phase transition from layered phase (R-3m) to the spinel phase (Fm3m) starting at around 350 °C. In contrast, the starting temperature for this phase transition from layered to spinel for the fully charged ALD coated sample moved up to 450 °C range, a more than 100 °C increase. These results clearly demonstrated the significant improvement in thermal stability obtained by the ALD coating of Al_2O_3 on the surface of $Li_{1.2}Ni_{0.17}Co_{0.07}Mn_{0.56}O_2$ materials.

(c) Summary of work in the past quarter related to milestone (c)
Studies of charged $Li_xNi_{1/3}Co_{1/3}Mn_{1/3}O_2$ (NCM) cathode material using TR-XRD and MS are underway.

(d) Summary of work in the past quarter related to milestone (d)
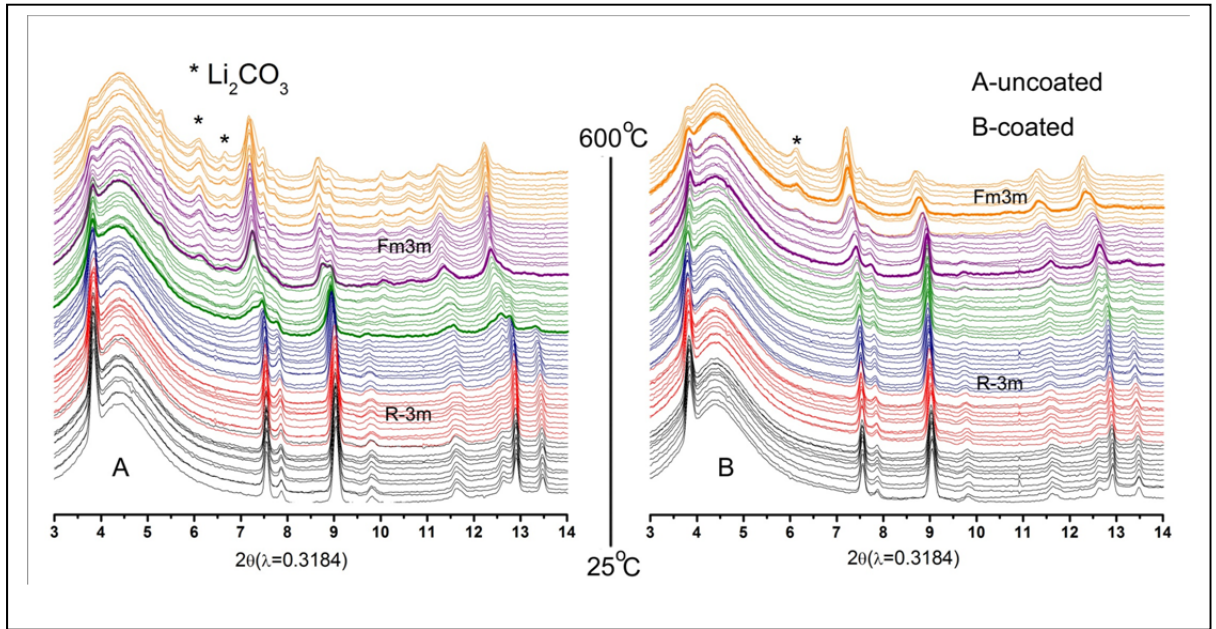The in situ XRD studies of $Li_{1.2}Ni_{0.15}Mno_{0.55}Co_{0.1}O_2$ (Toda HE5050) cathode material during charge-discharge cycling are underway.

Figure. 1 Crystal structure changes of fully charged cathode material $Li_{1.2}Ni_{0.17}Co_{0.07}Mn_{0.56}O_2$ studied by TR-XRD during heating from 25 °C to 600 °C

Project Number: FY12 New task (building on developed technology from ID39)

Project Title: Online and offline diagnostics for electrodes for Advanced Lithium Secondary Batteries

Project PI, Institution: David Wood, Oak Ridge National Laboratory

Collaborators: Argonne National Laboratory, Keyence, Solar Metrology

Project Start/End Dates: 10/1/11 to 9/30/14

Objectives: Due to high scrap rates of 10-20% or more associated with lithium secondary cell production, new methods of quality control (QC), which have been successful in other industries, must be implemented. Often flaws in the electrodes are not detected until the formation cycling when the entire series of manufacturing steps has been completed, and the associated scrap rates drive the costs of lithium secondary cells to an unacceptable level. If electrode flaws and contaminants could be detected in line near the particular processing steps that generate them, then the electrode material could be marked as unusable and the processing equipment could be adjusted to eliminate the defects more quickly. ORNL is considering in line analysis methods such as X-ray fluorescence spectroscopy (XRF) for electrode component uniformity and metal particle detection and laser thickness sensing of the electrode wet thickness measurement. In addition, on-line laser thickness measurement and IR imaging of wet and dry electrode coatings will be implemented for thickness uniformity and coating flaw detection. These methods have been effectively utilized in other industries such as photovoltaic, flexible electronics, and semiconductor manufacturing, but the equipment and measurement methods must still be tailored for lithium secondary cell production. The object of this project is to raise the production yield of lithium secondary battery electrodes from 80-90% to 99% and reduce the associated system cost by implementing in line XRF and laser thickness control. In addition, ORNL is providing its diagnostics capabilities and expertise to address materials issues with ABR cathode materials.

Approach:
Online diagnostics: Solar Metrology has been identified as a top manufacturer of in line XRF instruments for roll-to-roll applications and has a great deal of experience with the photovoltaics industry. ORNL will work closely with them to establish this technology for the lithium secondary battery industry. ORNL will produce tape casted and slot-die coated electrode rolls (anodes and cathodes) with deliberately introduced flaws to test the appropriateness of the method and the equipment modifications to the standard model. All key process parameters, such as line speed, coating thickness range, metal particle density, elemental homogeneity, etc., will be examined. In-line XRF data will also be correlated with ex-situ XCT data to gain a complete chemical and structural picture of the electrode as it is coated and dried.

Keyence has been selected as the partner for developing a laser thickness senor, or set of sensors, for lithium secondary battery electrode production. ORNL has a single-sided slot-die coating system, so only single-sided electrode coatings will be evaluated. ORNL will rent the sensors from Keyence and integrate them directly into ORNL's slot-die coating line for the proof-of-concept experiments.

The output data from the wet layer thickness measurements using the laser sensor(s) will be correlated with the thickness measurement capability by marking the regions that are out of specification during the coating process. The coated electrode rolls with markings will be fed into the in line XRF equipment to determine if wet regions out of specification match with dry regions that are determined to be out of specification. A feedback mechanism will be designed that considers whether the wet or dry thickness is a better input for adjusting the dispersion flow rate into the slot-die coater. The IR imaging QC will be correlated with thickness variation data to determine any further systematic flaw formation mechanisms.

Offline diagnostics:
ORNL characterization capabilities in acoustic emission detection, in-situ and ex-situ X-ray diffraction, neutron scattering, and magnetic property determination will be utilized to investigate cathode materials issues with ABR developed materials.

Milestones:
   a) Obtain in-line IR imaging data where different types of electrode coating flaws (pinholes, blisters, etc.) are identified (May 2012); on schedule.
   b) A method of correlating wet and dry thickness using laser thickness measurement and in line XRF, respectively (June 2012); on schedule.
   c) An in line XRF prototype(s) designed by Solar Metrology that measures electrode component uniformity, metal particle position, and dry electrode thickness (Sept. 2012); on schedule.
   d) A new or modified model of Keyence laser thickness sensor(s) specially designed for lithium secondary battery electrode dispersion deposition control (Sept. 2012); on schedule.
   e) Provide characterization and analysis for ABR developed HE5050 material provided by ANL

Financial data: $300k/year for FY12

PROGRESS TOWARD MILESTONES

Project 1: Investigating the phase transformation pathways in TODA-HE5050 ($Li_{1.2}Ni_{0.15}Mn_{0.55}Co_{0.55}O_2$ or $0.5Li_2MnO_3 - 0.5LiNi_{0.375}Co_{0.25}Mn_{0.375}O_2$) cathode during electrochemical cycling; an in-situ XRD study.

Goal:

- Study the major structural changes in HE5050cathode during electrochemical lithiation and delithiation in a voltage window of 2.4V-4.8V.
- Determine the lattice parameters and change in phase percentages as a function of charge/discharge cycles.
- Correlate the results with the electrochemical performance (voltage/ capacity fade).

Experiment:

The experiments were performed on cathodes with Toda HE5050 lithium rich material with composition $0.5Li_2MnO_3 - 0.5LiNi_{0.375}Co_{0.25}Mn_{0.375}O_2$. The electrochemical cycling was performed in a half-cell configuration with lithium metal as a counter electrode. A specially designed cell for in-situ XRD with large (9.8 mm in diameter) Kapton window was used. The coin cell 2032 hardware was used. 1.2M $LiPF_6$ in ethylene carbonate / dimethyl carbonate (EC/DMC 3:7 per volume) mixture was used as electrolyte (Purolyte®, Novolyte) and Celgard 2500 separator was placed between the electrodes in the cell. The electrodes had the following composition: 86%wt Toda HE5050 – 8%wt PVDF binder – 4%wt Timcal SFG-6 Graphite – 2%wt Timcal Super P. Experiments were controlled by BioLogic VMP3 potentiostat and the cell was positioned inside a cell holder within the XRD (Panalytical Instruments) enclosure for simultaneous collection of diffraction data. The in-situ experiments were performed for freshly prepared electrode (after zero cycles), after 16 cycles and after 36 cycles. The electrochemical experiments were done at the rate of 9mA/g.

Results:
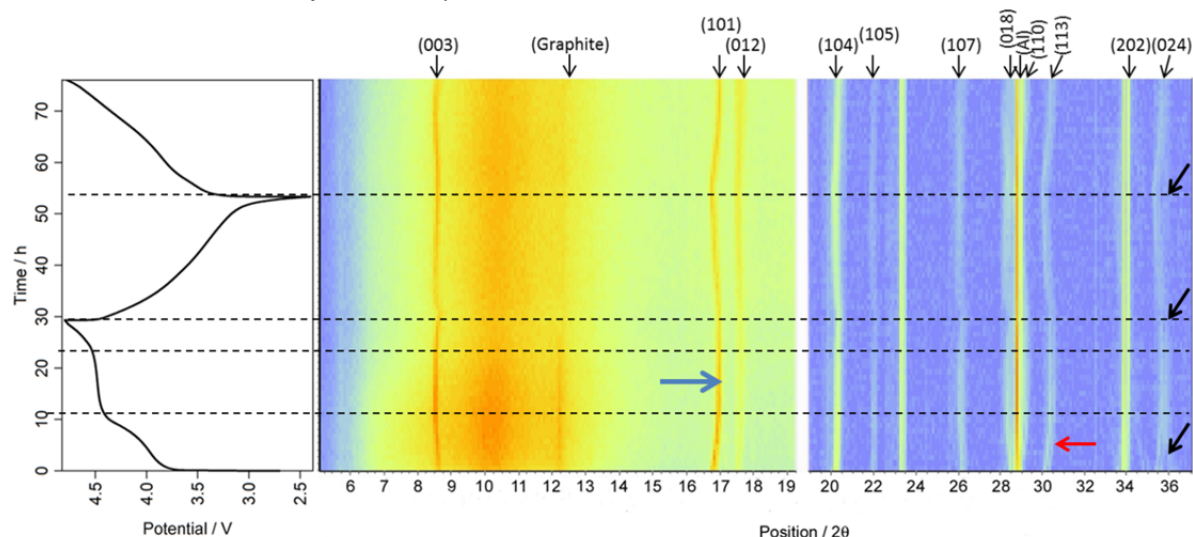
a. In-situ XRD results after zero cycles

Figure 1: In-situ XRD (Mo source) iso plots of HE5050 and the state of electrochemical cycling (left). The color scale represents the intensity of the particular crystallographic plane.

Figure 1 shows the electrochemical cycling data together with the plots showing the evolution of XRD peak within the corresponding time intervals. All the peaks can be indexed by taking rhombohedral symmetry with R$\overline{3}$m space group. Due to high background at lower 2-theta region, the monoclinic phase was not observed. However, the ex-situ XRD confirms that HE5050 cathode has both the hexagonal and monoclinic phase. The detailed observation from figure 1 shows that (101) planes shifts towards higher 2- theta up to plateau region and does not change up to 4.8V upon charging (see the blue arrow mark). Upon discharging, it shifts towards lower 2-theta region. (113) Planes shows same behavior as (110) planes (see the red arrow). A doublet near 2-theta ~ 36 degrees merge upon charging and again appears upon discharging (see the black arrows). Figure 2 represents the refined lattice parameters with the error bar calculated from Rietveld analysis.

From figure 2 (a) it can be seen that during charging, c-lattice parameter increases up to 4.4 V which clearly suggests that lattice expansion along c-direction. The lattice expansion along c- direction is mainly due to increase in electrostatic repulsion force between oxide layers which results due to lithium ion extraction from the host structure. In the plateau region (4.4-4.6V) the c-lattice parameter tends to decrease in a smooth manner and then decreases up to further charging up to 4.8V. During initial discharging, the c-lattice parameter increases and then decreases on further lithium intercalation. Similarly, the a-lattice parameter decreases up to 4.4 charging state and then increases smoothly on further charging. In figure, 2 (c) the relative phase
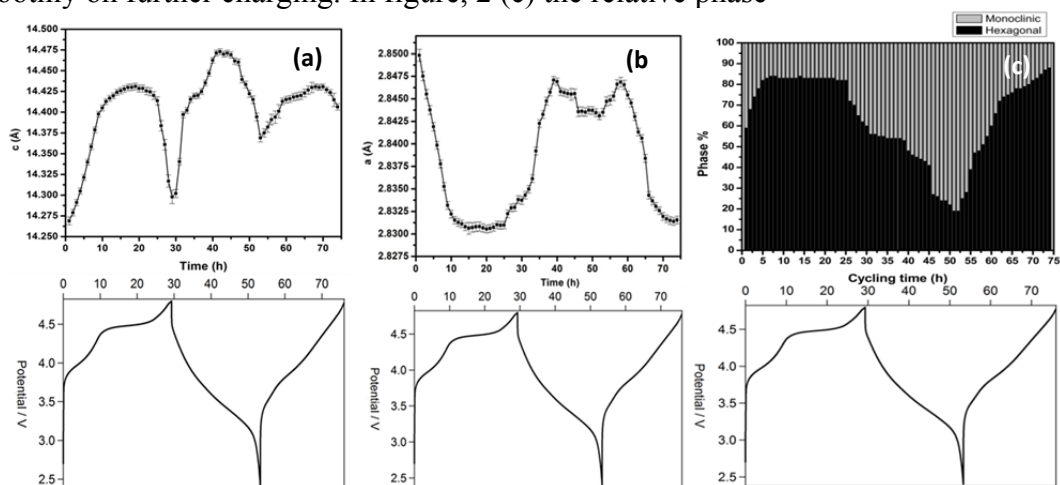

Figure 2: Change in c- lattice parameter (a), a- lattice parameter (b) and relative phase change (c) as function of charge/discharge cycles.

percentages were shown as a function of charge/discharge cycles. The monoclinic and hexagonal phases were taken into consideration and relative change in phase percentage was studied. Upon charging, the hexagonal phase is increased and then remains constant in the plateau region. The monoclinic phase increases during discharging. This process is repeated for next cycle.

b. In-situ XRD results 16 cycles

In-situ XRD was collected from the HE5050 electrode, which has been undergone 16 cycles. Figure 3 represents the refined lattice parameter along with the percentage of phase changes calculated from the Rietveld analysis.
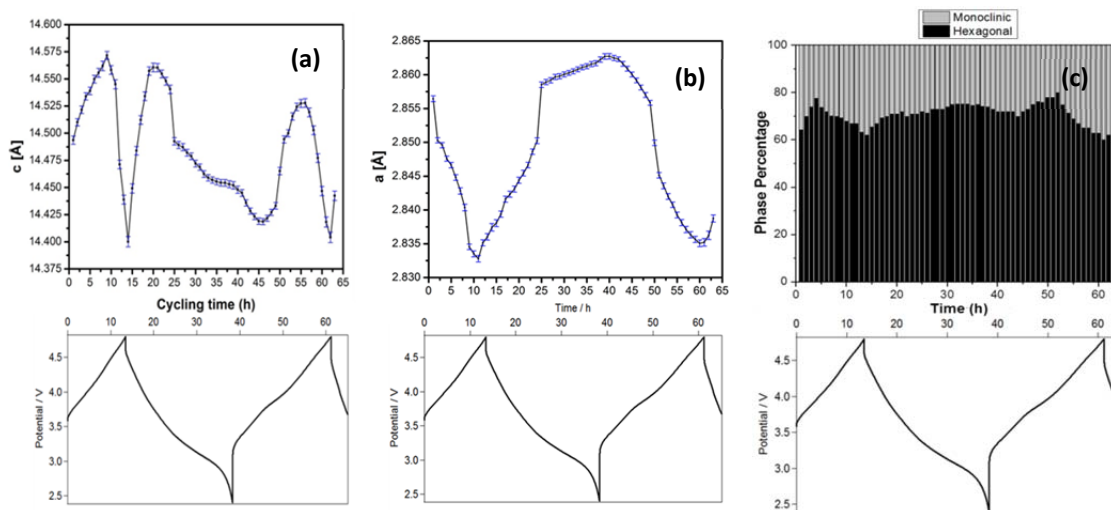

Figure 3: Change in c- lattice parameter (a), a- lattice parameter (b) and relative phase change (c) as function of charge/discharge cycles.

The c-parameter changes as a function of charge/discharge cycles, which is comparable to the trend, observed in figure 2(a). The difference is manly at the plateau region, where there is a sudden change in the values can be observed in the present case. The a lattice parameter decreases upon charging and increases upon discharging (see figure 4 b)which clearly describes the metal ion –metal ion distance changes during lithiation and delithiation. The decrease in a-lattice parameter can be attributed to the formation of smaller ionic radius ion, Ni^{+4} which is formed during charging. The increase in a lattice parameters suggests the formation of ion having larger ionic radius, Ni^{+2} which is formed during discharging. In figure 4-c the relative phase changes is presented. The trend is different as compared to the fresh electrode. The hexagonal phase increases upon charging to 4.4 V and then decreases on further charging to 4.8V and then increases upon discharging. The process was repeated for next cycle.

c. In-situ XRD results 36 cycles

Figure 4 (a) represents the in-situ XRD along with the electrochemical of the HE5050 cathode, which has been undergone for 36 cycles prior to in-situ experiment. The peaks were indexed based on the rhombohedral symmetry with R$\overline{3}$m space group. The (101) peaks shifts to the higher 2-theta value upon charging and the to lower 2-theta value upon discharging (see figure 4-b). The refined lattice parameters along with the percentage of phase changes calculated from the Rietveld analysis are shown in Figure 5.
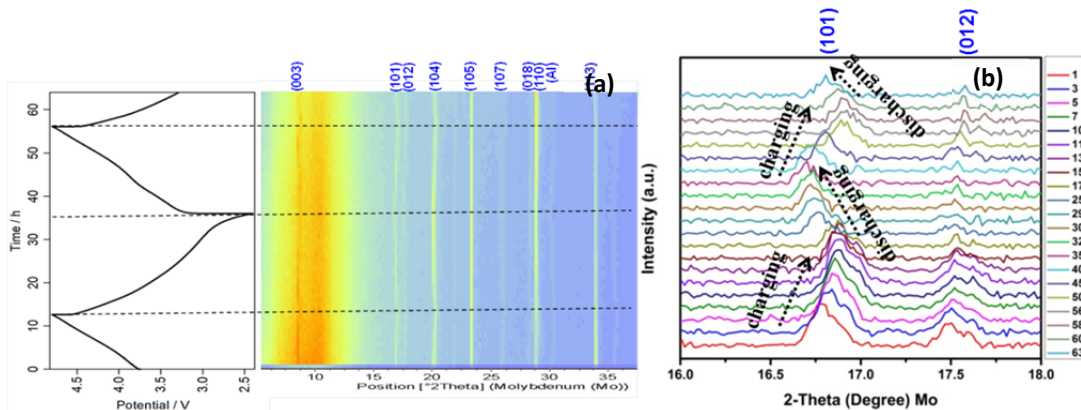
Figure 4: In-situ XRD (Mo source) iso plots of HE5050 after 36 cycles and the state of electrochemical cycling (left). The color scale represents the intensity of the particular crystallographic plane (a). The displacement of (101) plane as a function of charging/discharging processes (b). The number at right hand side of the figure represents the time in hour.
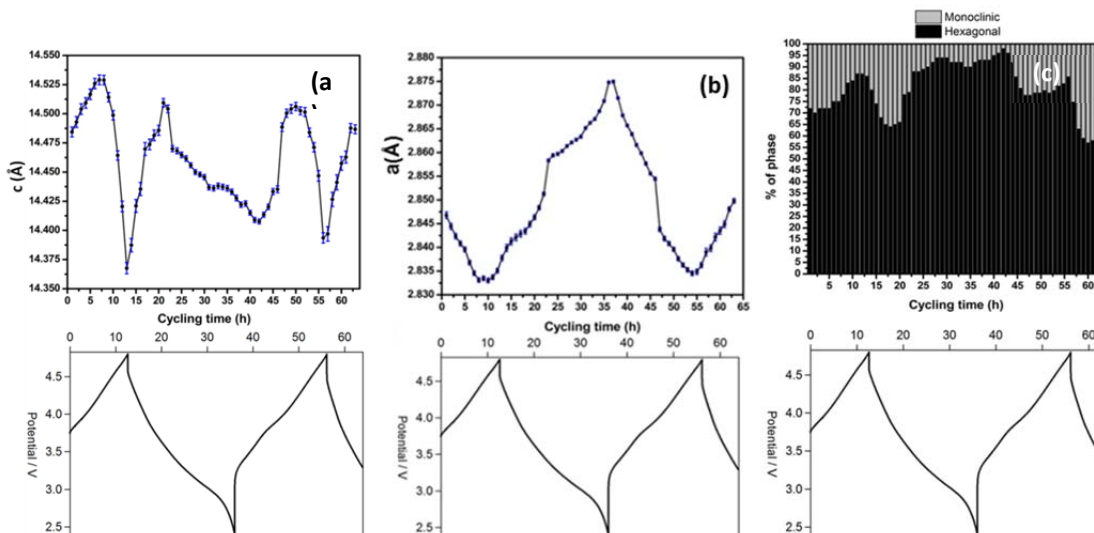

Figure 5: Change in c- lattice parameter (a), a- lattice parameter (b) and relative phase change (c) as function of charge/discharge cycles.

Interestingly, the relative phase change was different as compared to the other systems (fresh electrode and electrode undergone 16 cycles). The reason for this behavior and detailed analysis is under progress.
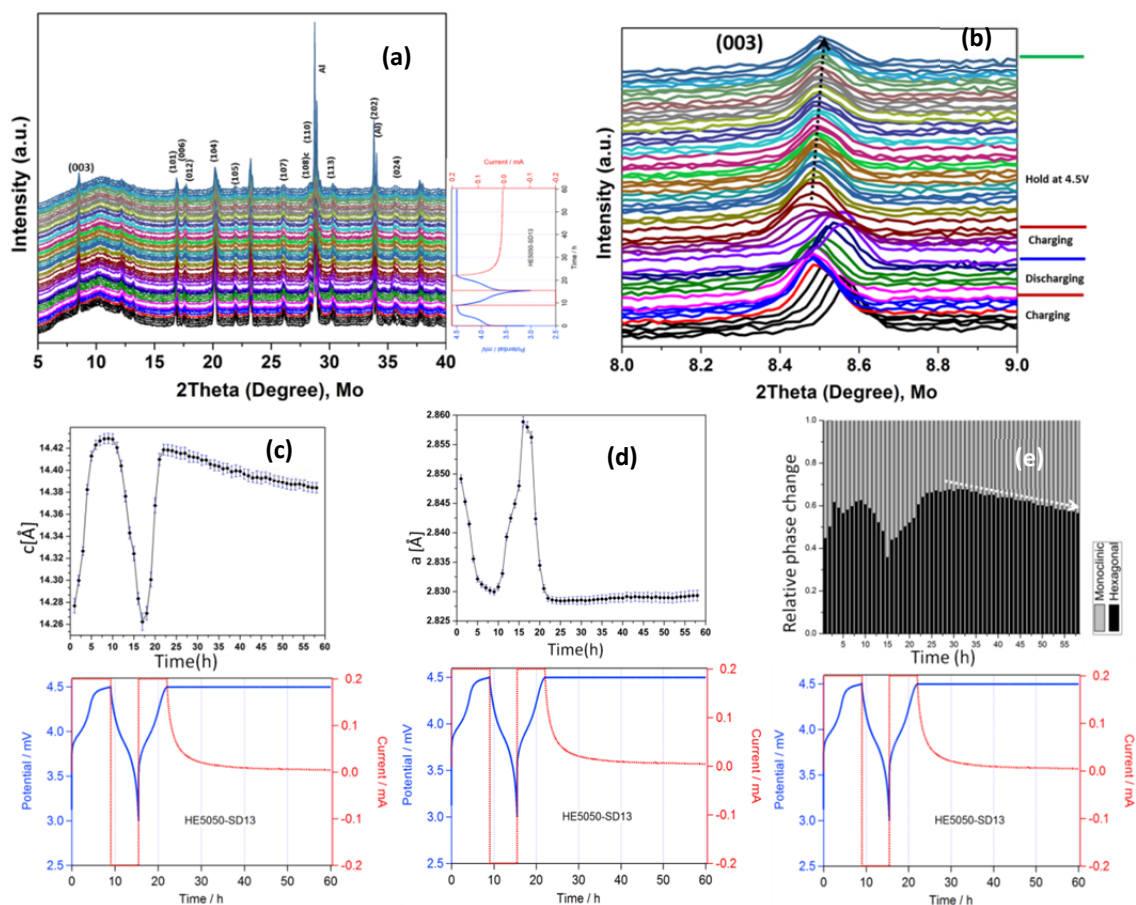
Figure 6: In-situ XRD along with the electrochemical data (a), (003) peak shift during voltage hold (b), change in c- lattice parameter (c), a- lattice parameter (d) and relative phase change (e) as function of charge/discharge cycles.

Project 2: Investigating the structural changes in TODA-HE5050 ($Li_{1.2}Ni_{0.15}Mn_{0.55}Co_{0.55}O_2$ or $0.5Li_2MnO_3 - 0.5LiNi_{0.375}Co_{0.25}Mn_{0.375}O_2$) cathode during high –voltage hold via in-situ XRD studies.

Goal:
- Investigate the structural changes in TODA- HE5050 cathode materials during high-voltage hold.
- Correlate those structural changes with the battery performance.

Experiment:
The fabrication of in-situ XRD cell was similar as explained for project 1 above. The electrochemical reaction was performed in the voltage window of 3 - 4.5 V and after 1.5 cycle the cell was hold at 4.5V for 40 h and in-situ XRD was collected during that hold duration to observe any structural changes during the high voltage hold.

Results: Figure 6 represents the results from the voltage hold experiment. It is evident that, the (003) peak shifts towards the higher 2-theta value during prolonged voltage hold (figure 6-b) which is in agreement with the decrease in refined c-lattice parameter

values (figure 6-c). The a-lattice parameter increases during the voltage hold process. However, this is not as significant as compared to change in c-lattice parameter values. It is also observed that the material relaxes to the original composition during prolonged voltage hold, which is also in agreement with the decrease in c-lattice parameter values.

The decrease in c-lattice parameters is due to contraction of the unit cell along c-direction. This can be explained based on following models. *Model 1*: Diffusion (migration) of lithium ions within the cathode structure. *Model 2:* Migration of transition metal ions from transition metal layers to octahedral vacancy of lithium layer. *Model 3:* Formation of oxygen vacancy in the cathode structure, which will decrease the electrostatic repulsion between oxide layers and ultimately decreases the c-lattice parameters. *Model 4:* Self discharge of lithium ions due to structural instability of cathode at low lithium concentration (high voltage hold). The verifications of these models are in progress and will be presented in next quarterly report.

Project 3: Understanding the cation- ordering of TODA-HE5050 ($Li_{1.2}Ni_{0.15}Mn_{0.55}Co_{0.55}O_2$ or $0.5Li_2MnO_3 - 0.5LiNi_{0.375}Co_{0.25}Mn_{0.375}O_2$) cathode in order to predict the capacity decaying pathways.

Goal:
- Study the local structure and cation -ordering of TODA-HE5050 cathode material before and after electrochemical cycling by ex-situ XRD, SQUID, TEM, and neutron scattering techniques.
- Structure-electrochemical property- correlation in order to determine the voltage/capacity fading pathways and propose the routes to overcome this problem.

Experiment: The HE5050 electrode prior to electrochemical cycling is characterized by XRD, TEM, and SQUID magnetometer. The cell fabrication procedure is similar to the in-situ experiment as explained in page 1. However, in this experiment, the Kapton window was replaced by stainless steel (coin cell 2032 hardware). The cells were cycled at 2.4-4.8V at 20 mA/g. After completion of electrochemical reaction, the cells were disassembled and the cathode was rinsed with dimethyl carbonate to clean the surface of electrode from the electrolyte contamination. The electrode was dried in the glove box and various characterizations were performed. In this report, we only present the selected area electron diffraction of starting material and magnetic response from the starting electrode after 0.5 cycles (charged state) and
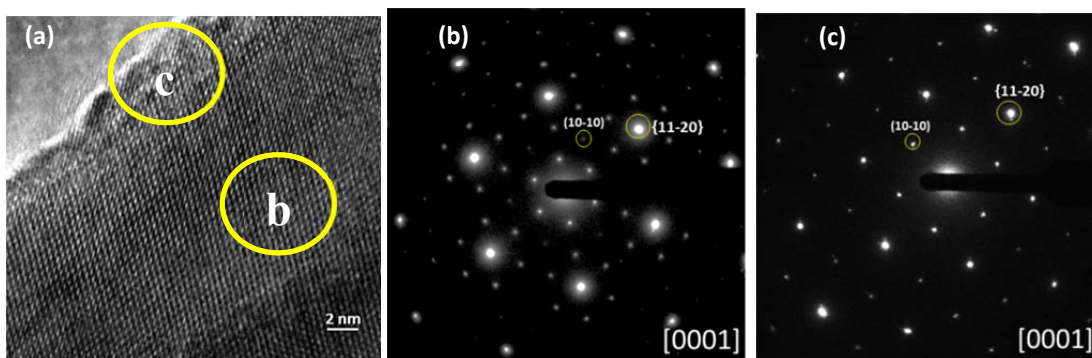
Figure 7: High resolution TEM of HE5050 fresh electrode (a). The corresponding selected area electron diffraction (SAED) taken from core of the particle (b) and edge of the particle (c). The particle was oriented along [0001] direction to observe the superlattice reflections.

after 10.5 cycles (charged state). The detailed results and analysis will be presented in next quarterly report.

Results:
The HRTEM image of HE5050 starting material is shown in figure 7(a). The trigonal symmetry was clearly observed from the lattice fringes. The particle was oriented in [0001] zone axis and SAED patterns were collected from the core of the particle as well as edge of the particle. The SAED that was collected from middle core of the particle shows superlattice reflections, which appear in between two fundamental O3 (hexagonal) reflections. These superlattice reflections referred to $\sqrt{3} \text{ X} \sqrt{3} \text{R} \, 30°$ ordering, which is due to ordering of lithium in the transition metal layer. However, the ordering was not observed in the edge of the particle. This clearly suggests the presence of composition gradient with in the particle.
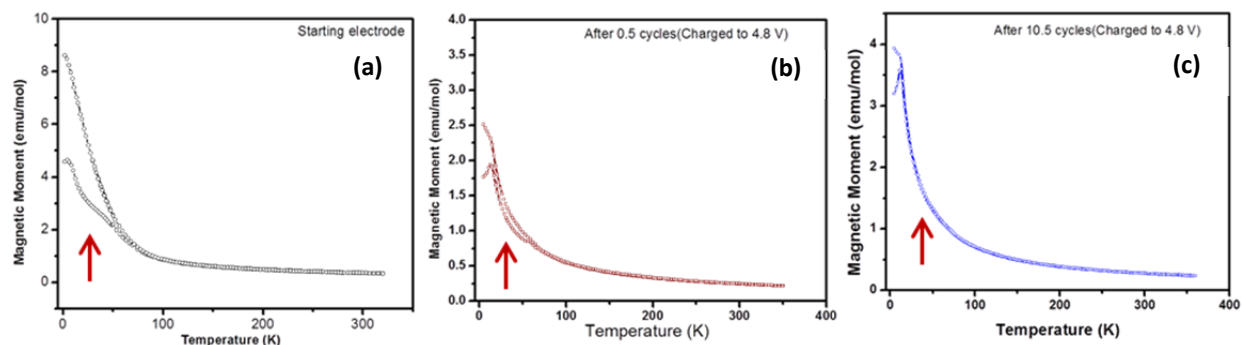

Figure 8: Variation of magnetic susceptibility with temperature for starting HE5050 electrode after 0.5 cycles (b) and after 10.5 cycles (c).

Figure 8 represents the magnetic susceptibility data for the HE5050 electrodes collected at magnetic field of 100 Oe. Starting electrode show magnetic ordering at low temperature region, which is minimized after 0.5 cycles and vanished after 10.5 cycles (see the arrow marks). Which clearly indicates that the structural modification after 10 cycles. The disappearance of ordering suggests that the crystal structure after 0.5 cycles (delithiated state) is not similar to the crystal structure after 10.5 cycles (delithiated state). Detailed analysis is underway.

Project 4. Non-Destructive Evaluation (NDE) for Advanced Lithium Secondary Batteries
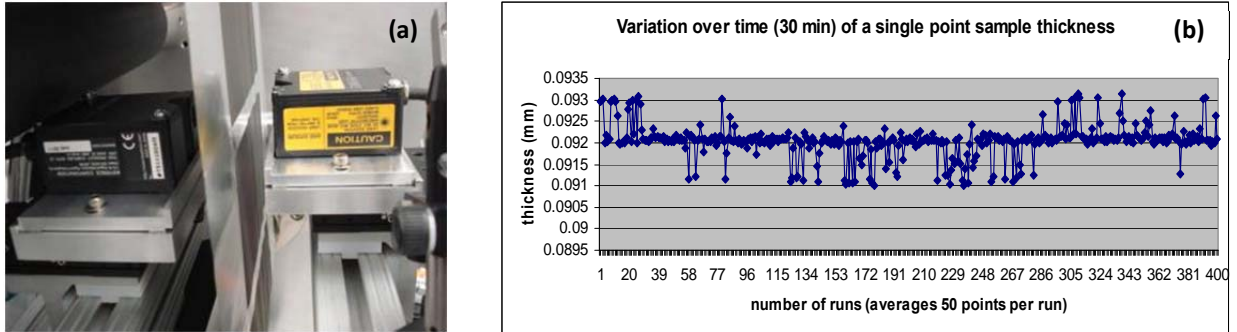
   a. Laser thickness measurement

Figure 9: The laser caliper set-up (a) and obtained base noise of the obtained by using calibration shim.

Progress:
- The Keyence lasers were successfully calibrated for thickness measurement experiment.
- Method to measure the electrode thickness by utilizing lasers was achieved.
- Initial thickness measurements were performed on patch coated electrodes as well as continuous electrode to determine the validity of the present approach.
- Thickness measurements were sensitive to the defects and flaws present in the electrode.

Figure 9 represents the laser caliper set-up system (a). To obtain the base noise from the thickness measurement, a calibration shim was used. Throughout the 30 minute data acquisition period, the data are clustered at 92 microns. Variation does occur from this average, but there is only a 2.2 micron difference, or +/- 1 micron from the average which validates the approach for measuring the thickness.
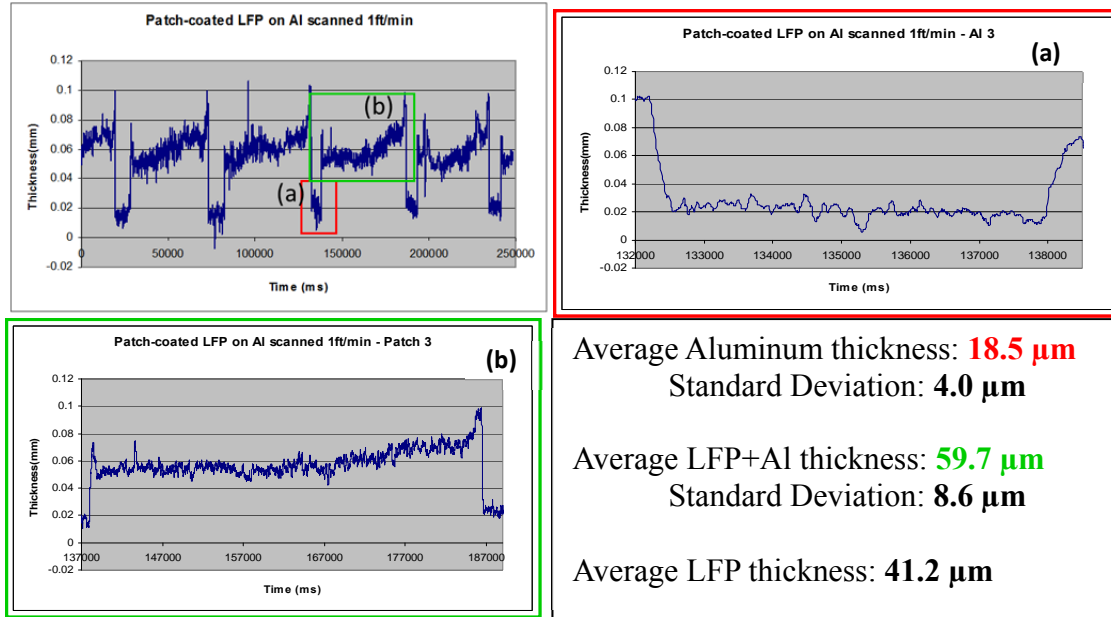
Figure 10: Laser thickness measurement on patch coated lithium iron phosphate electrode and the area a and b is highlighted.

One example of data from a thickness measurement experiment is shown in Figure 10. The thickness of patch coated lithium iron phosphate (LiFePO$_4$) coated on Al was measured and the highlighted areas are presented in figure 2 (a) and (b). The data accusation speed was 1ft/minute. The calculated coating thickness was found to be 41.2µm. The experiment was also performed on continues coated electrode at two different regions to verify any inhomogeneity in the coating. The results are shown in Table 1. It can be seen that the standard deviation is high in region 2 as compared to the region 1 for continuous coating. This may indicate inhomogeneity in the coating or any flaws (large pores) on the electrode surface. The detailed studies are in progress.

b.   IR imaging

Progress:
- Initial tests were performed on the Mylar coated electrode.
- From the image the flaws in the electrode could be detected.
- Temperature profile was used to detect the thickness across the electrode surface.

Results:
In Figure 11, the IR image from the electrode is presented. Visual inspection reveals little detail (Figure 11a). During the IR flashing, very thin spots and several thin lines across the electrode surface were revealed (Figure 11b). This clearly shows the presence of flaws in the electrode which could be detected from IR image.   The temperature profile of the electrode is presented in Figure 11c. The red and orange areas are thinner compared to the green area. This data also suggests the thickness variation across the electrode. To complement this results the high power quartz lamp is viewed through the

electrode and the image is presented in Figure 11d. Clearly, the thin areas show up as bright spots and thick areas show up as dark spot. Detailed studies are in progress.
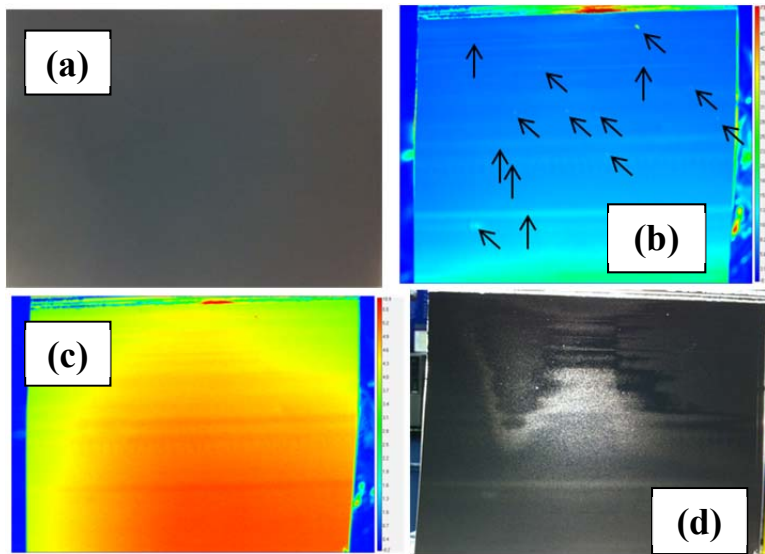

Figure 11: visual digital image (a), IR image (b), temperature profile (c), and image taken when quartz lamp is viewed through the electrode (d).

Planned Publications for next quarter.

- "In-situ XRD evaluation and microstructural transformation of $0.5Li_2MnO_3 - 0.5LiNi_{0.375}Co_{0.25}Mn_{0.375}O_2$ cathode during voltage cycling," *Journal of Power Sources* (2012).
- "Investigating phase transformation pathways during high-voltage hold in $0.5Li_2MnO_3 - 0.5LiNi_{0.375}Co_{0.25}Mn_{0.375}O_2$ cathode materials by in-situ XRD," *Journal of Power Sources* (2012).
- "Studying the cation-ordering and crystal structure of $0.5Li_2MnO_3 - 0.5LiNi_{0.375}Co_{0.25}Mn_{0.375}O_2$ cathode for high-voltage lithium ion batteries: magnetic and analytical TEM investigations," *Journal of Materials Chemistry* (2012).
- "Investigating phase transformation pathways during high-voltage hold in $0.5Li_2MnO_3 - 0.5LiNi_{0.375}Co_{0.25}Mn_{0.375}O_2$ cathode materials by magnetic responses and selected area electron diffraction studies," *RSC Advances* (2012).
- "Thickness evaluation of slot-die coated electrodes by IR imaging and laser techniques," *Journal of Materials Processing Technology* (2012).

TASK 2
Calendar & Cycle Life Studies

Project Number: 2.2A (ES111)

Project Title: Battery Design Modeling (PHEV Battery Cost Assessment)

Project PI, Institution: Kevin Gallagher, Dennis Dees, and Paul Nelson, Argonne National Laboratory

Collaborators (include industry):
Ira Bloom, Argonne National Laboratory
Dan Santini, Argonne National Laboratory

Project Start/End Dates: August 2010/ September 2014

Objectives: The objective of this task is to develop and utilize efficient simulation and design tools for Li-ion batteries to predict precise overall (and component) mass and dimensions, cost and performance characteristics, and battery pack values from bench-scale results. Through these means, researchers and manufacturers will be able to better understand the requirements in the material and battery design to reach DOE cost and specific energy goals.

Approach: Our approach is to design batteries based on power and energy requirements for any chosen cell chemistry and then feed this design into a cost calculation that accounts for materials & processes required. Coupling design and cost allows the user to quantify the impact of underlying properties on the total battery pack cost (cell chemistry, parallel cells, electrode thickness limits, P/E). Furthermore, the efficient nature of these calculations means that various scenarios may be characterized in a short time span – analysis limited by the user not the model.

Milestones:
(a.) Produce version 2.0 of the Battery Performance and Cost model (BatPaC) with documentation. October 2012 (On schedule)
(b.) Implement liquid and air thermal management and evaluate role in design and cost. May 2012 (Complete)
(c.) Support EPA and NHTSA use of BatPaC for 2017-2025 GHG regulation and CAFE standards rule making. March 2012 (Complete)
(d.) Support the public distribution of the model and report. October 2012 (On schedule)
(e.) Evaluate design and cost modeling of advanced Li-ion electrochemical couples. October 2012 (On schedule)

Financial data: $300K/year

PROGRESS TOWARD MILESTONES

(a) Creation of battery performance and cost model BatPaC v2.0: BatPaC v2.0 now includes air and liquid thermal management options as well as automatic error bar generation. Refinement of the model and the user interface is still ongoing. The 2.0 version is targeted for public distribution of late summer 2012.

(b) Implement thermal management options: Complete

(c) Support EPA 2017-2025 rule making: Complete. We will continue to support if new requests are made.

(d) Support public distribution: Interacted with multiple small and large companies to discuss BatPaC v1.0 availability, results of the model and some initial tips for use.

(e) Design & cost of advanced Li-ion: Advanced Li-ion electrochemical couples are one pathway to significantly lower battery cost by raising the active material energy density. While improving one electrode may result in modest advances, improvements in both positive and negative electrodes are necessary to produce a battery pack cost that achieves DOE goals.

Cathodes to be analyzed include one improved 'standard' material, NMC441, as well as two advanced Li-ion materials, LMR-NMC and LNMO. The NMC441 was published by Sun-Ho Kang et al (JES 2011) and can be considered a stepping stone to move from today's commercial materials to the more advanced cathodes.

- $Li_{1.05}(Ni_{4/9}Mn_{4/9}Co_{1/9})_{0.95}O_2$ **NMC441**: 175 mAh/g, 420 mAh/cm^3, U_{avg} = 3.82 V vs Li
- $xLi_2MnO_3(1-x)LiMO_2$ **LMR-NMC**: 250 mAh/g, 565 mAh/cm^3, U_{avg} = 3.75 V vs Li
- $LiNi_{0.5}Mn_{1.5}O_4$ **LNMO**: 130 mAh/g, 268 mAh/cm^3, U_{avg} = 4.75 V vs Li

The advanced negative electrode must improve on the volumetric specific capacity of graphite while not raising the electrode voltage significantly (e.g. not lower the cell voltage significantly). Various alloys such as tin and silicon have high theoretical capacities, but suffer from poor cycle life due to large volumetric expansions. Recent advances have shown exciting improvements in properties such as cycle life and coulombic efficiency. These problems are considered to be solved for the following cost and performance projections. The properties of the advanced Li-ion anode material evaluated are as follows:

- Capacity determined from parametric study below (> 800 mAh/cm^3 and 900 mAh/g)
- Assume 80% 1st cycle efficiency
- 50% electrolyte porosity in the discharge state
- 80:10:10 active:binder:carbon
- Target V/U = 0.7 (efficiency) for pulse power

The advanced anode potential profile as function of state of charge is taken from the graphene/graphite-silicon (GrSi) composite developed by Junbing Yang and Khalil Amine at Argonne. Figure 1a displays a normalized charge and discharge curve this material. The potential of the electrode on discharge is significantly higher than a graphite electrode, 0.4 vs 0.15 V vs Li, under the same cycling conditions (C/10). The effect of the capacity of the anode on projected price is evaluated in Figure 1b for two material cost values. The GrSi is paired with the LMR-NMC cathode material for these calculations of a 60 kW, 17 kWh 360V PHEV40 battery. Standard graphite electrodes commonly cost between 15 and 25 \$/kg. The GrSi anode with material cost of \$25/kg appears to reach diminishing returns at capacities higher than 800 mAh/cm^3 or 900 mAh/g. A value of 1300 mAh/g is used for the remainder of the studies to avoid hitting the knee in the cost curve.
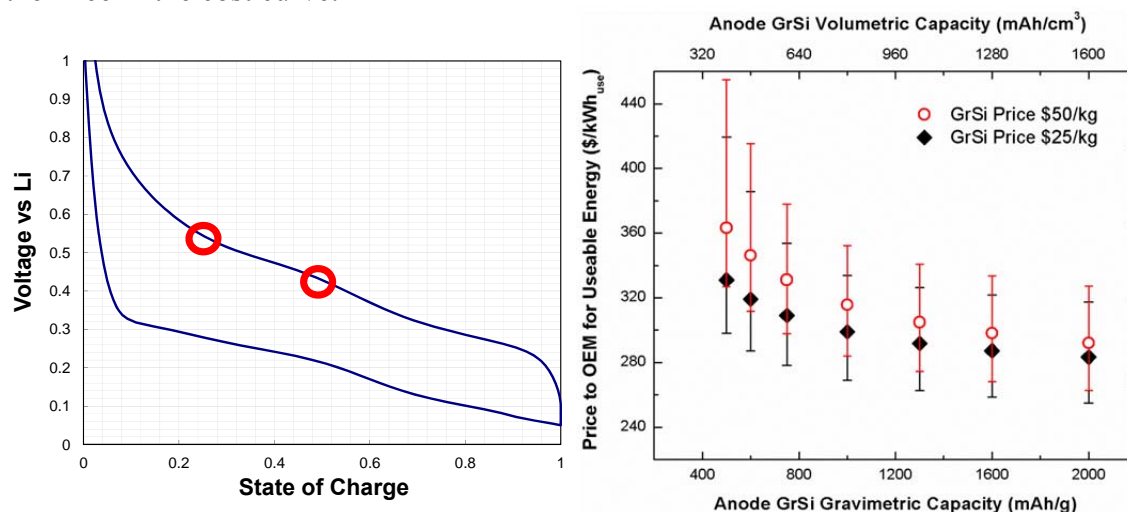

Figure 1: a) Charge and discharge curve of a graphene-silicon composite material from Junbing Yang and Khalil Amine at Argonne. This curve was used to estimate the potential of the negative electrode at 50 and 25% SOC during discharge. b) Results from BatPaC for a LMRNMC-GrSi couple for varying values of the specific capacity and raw material cost in a 17 kWh 60 kW 360 V battery.

Figure 2 evaluates the benefits of moving to the advanced GrSi electrode for the three cathodes detailed above. The NMC441 and LMRNMC cathodes realize some benefit from moving to the advanced anode, while LNMO (5V spinel) becomes more costly. The LNMO electrode is attractive due to the high cell potential (4.6 V) when coupled to graphite, but is most hindered by the cathode's low volumetric capacity. Thus, pairing this electrode with GrSi reduces the cell's strongest attribute without improving the cathode material's largest limitation.
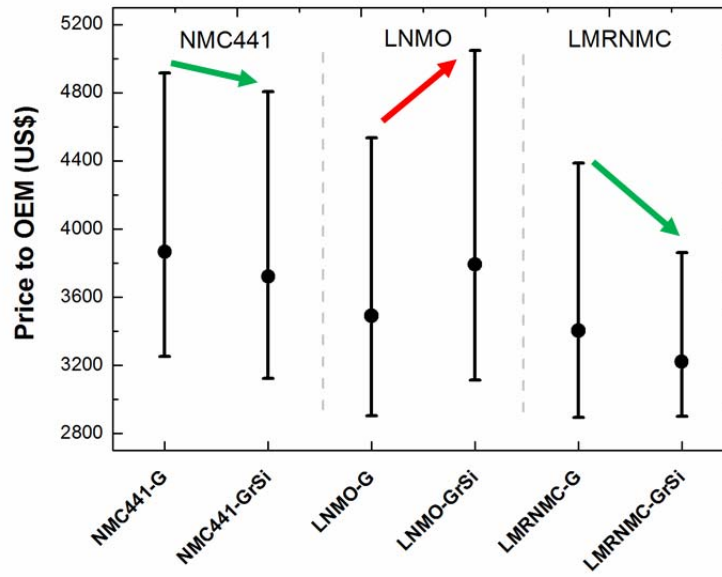
Figure 2: Predicted costs for a 17 kWh, 60 kW 360 V PHEV battery

The error bars in Figure 2 include contributions from materials, processing, and design uncertainties. The largest design contributor is the electrode thickness limitation. Current transportation batteries are limited to thickness near 50 microns due to transportation limitations in the electrolyte, lithium plating on the graphite electrode, as well as manufacturing issues. We consider these electrochemical couples with a 50 micron limitation in Figure 3.

Here again, we see the LNMO cathode does not pair well with the advance anode while the other materials see some benefit. The LMR-NMC material has the greatest synergy with this anode material due to two main reasons. First, the higher volumetric capacity of LMR-NMC means the graphite electrode is limiting. Replacing this electrode with the higher volumetric capacity of GrSi allows for a greater mAh/cm^2 loading. Second, the first cycle irreversible capacity of the LMR-NMC electrode can be used to seed the formation of the SEI layer on advanced anodes that may have a lower coulombic efficiency in initial cycles. The lower overall cell potential of a LMRNMC – GrSi couple will be problematic for higher power-to-energy ratio designs (e.g. Chevrolet Volt or a PHEV10). The lower voltage at bottom of state-of-charge is also more sensitive to ASI requirements leading to a cell that may operate at lower efficiency, perhaps leading to larger heat removal requirements and more expensive thermal management. However, this combination of anode and cathode materials appears to be the most promising pathway to achieving the DOE targets as demonstrated in Figure 3.
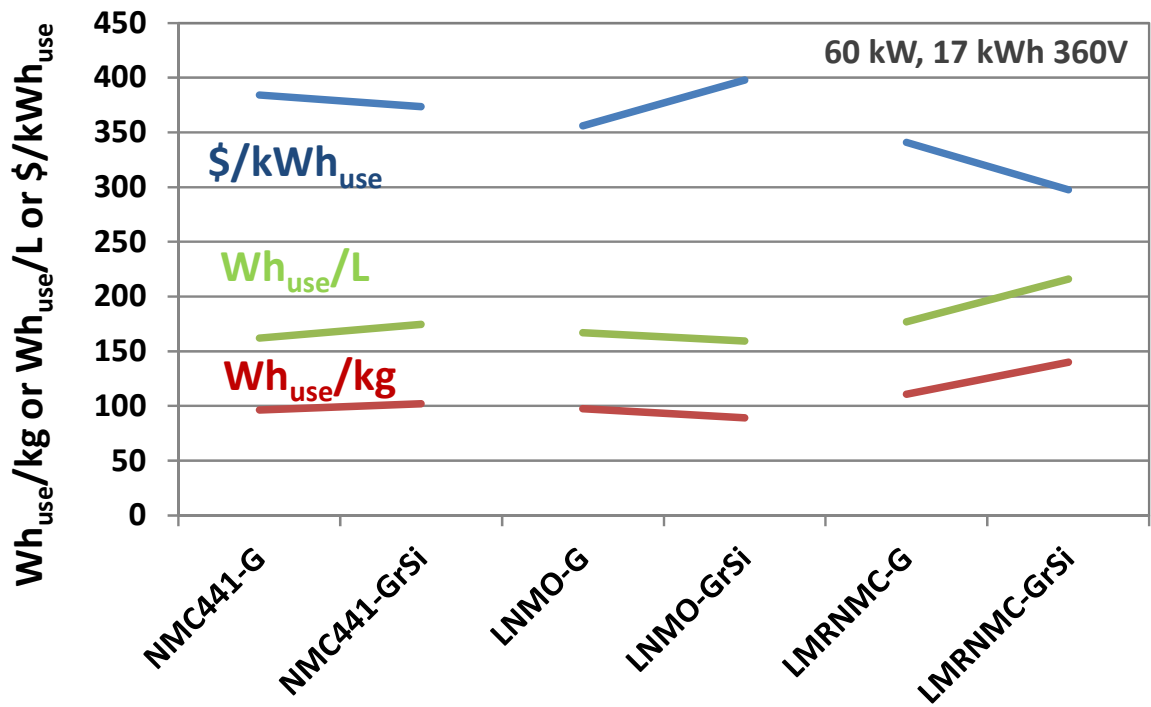
Figure 3: Performance and cost for advanced Li-ion cell chemistries for a 17 kWh, 60 kW 360 V PHEV battery with a 50 micron maximum electrode thickness limitation.

Publications, Reports, Intellectual property or patent application filed this quarter. (Please be rigorous, include internal reports--invention records, etc.)

Kevin G. Gallagher, Paul A. Nelson, and Dennis W. Dees, "Examining the Role of Battery Design and Performance on Manufacturing Cost" Abstract submitted for IMLB 2012

Kevin G. Gallagher, Dennis Dees, and Paul Nelson, "PHEV Battery Cost Assessment" 2012 DOE Annual Merit Review presentation submitted

TASK 3
Abuse Tolerance Studies

Project Number: 3.1 (ES035)

Project Title: Develop & evaluate materials &additives that enhance thermal & overcharge abuse

Project PI, Institution: Zonghai Chen & Khalil Amine, Argonne National Laboratory

Collaborators (include industry): Yang Ren, Yan Qin, Chi-Kai Lin, Lu Zhang, Superior Graphite

Project Start/End Dates: 10/01/2008~09/30/2014

Objectives: Identify the role of each cell material/components in the abuse characteristics of different cell chemistries; Identify and develop more stable cell materials that will lead to more inherently abuse tolerant cell chemistries; Secure sufficient quantities of these advanced materials (and electrodes) & supply them to SNL for validation of safety benefits in 18650 cells.

Approach: Three-phase strategy is adopted for the thermal property improvement, including securing material, tests on cell components, and validation at cell level. In-house synthesis, commercial source and partners are used to secure materials, and various electrochemical and thermal analysis are conducted at cell components level in the second phase, and finally the thorough validation is executed at cell level. At the second and third phase, certain feedbacks can be obtained to phase one. For overcharge study, similar strategy is applied but in the first phase organic synthesis is the major source to secure materials. In addition, when feedbacks go to phase one, new design can be achieved using organic knowledge to improve the performance in certain aspect.

Milestones
(a) Investigating potentially negative impact of ANL-RS2 as redox shuttle additive (ongoing);
(b) Investigating the thermal decomposition of SEI layer on graphite (ongoing).

Financial data: $500K/FY2012

PROGRESS TOWARD MILESTONES

(a) Summary of work in the past quarter related to milestone (a).
In the past years, we have reported that 2,5-di-tert-butyl-1,4-bis(2-methoxyethoxy)benzene (ANL-RS2) can be stable redox shuttle for overcharge protection and automatic capacity balancing of lithium-ion batteries using $LiFePO_4$ as the cathode material. It is also important to demonstrate that the added electrolyte additive will not significantly compromise the other performance of lithium-ion

batteries. This demonstration activity was based on electrochemical couple using MCMB as the anode, LiFePO$_4$ as the cathode. The baseline electrolyte used was 1.2 M LiPF$_6$ in EC/EMC (3:7 by weight) (Gen 2 electrolyte). In order to maximize the impact of ANL-RS2, if there is any, the concentration of ANL-RS-2 as additive was raised to 0.35 M in the final electrolyte. Figure 1a shows the discharge capacity of lithium-ion cells as a function of discharge C-rate with and without 0.35 M ANL-RS2 in the electrolyte. When the discharge current was less than 5C, insignificant impact of the added ANL-RS2 was observed. However, when the discharge current was increased to 5c and above, a decrease of discharge capacity up to 20% was observe due to the reduction of electrolyte conductivity caused by the addition of ANL-RS2. When the cells were continuously charged/discharged at C/3 rate at room temperature, excellent capacity retention was obtained for those with and without ANL-RS2; no capacity fade was observed for up to 200 cycles. In other word, the addition of ANL-RS2 has insignificantly negative impact on the low rate cycling performance (see Figure 1a). However, serious attention should be paid to the heat generated when the redox shuttle is activated (see Figure 2, previously reported).
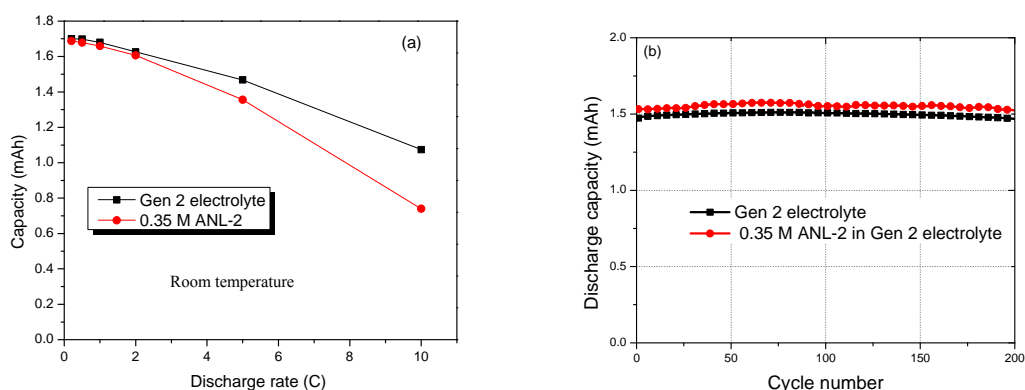

Figure 1 (a) Rate capability and (b) discharge capacity (C/3) of lithium-ion cells with/without ANL-RS2 redox shuttles showing that the addition of 0.35 ANL-RS2 in the electrolyte does decrease the electrolyte conductivity lead to the reduction of discharge capacity at high rate (>5C), and no impact of cycling performance at C/3 rate at room temperature.
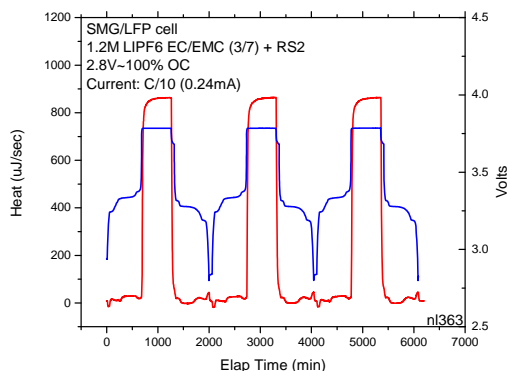
Figure 2 charge/discharge capacity of a $Li_4Ti_5O_{12}/LiFePO_4$ lithium-ion cell during overcharge test.

(b) Summary of work in the past quarter related to milestone (b)

We have demonstrated previously that the thermal decomposition of SEI layer played a critical in the safety of lithiated graphite. Our previous study showed that natural graphite, a mixture of 2H graphite and 3R graphite, has a better thermal stability than conventional MCMB. In order to validate the impact of surface functional group on the safety of graphite, natural graphite coated with carbon source was acquired from Superior Graphite. Different thermal processing conditions were applied to the precursor, assuming that the content and type of surface functional groups varies with the processing condition/temperature. The first batch of experiment was to treat the sample at different temperatures in inert atmosphere. The treating temperature varies from 700°C to 1080°C. Figure3a shows the Raman spectroscopies of natural graphite treated at different temperatures. It is clear that the surface coating layer shows more graphitic characteristics when treated at higher temperature, which is shown as the intensity decrease of D band at 1350 cm^{-1} and the right shoulder of G band at about 1600 cm^{-1} (or D' band). In addition, the self-discharge current of fully lithiated natural graphite was also measured to study the stability of SEI layer (see Figure 3b). The self-discharge current measured is caused by the slow reaction of lithiated graphite with non-aqueous electrolyte. Small self-discharge current is a indication of stable SEI layer and better safety characteristics. Figure 3b shows that the self-discharge current consistently decreases with the treating temperature. Characterization of theses samples using differential scanning calorimetry (DSC) is ongoing.
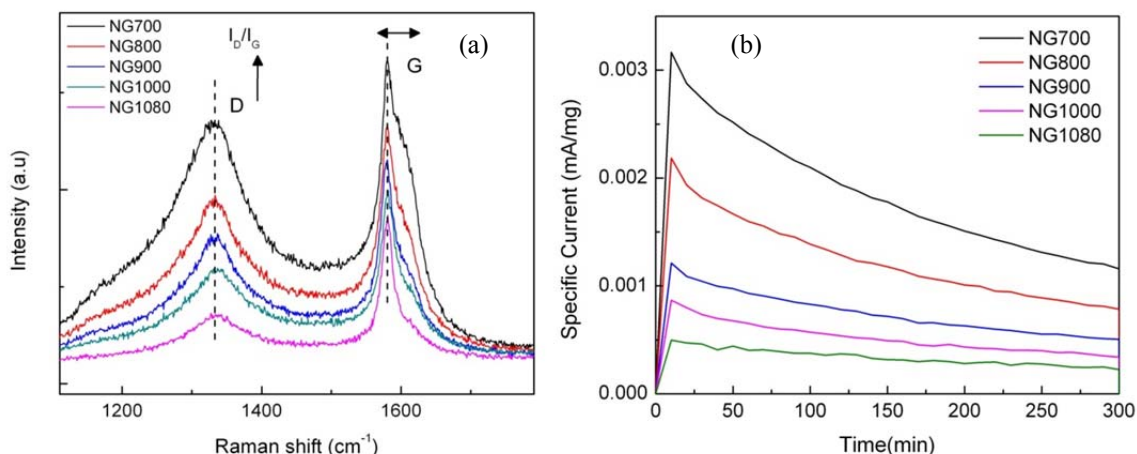
Figure 3 (a) Raman spectroscopy of natural graphite at different temperatures showing that the surface coating layer has more graphitic characteristics with the treating temperature; (b) self-discharge current of fully lithiated natural graphite at 1 mV to monitor the stability of SEI layer.

Publications, Reports, Intellectual property or patent application filed this quarter. (Please be rigorous, include internal reports--invention records, etc.)

1. Yang-Kook Sun, Zonghai Chen, Hyung-Joo Noh, Dong-Ju Lee, Hun-Gi Jung, Yan Ren, Steve Wang, Chong S. Yoon, Seung-Taek Myung, and Khalil Amine, Nano-Structured High-Energy Cathode Materials for Advanced Lithium Batteries, submitted *Nature Materials*, (**2012**).
2. Zonghai Chen, Ilias Belharouak, Y.-K. Sun, and Khalil Amine, $Li_4Ti_5O_{12}$ for High-Power, Long-Life and Safe Lithium-Ion Batteries, submitted book chapter, (**2012**).
3. Zonghai Chen, Ilias Belharouak, Y.-K. Sun, and Khalil Amine, Titanium-Based Anode Materials for Safe Lithium-Ion Batteries, submitted to *Advanced Functional Materials*, (**2012**).

TASK 3
Abuse Tolerance Studies

Project Number: 3.2 (ES036)

Project Title: Abuse Tolerance Improvements

Project PI, Institution: Chris Orendorff, Sandia National Laboratories

Collaborators (include industry): ANL, INL, BNL, ORNL, NREL, Binrad Industries, Physical Sciences Inc., A123

Project Start/End Dates: 10/1/2011-9/30/2012

Objectives: The objective of this work is to develop inherently abuse tolerant lithium-ion cell chemistries. This involves understanding the mechanisms of cell degradation and failure, determining the effects of new materials & additives on abuse response, and cell level abuse testing and cell characterization to quantify improvements

Approach: Materials to full cell characterization to determine inherent safety and reliability of the most advanced lithium-ion chemistries. Approaches include a suite of battery calorimetry techniques (microcal, DSC, TGA/TDA, isothermal, ARC), abuse tests (electrical, mechanical, thermal), and analytical diagnostics (electrochemical characterization, optical spectroscopy, mass spectrometry, computed tomography, electron microscopy, etc.)

Milestones:
(a) LiF/ABA electrolyte development (ON GOING, on schedule)
(b) Ionic liquid electrolyte development (ON GOING, on schedule)
(c) Cell prototyping optimization & collaboration with other Labs (ON GOING, on schedule)
(d) Overcharge shuttle evaluation in full cells (DUE 9/30/2012, on schedule)
(e) Support INL phosphazene electrolyte development (DUE 9/30/2012, on schedule)
(f) Evaluation of phosphate-coated NMC (DUE 9/30/2012, on schedule)
(g) Evaluation of ALD-coated NMC electrodes (DUE 9/30/2012, on schedule)

Financial data: Total budged $1.0M; received $640K (from SNL); $45K subcontract to Binrad Industries (ABA), $10K subcontracted to Physical Sciences Inc. (phosphate coated NMC)

PROGRESS TOWARD MILESTONES

(a) LiF/ABA electrolyte development. FY12 will focus on (1) developing new ABA molecules with improved voltage stability and (2) characterization of the degradation mechanisms of ABAs that lead to cathode passivation during runaway. DSC measurements on Toda NMC111 show a reduction in the heat release for the cathode in

1.0 M LiF/ABA in EC:EMC (3:7) compared to in 1.2 M LiPF$_6$ in EC:EMC (3:7) (Figure 1a) at 100% SOC. Results are consistent with observations made in FY11 for different NMC materials with ABA and suggests potential improvement in cell safety. However, SEI formation using LiF/ABA appears to be problematic as shown by the significant capacity fade in graphite anode half cells (Figure 1b). Efforts are underway to improve this fade and SEI film formation using additives (VC, PF$_6^-$) and coated anode electrodes. Synthesis of new ABAs should be completed in Q3.
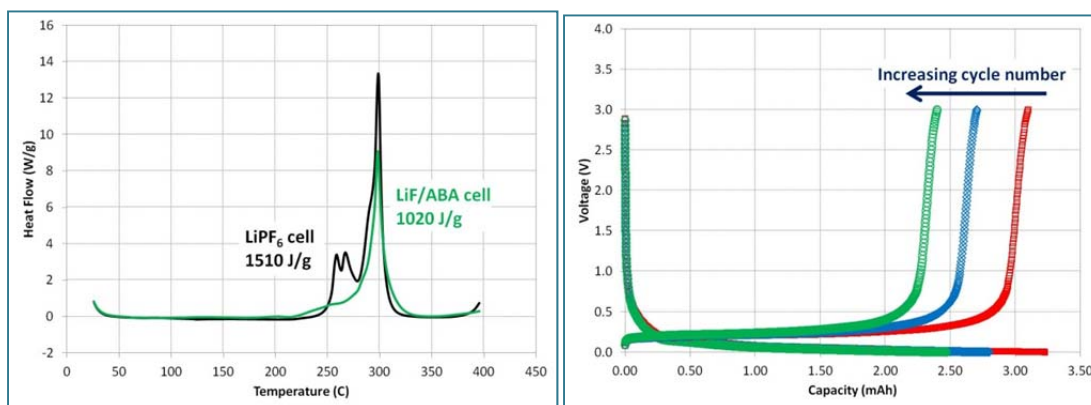
Figure 1. (a) Heat flow (W/g) as a function of temperature for Toda NMC111 in 1.2 M LiPF$_6$ in EC:EMC (3:7) (black trace) and in 1.0 M LiF/ABA in EC:EMC (3:7) (green trace) measured by DSC and (b) D/C capacity of anode ½ cells in 1.0 M LiF/ABA in EC:EMC (3:7)

(b) Ionic liquid electrolyte development. Based on the two ionic liquid (IL) candidates synthesized in Q1, the decision was made to move forward with cell measurements on IL-2 (ammonium-based IL), based on the improved low voltage stability. The viscosity of IL-2 is ~90 cP at ambient temperature (Figure 2a). In addition, lithium salts (LiTFSI) are soluble to ~ 0.7 M in IL-2. Cell measurements are made using a 50:50 mixture of 0.7 M LiTFSI in IL-2 and 0.7 M LiTFSI in EC/EMC (3:7) to improve the viscosity, but alternative co-solvents are currently being evaluated. A request was made to ANL to provide LTO/HV spinel electrodes for evaluation of IL-2 at SNL in coin cells in Q1. In the meantime, cell measurements were made using graphite/NMC111. Initial discharge curves are shown in Figure 2b, where the discharge capacity of the IL electrolyte cell at 400 mA is ~10-15% less than that for the conventional LiPF$_6$ in EC:EMC (3:7) electrolyte. This could be a rate limitation of the electrolyte at lower salt concentration and higher viscosity. Experiments are currently in progress to determine the effect of C/D rate on the performance of the IL-based electrolytes.
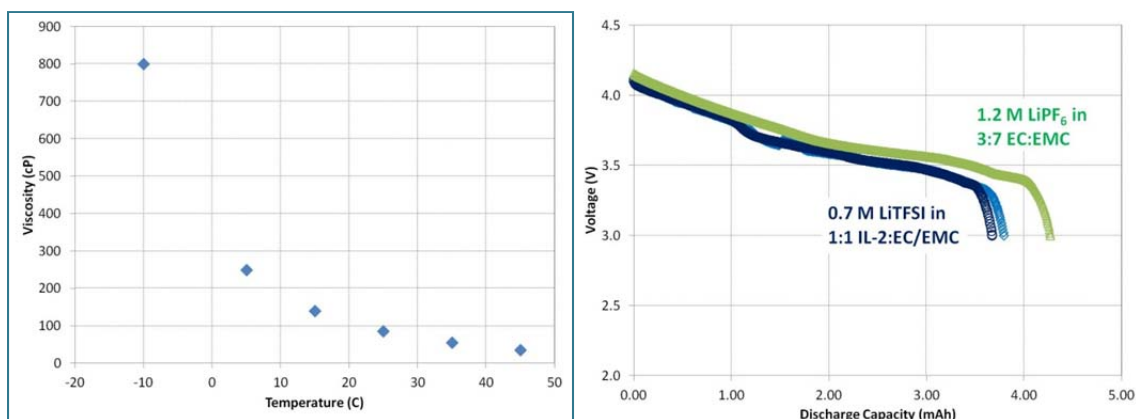
Figure 2. IL-2 viscosity (cP) as a function of temperature and (b) discharge capacity of NMC111 2032 coin cells with carbonate (green) and IL-based electrolytes (blue)

(c) Cell prototyping optimization & collaboration with other Labs. At the end of FY11, SNL and DOE agreed to use the Toda NMC (111)/Conoco Phillips A10 graphite electrochemical couple for the early FY12 cell builds to support the electrolyte thrust/materials development efforts in ABR. In Q1 FY12, SNL optimized a 1.5 Ah design for this couple in 18650 cells and coated ~150 electrode pairs to support the effort. In addition, SNL has coated the first run of LFP electrodes to support the ANL-RS-2 shuttle development. LFP cells have been built with the shuttle and the first NMC cells have been built with the INL electrolyte. The quantity of cells to support these different programs is 40 (INL Phosphazene), 24 (JPL electrolyte, 24 (ANL-RS-2 shuttle, LFP), ~40 (SNL ABA), and 6-10 (NREL ALD coating).

The electrode processing standardization effort between ANL/ORNL/SNL is underway with an electrode formulation of Toda 523 NMC:Denka carbon:Solvay binder (90:5:5). Electrodes have been cast at Sandia giving 157 mAh/g and the round robin testing activity is in progress Figure 3). SNL will also deliver 523 electrodes with this formulation to NREL for ALD/Al_2O_3 coating.
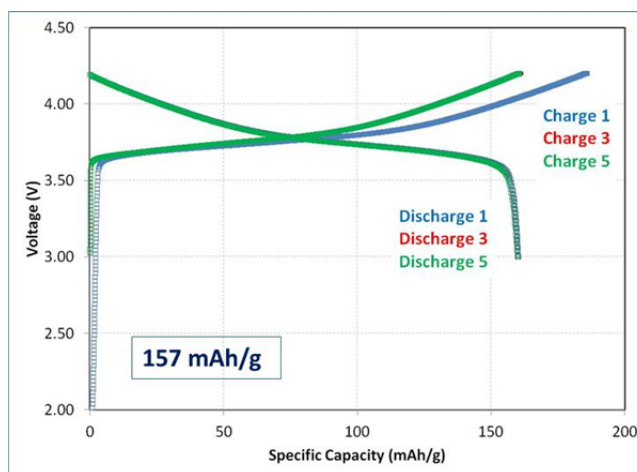

Figure 3. Charge and discharge capacity of NMC523

(d) Overcharge shuttle evaluation in full cells. Two-cell batteries (LFP, 18650s) were made with cells containing the redox shuttle to determine the utility of the shuttle for cell balancing. Cells were offset to 100% SOC (3.6 V) and 50% SOC (3.25 V) and charged at 200 mA (Figure 4a) and 1 A (Figure 4b). At 200 mA, the cells are balanced in ~4.5 hr with very little cell heating (max. temperature = 32 C). At 1A, the cells were balanced in ~90 min, with a much more significant temperature increase to 72-78 C. This represents an extreme case for cells to be out of balance and work is in progress to evaluate the rebalancing ability at more moderate states of cell imbalance. Cells were also evaluated under constant current overcharge abuse conditions (Figure 5). At 1A overcharge, the cell without the shuttle begins to heat immediately and undergoes a runaway reaction at 130% SOC (a known problem with LFP). With the shuttle, the cell voltage peaks at 4 V, equilibrates to 3.8V and the cell skin temperature increases and equilibrates at 90 C. The test was terminated at 260% SOC without any cell venting or catastrophic failure. This result represents a significant improvement in overcharge abuse response for LFP cells using the redox shuttle.
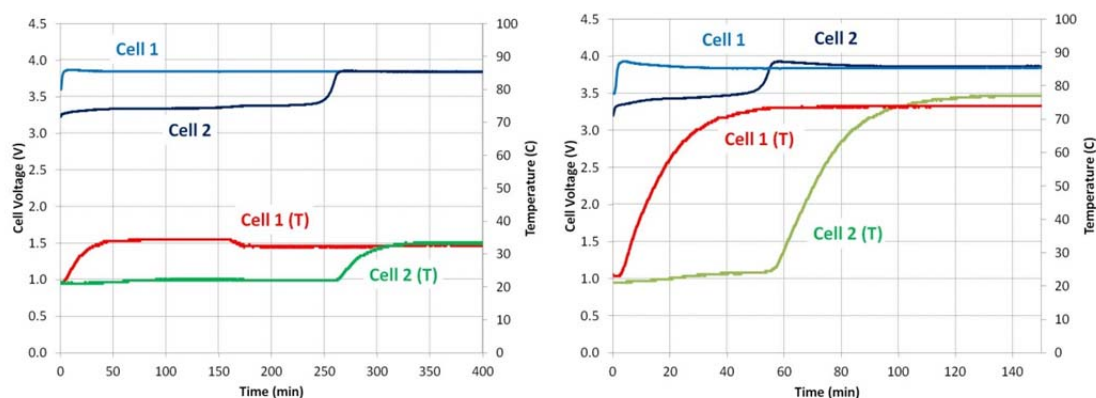
Figure 4. Cell voltage and skin temperature during cell
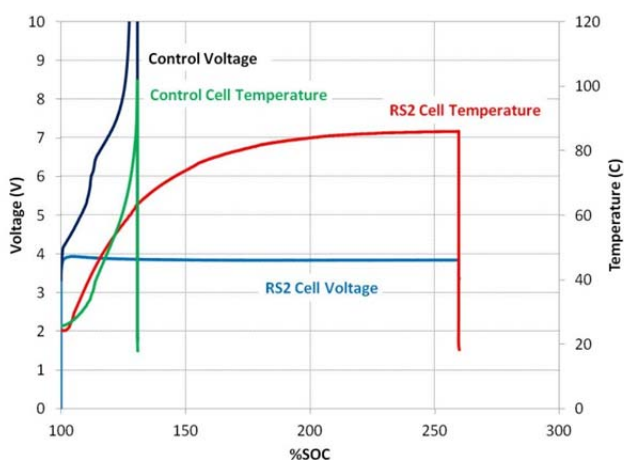balancing at (a) 200 mA and (b) 1 A charge current

Figure 5. Cell voltage and skin temperature during a 1 A overcharge
abuse test for cells with and without the redox shuttle

(e) Support INL phosphazene electrolyte development. Electrolytes were received from INL in early Q1 FY12. These include a control (1.2 M LiPF6 in EC:EMC (2:8)) and phosphazene containing electrolytes SM-6, FM-2, and PhIL-1 (up to 3% by wt).. ARC measurements were made in Q2 on individual cells with the phosphazene additives (Figure 6). Results show no change in the onset temperature for the cathode runaway, but a slight decrease in the peak heating rate for the cells with the additive. Replicates of these measurements will be done in Q3 as well as gas volume analysis to determine the effect of the additives of gas generation and flammability measurements to measure their efficacy as a flame retardant in cells.
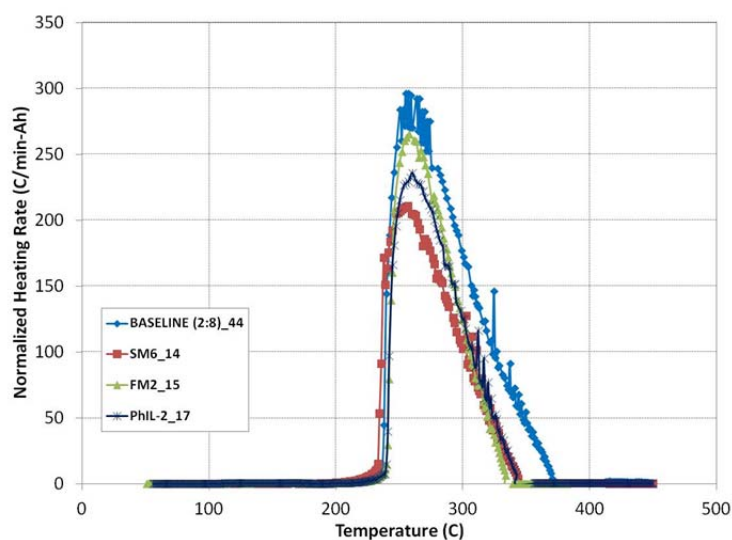

Figure 6. Cell heating rate (C/min) as a function of temperature during cell runaway for phosphazene containing electrolyte measured by ARC

(f) Evaluation of phosphate-coated NMC. SNL is contracting with Physical Sciences, Inc. (PSI) to evaluate phosphate-coated NMCs using their process developed under a NASA NRA proposal in FY09/FY11. Initial performance measurements on the coated-NMC show no statistical difference is charge/discharge capacity compared to the uncoated-control. DSC measurements on the coated cathodes (w/o excess electrolyte) show the onset temperature for the decomposition of the coated NMC to be shifted to higher temperature, compared to the uncoated control (Figure 7). Results are consistent with observations made for the AlF_3-coated NMC, suggesting a slowing of the decomposition and combustion reactions at the particle interface.
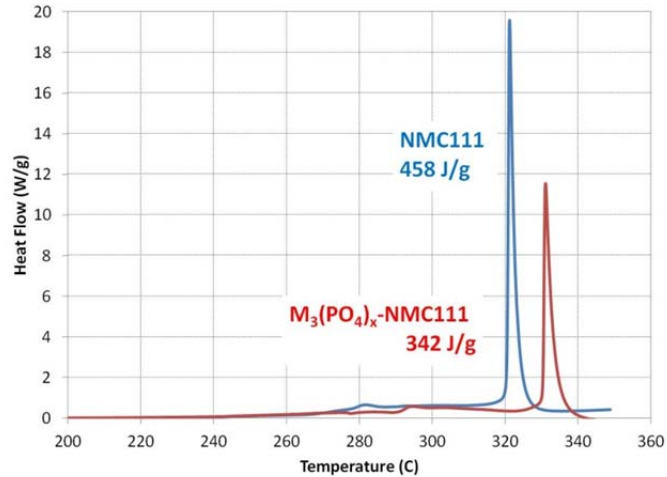
Figure 7. Heat flow (W/g) as a function of temperature for phosphate-coated NMC111 (red) and uncoated NMC111 (blue) without excess electrolyte measured by DSC

(g) Evaluation of ALD-coated NMC electrodes. CP A10 and Toda NMC111 18650 electrodes prepared at SNL were Al_2O_3-coated by ALD at NREL/CU (4 each) in Q2. 18650 cells were built at SNL using coated anodes/uncoated cathodes and uncoated anodes/coated cathodes to separate out the contributions from coating each electrode. Once coated-anode cell was measured by ARC at the end of Q2 and compared to the baseline (uncoated electrodes). Results show a shift in the high rate runaway onset temperature by ~20 C (Figure 8). This suggests a passivation of the high temperature anode decomposition (~200 C for graphite anodes) and a delay in the cathode decomposition, as a result. It is important to note that this is a single cell measurement and replicates will confirm this observation. Coated-cathode ARC measurements in cells, coated-electrode DSC, and additional coating work on NMC powders will be done in Q3.
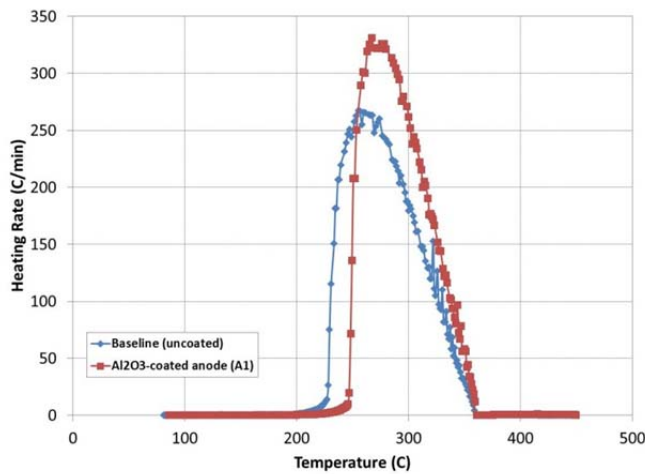

Figure 8. Cell heating rate (C/min) as a function of temperature during cell runaway for a control cell (blue) and an Al_2O_3-coated anode cell (ALD) measured by ARC

TASK 3
Abuse Tolerance Studies

Project Number: 1.2.1 (ES037)

Project Title: Overcharge Protection for PHEV Batteries

Project PI, Institution: Guoying Chen and Thomas Richardson, Lawrence Berkeley National Laboratory

Collaborators: Robert Kostecki, John Kerr, Vince Battaglia, Marca Doeff, Gao Liu, Yuegang Zhang (Molecular Foundry)

Project Start Date: March 2009

Objectives: Develop a reliable, inexpensive overcharge protection system. Use electroactive polymers for internal, self-actuating protection. Minimize cost, maximize rate capability and cycle life of overcharge protection for high-energy Li-ion batteries for PHEV applications.

Approach: Our approach is to use electroactive polymers as self-actuating and reversible overcharge protection agents. The redox window and electronic conductivity of the polymer will be tuned to match the battery chemistry for non-interfering cell operation. Rate capability and cycle life of the protection will be maximized through the optimization of polymer composite morphology and cell configuration.

Milestones:
a) Investigate overcharge protection performance of polymer fiber incorporated composite separators (Jun. 2012). **On Schedule**

b) Evaluate the property and performance of new high-voltage electroactive polymer candidates (Jul. 2012). **On Schedule**

c) Report overcharge protection for pouch and other large-scale battery cells (Sep. 2012). **On Schedule**

Financial data: $190K (FY2009), $190K (FY2010), $250K (FY2011)

PROGRESS TOWARD MILESTONES

We recently reported the excellent cyclability of lithium battery cells overcharge-protected by a GF/D-type glass fiber separator impregnated with electroactive polymers. The performance improvement over the previously used Celgard composite separator was attributed to better polymer utilization on a substrate with more open pore structure and higher porosity. In this quarter, we further investigated alternative membrane substrates and their effect on the sustainable overcharge current densities. Three types of commercial glass fiber membranes, Whatman GF/D, GF/A, and GF/C, with compressed thicknesses of 160, 85 and 85um, respectively, were used in this study. The membranes had similar pore structures and porosities, although the fiber diameters in GF/C were noticeably smaller, as shown in Fig. 1.

Composite separators were prepared by solution impregnating poly(3-butylthiophene) (P3BT) into the glass fiber membranes at a weight loading of 5%. Fig. 2a shows the performance of the P3BT-GF/C composite at different current densities, evaluated in a "Swagelok - type" cell with the composite membrane as cathode and Li foil anode and reference electrode. The cell was able to hold constant potentials at a range of current densities by shorting through the conductive polymer, with steady state reached at a current density as high as $20mA/cm^2$. Fig. 2b compares the sustainable current densities of the P3BT composites on the various substrates. All glass fiber composites showed improved performance over that of the Celgard, which only had a maximum current density of $0.5mA/cm^2$. Both GF/D and GF/A attained a highest current density of $10mA/cm^2$, with the cell potentials noticeable lower on the latter owing to its decreased thickness. The maximum sustainable current density was achieved using the GF/C composite, 20 times higher compared to that of the Celgard composite (Fig. 2b). The superior performance of the GF/C composite is likely a result of more uniformly distributed, smaller fibers that lead to better pore structure for the distribution and utilization of the electroactive polymer. The results further demonstrate the important role of the composite substrate. The cycling performance of the cells protected by a GF/C composite is currently under investigation.
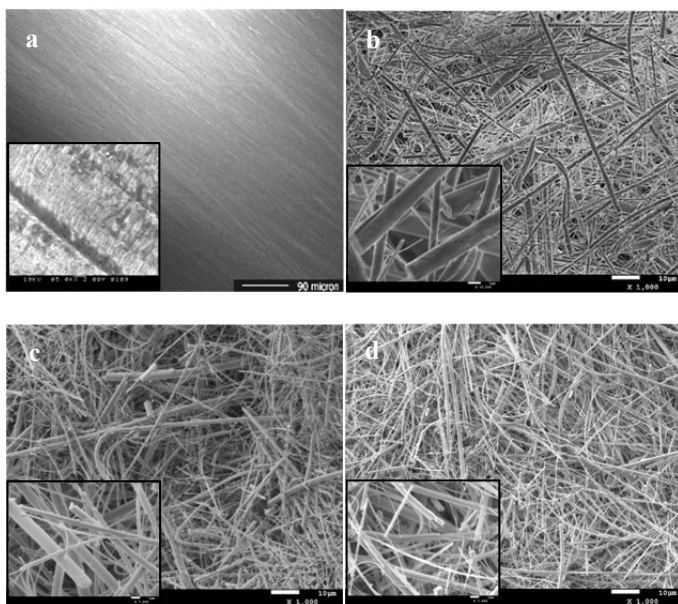
Figure 1. SEM images of membrane substrates: (a) Celgard, b) GF/D-type, (c) GF/A-type, and (d) GF/C-type glass fiber membranes.
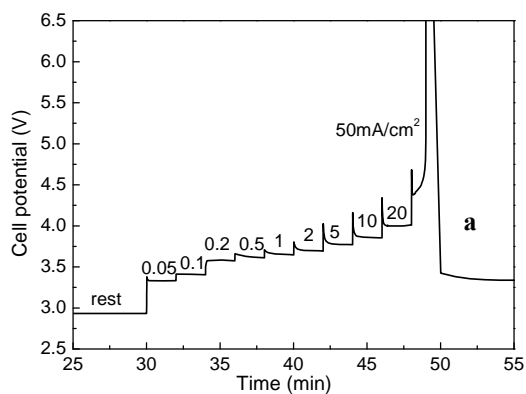

Figure 2. (a) Voltage profile of the P3BT-GF/C composite at the indicated current densities and (b) comparison of the sustainable current densities achieved by the P3BT composites on various substrates.